NF-κB PLAYS A ROLE IN CARDIAC FIBROBLAST SURVIVAL UNDER HYPOXIA

SANGEETHA MOHAN

PhD Thesis – February, 2009

SREE CHITRA TIRUNAL INSTITUTE FOR MEDICAL SCIENCES AND TECHNOLOGY THIRUVANANTHAPURAM – 695 011, INDIA

NF-κB PLAYS A ROLE IN CARDIAC FIBROBLAST SURVIVAL UNDER HYPOXIA

A thesis presented

by

SANGEETHA MOHAN

Division of Cellular and Molecular Cardiology
Sree Chitra Tirunal Institute for Medical Sciences and Technology
Thiruvananthapuram 695 011, India

in partial fulfillment of the requirements for the degree of

Doctor of Philosophy

of

SREE CHITRA TIRUNAL INSTITUTE FOR MEDICAL SCIENCES AND TECHNOLOGY THIRUVANANTHAPURAM, INDIA

CERTIFICATE

I, **Sangeetha Mohan**, hereby certify that I had personally carried out the work depicted in the thesis entitled **"NF-κB plays a role in cardiac fibroblast survival under hypoxia"** under the direct supervision of **Dr. K Shivakumar**, Scientist F, Division of Cellular and Molecular Cardiology, Sree Chitra Tirunal Institute for Medical Sciences and Technology, Thiruvananthapuram, Kerala, India, except where external help was sought and is acknowledged.

Sangeetha Mohan

Sangeetha Mohan

Dr. K Shivakumar
Scientist F

Division of Cellular and Molecular Cardiology
Sree Chitra Tirunal Institute for Medical Sciences and Technology
Thiruvananthapuram 695 011, India

CERTIFICATE

This is to certify that **Ms. Sangeetha Mohan**, in the Division of Cellular and Molecular Cardiology of this institute, has fulfilled the requirements of the regulations relating to the nature and prescribed period of research for the PhD degree of the Sree Chitra Tirunal Institute for Medical Sciences and Technology, Thiruvananthapuram. The work relating to her thesis entitled **"NF-κB plays a role in cardiac fibroblast survival under hypoxia"** was carried out under my direct supervision.

K Shivakumar

12/2/2009

Dr. K Shivakumar
(Guide)

The thesis entitled

NF-κB PLAYS A ROLE IN CARDIAC FIBROBLAST SURVIVAL UNDER HYPOXIA

submitted by

Sangeetha Mohan

for the degree of

Doctor of Philosophy

of

Sree Chitra Tirunal Institute For
Medical Sciences and Technology
Thiruvananthapuram - 695 011, India

evaluated and approved by

K Shivakumar
9/10/2009

Dr. K Shivakumar
(Guide)

Madhu Khullar
9.10.0

Thesis examiners

CONTENTS

ACKNOWLEDGEMENTS

I consider myself privileged to have had the opportunity to carry out my doctoral work in the Division of Cellular and Molecular Cardiology, Sree Chitra Tirunal Institute for Medical Sciences and Technology, Thiruvananthapuram, India. I thank Professor K Mohandas, Director, for extending support and excellent facilities required for research programs in this institute. I also thank Dr AV George, the Registrar, for his help in coordinating the PhD program.

I express my heartfelt gratitude to my guide and supervisor, Dr. K Shivakumar, Scientist F, for his scholarly guidance, encouragement, advice, support and constructive suggestions over the years that have been of immense help in building my confidence throughout my research program, which has helped me greatly in the successful completion of my doctoral work. I will always treasure the excellent training in research that I have received from him and am also indebted for critically going through the manuscript and enabling me to present the same.

I express my sincere thanks to Dr. CC Kartha, Head of the Division of Cellular and Molecular Cardiology, and Dr. Renuka Nair, Division of Cellular and Molecular Cardiology, for their encouragement and advice. My thanks are also due to Dr. G Srinivas and Dr. Lissy K Krishnan, the members of my Doctoral Advisory Committee for their help and co-operation.

I feel privileged to place on record my sincere gratitude to Dr. Edward G Lakatta and Dr. Li Lin of the Laboratory of Cardiovascular Sciences, NIA-NIH, Baltimore, Maryland, USA, for supporting my visit to USA and providing facilities to perform a part of my work at the LCS.

I am glad to have been associated with this institute and I appreciate the goodwill extended to me by my colleagues. Above all, I am extremely fortunate to have a loving family and friends whose support and encouragement has been instrumental in my progress towards completion.

Sangeetha Mohan

LIST OF FIGURES

ABBREVIATIONS

AIF	Apoptosis-inducing factor
AEC	3-amino 9-ethyl-carbazole
AMPA	a-amino 3-hydroxy-5-methyl-4-isoxazolepropionic acid
Ang II	Angiotensin II
ANT	Adenine nucleotide translocase
Apaf-1	Apoptotic protease activating factor-1
APS	Ammonium persulphate
ARC	Apoptosis repressor with caspase recruitment domain
Bad	B-cell antagonist of cell death
Bak	Bcl-2-antagonist killer
Bax	Bcl-2-associated X protein
Bcl-2	B-cell leukemia/lymphoma-2
Bcl-xL	B-cell leukemia/lymphoma-X-linked
BH3	Bcl-2 homology domain 3
Bid	BH3-interacting domain death antagonist
Bim	Bcl-2 interacting mediator of cell death
Bmf	Bcl-2 modifying factor
BNip	Bcl-2 nineteen kDa-interacting protein
bp	Base pair

BSA	Bovine serum albumin
CF-H	Hypoxic cardiac fibroblasts
CF-N	Normoxic cardiac fibroblasts
CHO	Chinese Hamster Ovary
cIAP1	Cytosolic IAP1
cIAP2	Cytosolic IAP2
DEPC	Diethyl pyrocarbonate
DIABLO	Direct IAP-binding protein with low pI
DISC	Death-inducing signaling complex
DMSO	Dimethyl sulfoxide
DNase	Deoxyribonuclease
ECL	Enhanced chemiluminescence
ECM	Extracellular matrix
ECs	Endothelial cells
EDTA	Ethylene diamine tetraacetic acid
EGFP	Eukaryotic green fluorescing pigment
EMSA	Electroprotic mobility shift assay
ET-1	Endothelin-1
FBS	Fetal bovine serum
FLIP	Flice-linked inhibitor protein
H	Hypoxia

H-Bay	Hypoxic Bay 11-7085-treated cells
H-EGFP	Hypoxic EGFP-transfected cells
HEPES	N-[2-hydroxyethyl] piperazine-n'-[2-ethanesulfonic acid]
HFCM	Hypoxic fibroblast-conditioned medium
HIF	Hypoxia-inducible factor
H-IκB-sr	Hypoxic inhibitor kappa B-super repressor
Hm	Mutant NF-κB oligo-treated hypoxic cells
HRP	Horse radish peroxidase
Hsp	Heat shock protein
Hw	Wild-type NF-κB oligo-treated hypoxic cells
IAPs	Inhibitor of apoptosis proteins
IKK	Inhibitor kappa B kinase
IL	Interleukin
IκBs	Inhibitor of kappa B
IκB-sr	Inhibitor kappa B-super repressor
M199	Medium 199
MAPK	Mitogen-activated protein kinase
MOPS	(3-[N-morpholino] propane sulfonic acid)
MPT	Mitochondrial permeability transition
N	Normoxia

N-Bay	Normoxic Bay 11-7085-treated cells
N-EGFP	Normoxic-EGFP transfected cells
NES	Nuclear export signal
NFCM	Normoxic fibroblast-conditioned medium
NF-κB	Nuclear factor-kappa B
N-IκB-sr	Normoxic inhibitor kappa B-super repressor
NLS	Nuclear localization signals
NO	Nitric oxide
PBS	Phosphate buffered saline
PF-H	Hypoxic pulmonary fibroblasts
PF-N	Normoxic pulmonary fibroblasts
PI	Propidium iodide
PKB	Protein kinase B
PKC	Protein kinase C
Puma	p53 upregulated modulator of apoptosis
RNase	Ribonuclease
ROS	Reactive oxygen species
SAPK	Stress-activated protein kinase
SDS	Sodium dodecyl sulfate
siRNA	Small interfering RNA

Smac	Second mitochondria-derived activator of caspase
TEMED	N, N, N', N' - tetramethylethylenediamine
TGF-β	Transforming growth factor-β
TNF-α	Tumore Necrosis factor-α
TRADD	TNF-a receptor-associated death domain
β-TRCP	β-transducin repeat-containing protein
VDAC	Voltage-dependent annion channel
VSMCs	Vascular smooth muscle cells
xIAP	X-linked IAP

SYNOPSIS

The myocardium consists of two interdependent compartments: the parenchyma, composed of highly differentiated cardiac myocytes, and the stroma, comprising less differentiated pluripotent cells embedded in an ECM. Cardiac myocytes are terminally differentiated cells that are responsible for the contractile function of the heart. Cardiac fibroblasts, on the other hand, are pluripotent, undifferentiated cells that are a major source of fibrillar collagens type I and III, matrix metalloproteinases, tissue inhibitors of matrix metalloproteinases and several growth factors and cytokines with significant autocrine and paracrine effects upon resident cardiac cells. Cardiac fibroblasts play a central role in maintaining ECM homeostasis in the normal myocardium. Whereas myocytes respond to pathophysiological stimuli by hypertrophic growth, fibroblasts increase in number (hyperplasia) and synthesize ECM proteins, leading to structural and functional remodeling of the interstitium. However, maintenance of the quantitative relationship between the parenchymal and stromal compartments is critical for sustaining normal cardiac function.

Generally, during myocardial injury, when cardiac myocytes die in response to a myriad of stimuli including hypoxia, cardiac fibroblasts survive, re-enter the cell cycle, undergo phenotypic transformation into myofibroblasts, infiltrate into the site of injury, proliferate and take part in the wound healing response. Unlike wound healing response in other tissues, failure of myofibroblast apoptosis in the heart results in their persistence in the mature scar for prolonged periods of time. Over-expression of the fibroproliferative

response and associated matrix deposition result in fibrosis, progressive ventricular dysfunction and eventually heart failure. The ability to proliferate throughout adult life and relative resistance to injury are inherent attributes of cardiac fibroblasts that underlie their ability to influence myocardial remodeling *post-injury*.

A major factor influencing the extent of cell injury and response in acute and chronic myocardial ischemia and infarction is hypoxia. Unlike cardiac myocytes, cardiac fibroblasts are resistant to hypoxia. However, in spite of the ability of cardiac fibroblasts to survive hypoxia and other pathogenic stimuli prevailing in the injured myocardium, the survival mechanisms built into these cells have not been investigated, barring a single study that stresses the pro-survival role of constitutively expressed Bcl-2 under conditions of ambient stress.

Survival of cells under conditions of stress can either be by the suppression of the apoptotic pathways or by the recruitment of anti-apoptotic factors. The existence of a fine balance between these interdependent pathways ensures cellular homeostasis.

Two important families of anti-apoptotic proteins widely studied include the Bcl-2 family of anti-apoptotic proteins that protect against the mitochondria-dependent death pathway and the IAPs that inhibit both mitochondria-dependent and -independent caspase

activation. Bcl-2 sequesters pro-apoptotic Bid, Bax and Bak from forming pores in the outer mitochondrial membrane and prevents release of pro-apoptotic Smac/DIABLO/AIF/cytochrome C into the cytoplasm. IAPs, on the other hand, are dynamic regulators of apoptosis that directly bind and inhibit active executioner caspase-3, -7 and -9 to promote cell survival. NF-κB is a well-known stress-activated transcription factor that is reported to transcriptionally regulate the expression of these anti-apoptotic proteins.

NF-κB regulates a large number of genes involved in the synthesis of cytokines and chemokines involved in immune response, in embryo and cell lineage development, cell apoptosis, cell cycle progression, inflammation, ontogenesis and cell survival. NF-κB proteins that are basically sequestered in the cytoplasm by IκBs, the degradation of which allows active NF-κB to translocate into the nucleus, bind to its cognate DNA-binding site and regulate the transcription of genes. Post-translational modification regulates both the DNA binding and oligomerization properties of NF-κB. NF-κB is activated in the heart in response to various stimuli, including hypoxia, ROS and inflammatory cytokines during heart failure.

Against this backdrop, the broad objective of this study was to delineate the survival mechanisms recruited in adult rat cardiac fibroblasts in response to hypoxia.

Specific questions addressed:

- Are cardiac fibroblasts relatively resistant to hypoxia?
- Does hypoxia activate NF-κB in cardiac fibroblasts?
- Does NF-κB play a pro-survival role in cardiac fibroblasts under hypoxia?
- If so, does the transcription factor, NF-κB, regulate the expression of anti-apoptotic proteins, Bcl-2 and cIAP2, in hypoxic cardiac fibroblasts?

Approach

Adult rat cardiac fibroblasts were isolated by enzymatic digestion, cultured in M199 with 10% FBS, characterized by morphological and immunocytochemical methods and were exposed to hypoxia generated *in vitro* by commercially available hypoxia systems from Becton-Dickinson, USA. Pulmonary fibroblasts and cardiac myocytes from adult rats were used as "controls" to ascertain features of apoptosis resistance that are unique to fibroblasts of cardiac origin. Hoechst 33324 and Annexin V-FITC staining kit were used to detect loss of cell viability. DNA-binding activity of NF-κB in cardiac fibroblasts was determined by EMSA. The role of NF-κB in cardiac fibroblast survival was studied by its gene-based inhibition and was further confirmed using a pharmacological inhibitor (Bay 11-7085). Expression profile of anti-apoptotic Bcl-2 and cIAP2 was examined by western blot analysis.

Major findings

1. Cardiac fibroblasts, in contrast to cardiac myocytes and fibroblasts of non-cardiac origin (pulmonary), are resistant to hypoxic injury.

2. DNA-binding activity of NF-κB was detected in hypoxic cardiac fibroblasts.

3. NF-κB inhibition by genetic and pharmacological means renders cardiac fibroblasts susceptible to hypoxia, emphasizing the involvement of NF-κB in cardiac fibroblast survival under hypoxic conditions.

4. Cardiac fibroblasts express constitutive levels of Bcl-2 under hypoxic and normoxic conditions.

5. Hypoxia induces cIAP2 in cardiac fibroblasts.

6. Pulmonary fibroblasts do not express cIAP2 and Bcl-2, consistent with their susceptibility to hypoxia.

7. NF-κB inhibition did not affect Bcl-2 expression in hypoxic cardiac fibroblasts.

8. NF-κB inhibition attenuated cIAP2 expression in hypoxic cardiac fibroblasts, suggesting that NF-κB selectively regulates the expression of cIAP2 but not Bcl-2 in hypoxic cardiac fibroblasts.

Conclusions

The findings raise the possibility that constitutively expressed Bcl-2 and hypoxic-induction of cIAP2 may protect cardiac fibroblasts against hypoxic injury. Importantly, this study shows that NF-κB may play a pro-survival role in cardiac fibroblasts under hypoxic conditions and that regulation of cIAP2 expression by NF-κB may, at least in part, mediate the pro-survival role of NF-κB during hypoxia. In that sense, the findings significantly enlarge the earlier report that links survival of cardiac fibroblasts under conditions of ambient stress exclusively to basal levels of Bcl-2.

This is only the second study on survival mechanisms in cardiac fibroblasts and the first to demonstrate a pro-survival role for NF-κB in hypoxic cardiac fibroblasts.

Publication

Shivakumar K, Sollott SJ, **Sangeetha M**, Sapna S, Ziman B, Wang S, Lakatta EG. Paracrine effects of hypoxic fibroblast-derived factors on the MPT-ROS threshold and viability of adult rat cardiac myocytes. *Am J Physiol Heart Circ Physiol* 2008; 294: H2653-8.

I. INTRODUCTION

The myocardium consists of myocytes, non-myocytes and the ECM. Myocytes represent a third of the cell population in the heart whereas non-myocytes account for about two-thirds of myocardial cells of which over 90% are fibroblasts and the rest is made up of ECs and VSMCs [154]. Cardiac myocytes are terminally differentiated cells that are responsible for the contractile function of the heart. Cardiac fibroblasts, on the other hand, are pluripotent, undifferentiated cells that are a major source of fibrillar collagens (type I and III), matrix metalloproteinases, tissue inhibitors of matrix metalloproteinases and several growth factors and cytokines with significant autocrine and paracrine effects upon resident cardiac cells [87, 154, 158]. Cardiac fibroblasts play a central role in maintaining ECM homeostasis in the normal myocardium [90] and, over the years, it has become increasingly evident that they are an important determinant of the structural and functional remodeling of the myocardium in several pathological states [18].

I.1. Identification of the problem

I.1.1. Cardiac fibroblasts are relatively resistant to injury

In contrast to cardiac myocytes that lose their replicative capacity soon after birth and are susceptible to a variety of pro-apoptotic factors prevailing in the injured myocardium, cardiac fibroblasts retain their proliferative potential throughout adult life and are found to be relatively resistant to injury in response to several insults. These inherent attributes of cardiac fibroblasts underlie their ability to influence myocardial remodeling *post-injury*.

Generally, when cardiac myocytes die in response to stimuli such as hypoxia, ischemia-reperfusion, acidosis, oxidative stress, nutrient deprivation and cytokines [31], cardiac fibroblasts survive, re-enter the cell cycle, undergo phenotypic transformation into myofibroblasts, infiltrate into the site of injury, proliferate and take part in the wound healing response. Culmination of the wound healing response in tissues of non-cardiac origin is associated with the progression of the granulomatous tissue into a mature scar following myofibroblast apoptosis. In the heart, however, myofibroblasts are reported to persist in the mature scar for prolonged periods of time [140]. Failure of myofibroblast apoptosis may potentially result in over-expression of the fibroproliferative response and associated matrix deposition, resulting in fibrosis, progressive ventricular dysfunction and eventually heart failure [18]. Consistent with the reported persistence of myofibroblasts in the mature infarct scar following failure of mechanisms of elimination, several studies *in vitro* have reported that these cells are resistant to diverse insults such as hypoxia [88], growth factor deprivation and staurosporine [98].

I.1.2. Hypoxia in the heart

A major factor influencing the extent of cell injury and response in acute and chronic myocardial ischemia and infarction is hypoxia. Hypoxia is a condition in which diffusive oxygen transport fails to meet the metabolic demands of the tissue. Apart from its occurrence at high altitudes, hypoxia is associated with a variety of pathophysiological states, including pulmonary diseases, excessive exercise, myocardial ischemia and

infarction. Persistence of hypoxia may have severe pathological consequences, at the cellular and molecular levels [45, 57, 68, 101, 127, 161, 163].

Several investigators have demonstrated the susceptibility of cardiac myocytes to hypoxia *in vitro* [26a, 143]. Further, cardiac myocyte death occurs during myocardial infarction [13, 126], especially following reperfusion [50, 60], heart failure [108, 162], various cardiomyopathies [93], myocarditis [125] and transplant rejection [107], where hypoxia is a major component. On the contrary, cardiac fibroblasts are resistant to hypoxia. Surprisingly, however, in spite of the ability of cardiac fibroblasts to survive hypoxia and other pathogenic stimuli prevailing in the injured myocardium, the survival mechanisms built into these cells have not been investigated, barring a single study that stresses the overriding pro-survival role of constitutively expressed Bcl-2 under conditions of ambient stress [98].

I.1.3. Cell survival versus cell death

Survival of cells under conditions of stress can be either by the suppression of apoptotic pathways or by the recruitment of anti-apoptotic factors. The existence of a fine balance between these interdependent pathways ensures cellular homeostasis.

I.1.3.1. Apoptotic pathways

Apoptosis (programmed cell death) is essential for life, especially during embryonic development, maintenance of tissue homeostasis, remodeling, surveillance

and host defense in the postnatal tissue [31]. Excessive apoptosis is associated with stroke, myocardial infarction, heart failure and degenerative diseases, while too little causes neoplasia. Apoptosis within cells is mediated through two evolutionarily conserved, convergent caspase-dependent pathways: a) **Extrinsic pathway,** which utilizes cell surface death receptors, and b) **Intrinsic pathway,** involving the mitochondria and the endoplasmic reticulum [51]. The extrinsic pathway is initiated by the binding of death signals (like TNF-α) to their specific cognate cell surface receptors, which activate caspase-8 that subsequently activates executioner caspases-3. On the other hand, in the intrinsic pathway, death signals are funneled towards the mitochondria by pro-apoptotic Bid, Bax or Bak activated by diverse mechanisms that culminate in loss of mitochondrial membrane potential and destabilization of the outer mitochondrial membrane [31], leading to the release of mitochondrial apoptogens, such as cytochrome C, Smac, DIABLO and AIF, into the cytoplasm. Once in the cytoplasm, cytochrome C binds Apaf-1 along with ATP and pro-caspase-9 to form a multiprotein complex called the apoptosome. Within the apoptosome, pro-caspase-9 is activated by dimerization after which it cleaves and activates downstream pro-caspase, leading to cell death [31, 51]. However, irrespective of the pathways triggered, the aim of the process is to activate executioner caspases that directly mediate apoptotic cell death [31].

I.1.3.2. Survival pathways

The expression of anti-apoptotic proteins is tightly regulated, as it is the relative balance between the anti- and pro-apoptotic factors that determines whether a cell

survives or dies under given conditions. The Bcl-2 family of anti-apoptotic proteins protects against the mitochondria-dependent death pathway and the IAPs inhibit both mitochondria-dependent and -independent caspase activation [123]. Bcl-2/Bcl-xL sequesters pro-apoptotic Bid from activating Bax/Bak and blocks them from forming pores in the outer mitochondrial membrane and prevents release of pro-apoptotic Smac/DIABLO/AIF/cytochrome C into the cytoplasm [31]. IAPs, on the other hand, are dynamic regulators of apoptosis that directly inhibit active caspases (caspases-3, -7 and -9) to promote cell survival [123]. NF-κB is a well-known stress-activated transcription factor that is reported to transcriptionally regulate the expression of these anti-apoptotic proteins [49a, 78, 123].

NF-κB regulates a large number of genes involved in the synthesis of cytokines and chemokines involved in immune response, in embryo and cell lineage development, cell apoptosis, cell cycle progression, inflammation, ontogenesis and cell survival [24, 84]. The NF-κB family comprises five major members: RelA (p65), NF-κB1 (p50/p105), NF-κB2 (p52/p100), c-Rel and RelB. Each member of the NF-κB family, except RelB, can form homodimers as well as heterodimers with one another. NF-κB dimers bind to a cognate 10 bp DNA binding site on the DNA called the kappa B site (κB site) and directly regulate gene transcription [83]. NF-κB proteins are basically sequestered in the cytoplasm by IκBs. The degradation of IκB allows active NF-κB to translocate to the nucleus, bind to its cognate DNA-binding site and regulate the transcription of genes. On

activation by a variety of inducers, IκB becomes phosphorylated, ubiquitylated and degraded by proteasomes. Post-translational modification regulates both DNA binding and oligomerization properties of NF-κB. NF-κB is activated in the heart in response to various stimuli including hypoxia, ROS and inflammatory cytokines during heart failure [52].

I.2. Broad objective of the study

Against this backdrop, the major goal of this study was to delineate the survival mechanisms recruited in adult rat cardiac fibroblasts in response to hypoxia, focusing on a possible protective role for NF-κB.

The following specific questions were addressed:

- Are cardiac fibroblasts relatively resistant to hypoxia?
- Does hypoxia activate NF-κB in cardiac fibroblasts?
- Does NF-κB play a pro-survival role in cardiac fibroblasts under hypoxia?
- If so, does the transcription factor regulate the expression of pro-survival Bcl-2 and cIAP2 in hypoxic cardiac fibroblasts?

I.3. Major findings

a. In contrast to cardiomyocytes and fibroblasts of non-cardiac origin (pulmonary fibroblasts), cardiac fibroblasts are resistant to hypoxic injury

b. DNA-binding activity of NF-κB was detected in hypoxic cardiac fibroblasts by EMSA

c. NF-κB inhibition by genetic and pharmacological means renders cardiac fibroblasts susceptible to hypoxia

d. Cardiac fibroblasts express constitutive levels of Bcl-2 under hypoxic and normoxic conditions; in contrast, pulmonary fibroblasts do not express Bcl-2

e. Bcl-2 expression in cardiac fibroblasts is not under NF-κB control

f. Hypoxia induces cIAP2 in cardiac fibroblasts; in contrast, pulmonary fibroblasts do not express cIAP2

g. NF-κB selectively regulates the expression of cIAP2 in hypoxic cardiac fibroblasts

I.4. Conclusion

This study demonstrates for the first time that NF-κB may play a pro-survival role in hypoxic cardiac fibroblasts. Further, regulation of cIAP2 expression by NF-κB may, at least in part, mediate the protective role of NF-κB in these cells under hypoxia.

II. REVIEW OF LITERATURE

The myocardium consists of two interdependent compartments: the parenchyma, composed of highly differentiated cardiac myocytes, and the stroma comprising less differentiated pluripotent cells embedded in an ECM.

Cardiac myocytes account for one-third of the cardiac cell population in the heart and are responsible for the phasic contractile activity of the heart. They are terminally differentiated cells that lose their ability to divide soon after birth and further growth of the myocyte compartment occurs through enlargement or hypertrophy of individual cells. Myocyte hypertrophy can be physiological, resulting from normal growth and exercise, or pathological, associated with chronic hypertension, valvular disease and ischemia/infarction [15, 158].

The stromal compartment includes non-myocytes embedded in the cardiac interstitium that is composed of a structural protein network formed largely of fibrillar collagens. The non-myocytes account for two-thirds of the cell population of the heart. They include fibroblasts, ECs and VSMCs [154]. More than 90% of the non-myocyte population is formed of cardiac fibroblasts, which, unlike other non-myocytes, are free to move within the ECM [4a, 155].

While myocytes respond to pathophysiological stimuli by hypertrophic growth, fibroblasts increase in number (hyperplasia) and synthesize more ECM proteins, leading to structural remodeling of the interstitium [27]. The quantitative relationship between the

parenchymal and stromal compartments is critical for sustaining normal cardiac function [18].

II.1. Cardiac Fibroblasts

Cardiac fibroblasts play an essential role in myocardial function and pathophysiology, contributing to cardiac growth, development and maintenance of myocardial structure and electro-mechanical function in the healthy and diseased myocardium [20, 115a].

II.1.1. Cardiac fibroblasts in the normal myocardium

Cardiac fibroblasts are recognized as a major cell type responsible for the maintenance of ECM homeostasis within the normal myocardium. ECM is a highly differentiated, dynamic structure consisting primarily of fibrous collagens, type I (80%) and type III (10%), with smaller amounts of collagens, type IV, V, VI, elastin and laminin [18]. Type I collagen is present in the form of thick fibers having a tensile strength of steel, while type III collagen forms a reticular network within the myocardium [159]. Cardiac fibroblasts are the only source of fibrillar collagens, type I and III. They are also a major source of matrix metalloproteinases and tissue inhibitor of matrix metalloproteinases, key enzymes involved in ECM turnover within the heart [158]. Recent findings suggest that these cells are an intra-cardiac source of growth factors and cytokines, including Ang II, TGF-β, IL-1β, IL-6, IL-8, ET-1, prostaglandins and NO [14, 90] that can affect cardiac cell functions by autocrine and paracrine mechanisms [87].

These cells also serve as intermediate sensors and amplifiers of stimuli originating from other cells of the myocardium, including myocytes and infiltrating immune cells [8, 18, 170].

II.1.2. Cardiac fibroblasts in wound healing

Cardiac fibroblasts are key participants in any wound healing response within the injured heart because, in contrast to cardiac myocytes, they retain the ability to proliferate throughout adult life [20] and are relatively resistant to many pathogenic factors prevailing in the injured myocardium [98]. The sequential steps involved in a regular wound healing include: hemostasis, infiltration of immune/inflammatory cells, degradation and phagocytosis of necrotic myocytes and cellular debris, repopulation of cardiac fibroblasts within the site of injury by chemotaxis and increased proliferation, reconstruction of a granulomatous scar and subsequent ECM remodeling to produce a mature scar [18]. Normally, in any wound healing response, culmination of the process is associated with myofibroblast apoptosis leading to the progression of granulomatous tissue to a mature scar. But, in the heart, myofibroblasts are reported to persist in the mature scar for prolonged periods of time [140]. Failure of myofibroblast apoptosis may potentially result in over-expression of the fibroproliferative response and associated matrix deposition, leading to fibrosis, progressive ventricular dysfunction and eventually heart failure [18, 19a].

II.1.3. Cardiac fibroblasts in disease

In many pathological states of the heart such as myocardial ischemia and infarction, cardiac hypertrophy and heart failure, a disproportionate accumulation of ECM proteins, especially fibrillar collagens, lead to compromised cardiac function [28, 29, 159]. Generally, myocyte loss triggers a cascade of processes that includes enhanced degradation of the collagen matrix facilitating slippage and removal of dead myocytes followed by excessive cardiac fibroblast proliferation, leading to increased ECM deposition or fibrosis (reparative/replacement fibrosis) at the site of injury [23]. Further, hemodynamic changes within the myocardium, as in hypertensive cardiomyopathy, lead to enhanced synthesis and disproportionate accumulation of fibrillar collagen even in the absence of myocyte loss, a process referred to as 'reactive fibrosis' [7, 156]. Such alterations in the quantity and composition of the interstitial protein scaffold due to fibrosis are primarily physiological and adaptive, aimed at restoring normal myocardial function, but may eventually lead to distorted tissue structure, abnormal myocardial stiffness and electrical discontinuity between surviving myocytes [30].

In all of these conditions, the relative resistance of cardiac fibroblasts to many insults on the one hand and the susceptibility of cardiac myocytes on the other contribute to significant perturbations in the quantitative relationship between the parenchyma and stroma, impacting pump function. This necessitates an examination of the broader issue of cell death and cell survival in higher eukaryotes.

II.2. Cell death

Regulation of cell number or maintenance of numerical equilibrium is crucial in all complex multicellular organisms, and the evolution of differentiated cells has selected mechanisms to modulate the balance between cell survival and cell death [32]. Thus, cell death is an integral part of any complex multicellular organism for disposal of unwanted cells during embryogenesis, cellular turnover during proliferation and various pathologies [65]. Physiologically, three modes of cell death are defined within eukaryotes: autophagy, necrosis and apoptosis [146].

II.2.1. Autophagy

Autophagy is a dynamic cellular adaptive death response, activated during nutritional deprivation within cells. It is a highly regulated process [73] and is involved in cytoplasmic house keeping mechanisms for the selective removal of non-functional organelles and cellular components by degradation. Parts of cytoplasm and intracellular organelles are sequestered within characteristic 'double' or 'multi' membrane-bound membrane vesicles and finally delivered to lysosomes for bulk degradation. It can remove organelles in a generalized fashion or in a specific manner. Cells begin to cannibalize some of their cellular cargo whose components are later re-used as energy source [62b, 62c, 73, 91].

II.2.2. Necrosis

Necrosis is a passive, unregulated and irreversible form of cell death, occurring mainly under pathological conditions. A rapid loss of ion-flux control leads to swelling and rupture of the cell [118]. Cellular necrosis involves: cell swelling, appearance of holes in the plasma membrane, loss of calcium homeostasis, loss of control over intracellular processes and spilling out of intracellular materials that culminates in inflammatory response. However, mechanisms mediating necrosis in mammals are poorly understood.

II.2.3. Apoptosis

Apoptosis is an evolutionarily conserved, autonomously controlled, genetically programmed mode of cell death, functioning systematically within all metazoans, for cellular suicide. It is essential for life, especially during embryonic development, maintenance of tissue homeostasis, remodeling, surveillance and host defense in the postnatal tissue [31]. As a safeguard against disease, every cell in our body expresses the components of the apoptotic pathways and is ready for self-destruction. In fact, it has recently become clear that cells must receive the proper set of signals to prevent apoptosis or they will self-destruct. Excessive apoptosis is associated with stroke, myocardial infarction, heart failure and degenerative diseases while too little causes neoplasia.

Morphologically, apoptosis is manifested as cell and nuclear shrinkage. Nuclear chromatin condenses, which later marginates against the nuclear membrane, nucleus progressively condenses and breaks up (karyorrhexis). Other organelles also start condensing. Cell membrane starts detaching from the surrounding tissue, outline becomes convoluted and forms extension (blebbing). Blebs separate out into membrane-bound apoptotic bodies, which are phagocytosed by macrophages and neighboring cells. Because cellular contents are not released, this occurs with little inflammation [65].

Biochemical changes during apoptosis can be categorized into: changes within the nucleus, changes within mitochondria, changes in the plasma membrane and changes associated with the shape and structure of the cell [65]. Nuclear changes include condensation of the nuclear chromatin, degradation of nuclear proteins and degradation of nuclear membranes by caspases that are packaged into dense membrane-bound smaller bodies that are finally degraded. The chromosomal DNA gets degraded by endogenous DNase to form ~200bp fragments that are visualized as laddering observed on agarose gel. Mitochondria remain intact structurally until late in the process of apoptosis. However, release of mitochondrial proteins causes change in the ionic and electrochemical gradient finally leading to organelle condensation during apoptosis. A major change to plasma membrane includes loss of microvilli and expression of 'eat me' signals like the externalization of phosphatidyl serine. Towards the later stages, cells shrink, get rounded up and sever contact with neighboring cells and are packaged into membrane apoptotic bodies and degraded by phagocytic cells [65].

II.2.3.1. Molecular basis of apoptosis

Apoptosis within cells is mainly mediated through two evolutionarily conserved, convergent caspase-dependent pathways: a) **Extrinsic pathway,** which utilizes cell surface death receptors, and b) **Intrinsic pathway,** involving mitochondria and endoplasmic reticulum [51]. Irrespective of the pathways triggered, the aim of the process is to activate downstream pro-apoptotic proteins.

II.2.3.1.1. Pro-apoptotic proteins

Caspases are a family of cysteine-rich proteases, cleaving substrates after the aspartic acid residues and directly mediating apoptotic cell death [31]. These proteases are synthesized as inactive zymogens (pro-caspases). Caspases can be sub-divided into upstream or apical caspases-2, -8, -9, -10 and -12 and downstream/effector or executioner caspases-3, -6 and -7. Caspases are activated in a hierarchical order. Initiator caspases cleave the effector caspases, which in turn degrade a number of intracellular protein substrates leading to apoptosis [114]. Upstream caspases are activated by dimerization. In contrast, downstream pro-caspases exist as inactive dimers and are activated by proteolytic cleavage by the upstream caspases. Once activated, the downstream caspases orchestrate the demise of the cell through the cleavage of specific cellular substrates, resulting in the characteristic biochemical and morphological changes associated with apoptosis [31, 118, 122].

Caspases are generally activated within cells by pro-apoptotic Bcl-2 family proteins, which include a) multi-domain, and b) BH3-only pro-apoptotic members. Bax and Bak are pro-apoptotic multi-domain proteins, funneling upstream apoptotic signals towards mitochondria, stimulating the release into the cytosol of cytochrome C and other apoptogens required for caspases activation. Conformational changes regulate the activation of these proteins leading to their insertion into the outer mitochondrial membrane. Cells lacking these proteins are resistant to the intrinsic pathway of activation. The BH3-only Bcl-2 proteins include: Bim, Bid, Bad, Bmf, Noxa, Puma and BNip3. These are specialized to transfer specific sub-set of pro-apoptotic stimuli directly or indirectly to Bak and Bax [31, 62a].

II.2.3.1.2. Caspase-dependent apoptotic pathways

II.2.3.1.2.1. The extrinsic pathway

The extrinsic pathway is initiated by the binding of pro-apoptotic extracellular death signals, like TNF-α, to their specific cognate cell surface receptors. Ligand binding initiates the formation of a multi-protein complex termed as DISC. This recruits adaptor proteins called death domain - TRADD, which in turn employ pro-caspase-8 (initiator caspases) into the DISC. Activation of pro-caspase-8 by dimerization subsequently cleaves and activates (auto-activation) pro-caspase-3 (executioner caspases), which ultimately leads to the death of the cells [31, 51].

II.2.3.1.2.2. The intrinsic pathway

In contrast to the extrinsic pathway that is mediated by specialized subset of death signals, the intrinsic pathway is activated by a wide variety of extracellular and intracellular stimuli including loss of survival/trophic factors, toxins, radiation, hypoxia, oxidative stress, ischemia-reperfusion and DNA damage [51]. Pro-apoptotic Bid, Bax and Bak are activated by these peripheral signals, which triggers mitochondria to release apoptogens such as cytochrome C, Smac, DIABLO and AIF, into the cytoplasm. This is accompanied by loss of mitochondrial membrane potential and destabilization of the outer mitochondrial membrane [31]. Once in the cytoplasm, cytochrome C binds Apaf-1 along with ATP. This stimulates Apaf-1 to homo-oligomerize and recruit pro-caspase-9 into the multi-protein complex called the apoptosome. Within the apoptosome, pro-caspase-9 is activated by dimerization after which it cleaves and activates downstream pro-caspases [31, 51].

Recently, the endoplasmic reticulum has also been recognized as an important organelle in the intrinsic pathway [31]. Here, the increase in cytoplasmic Ca^{2+} concentration following release from endoplasmic reticulum causes mitochondrial permeability transition pore opening which in turn releases apoptogens into the cytosol. Activation of caspase-12 is also known to be mediated by increased Ca^{2+}. This mechanism may provide a means by which the endoplasmic reticulum can carry out the distal stage in the intrinsic pathway, independent of mitochondria [51].

II.2.3.1.3. Caspase-independent apoptotic pathways

Apart from caspase-dependent mechanisms, certain caspase-independent apoptotic mechanisms also exist within cells, which include: **Granzymes,** released by T-cells and natural killer cells, freeing DNase that cleaves DNA, nuclear lamins and histones directly; **Calpains**, which are Ca^{2+} dependent cysteine proteases; **AIF** and **Endo G** are located within the inter-mitochondrial membrane, which are released in response to apoptotic stimulus. Once released into the cytosol, they directly/indirectly mediate DNA fragmentation leading to cell death. On the other hand, **microRNA**, which are single stranded RNAs of 20-25 nucleotides transcribed from DNA, directly bind to functional mRNAs and block translation of survival proteins, causing apoptosis [31].

II.3. Pro-survival pathways

The apoptotic pathways within cells are held in check until triggered (by extrinsic or intrinsic death stimuli) by a variety of endogenous inhibitors of cell death. These anti-apoptotic pathways interfere with vital steps of either the extrinsic or the intrinsic pathway of apoptosis activation. Two most widely studied classes of such anti-apoptotic proteins include: Bcl-2 family of anti-apoptotic proteins that protect against the mitochondrial route of apoptosis and IAPs that protect against both intra- and extra-mitochondrial route of caspase activation leading to cell death.

II.3.1. Bcl-2 family of anti-apoptotic proteins

Mitochondria are the main target for the Bcl-2 family of anti-apoptotic factors. Bcl-2 and Bcl-xL are the two well-studied anti-apoptotic members of the Bcl-2 family of proteins involved in programmed cell survival. They were the first regulators of apoptosis to be discovered. Bcl-2 is constitutively localized in the outer mitochondrial membrane facing the cytoplasm, while a significant pool of Bcl-xL is not membrane-bound. The ratio of anti-apoptotic Bcl-2 to pro-apoptotic Bax/Bak determines whether a cell lives or dies. Bcl-2/Bcl-xL sequesters pro-apoptotic Bid from activating Bax/Bak and blocks these pro-apoptotic members from forming pores in the outer mitochondrial membrane and prevents release of apoptotic Smac/DIABLO/AIF/cytochrome C into the cytoplasm [31, 112a]. Certain threshold of growth factors is reported to sustain up-regulation of Bcl-2/Bcl-xL expression within cells to prevent the early onset of death. Bcl-2/Bcl-xL is also reported to prevent cell death induced by hypoxia by decreasing the production and action of ROS within cells [132].

II.3.2. Inhibitors of apoptosis proteins

IAPs are dynamic regulators of apoptosis that directly inhibit active caspases (caspases-3, -7 and -9) to promote cell survival [123]. IAPs suppress both mitochondria-dependent and -independent caspase activation and apoptosis [123]. Structurally, two motifs were identified to be important in their function, a Zn-binding baculovirus IAP repeat (BIR) and a RING domain. BIR is responsible for the anti-apoptotic property of IAPs. It binds directly to the caspases suppressing their activation. RING-containing

proteins can catalyze self-degradation and select target proteins through ubiquitylation. Eight human IAPs have been identified thus far: cIAP1, cIAP2, xIAP, ILP-2, ML-IAP, NAIP, survivin and Apollon. Among them, only cIAP1 and cIAP2 are identified biochemically. The release of Smac/DIABLO from mitochondria is inhibited mainly by xIAP [98, 134]. Level of IAPs within the cell is controlled by IAPs themselves by their self-ubiquitilyation properties [168].

II.3.3. Bcl-2 and IAPs in cell cycle

In addition to their anti-apoptotic roles, Bcl-2/Bcl-xL and IAPs are also reported to have anti-proliferative action, thereby promoting cell survival. Bcl-2 prolongs the G_0 phase in cell cycle, thus delaying cell cycle progression by increasing the expression of a cell cycle inhibitor, p27 in lymphocytes [148]. However, it still remains largely unclear whether the dual function of Bcl-2/Bcl-xL in the cell cycle is just a secondary consequence of enhanced survival [69]. IAPs are also reported to induce cell cycle arrest, which in turn suppresses cell death by mechanisms independent of caspase inhibition [123]. It has been reported that G_2/M phase-specific expression of cIAP2 contributes to survival of mitotically arrested cells [70].

II.3.4. Other anti-apoptotic proteins

Apart from these two important classes of anti-apoptotic proteins, there are also other pro-survival factors/pathways mediating cell survival. Some of the widely studied

members include: PI3K/Akt and PKB/Akt cellular survival signaling pathways, cFLIP, ARC and Hsps.

It has been reported that constitutive activation of Akt family of serine-threonine kinase signaling within cells is sufficient to block cell death induced by diverse factors [35, 147]. It is a critical regulator of PI3K-mediated cell survival. PI3K activity is found to be required for growth factor-dependent survival of a variety of cells [35]. Akt1 and 2 are abundant within the myocardium, and Akt2 is also known to regulate cardiac metabolism and cardiac myocyte survival [38]. Cell survival is also mediated by other signaling pathways, including the Ras/Raf/MAP kinase pathways [56].

ARC is a ~22kDa protein, highly expressed in heart and skeletal muscles, and is reported to protect the heart against ischemia-reperfusion injury by interfering with the activation of the mitochondrial apoptotic pathway. ARC over-expression inhibited oxidant stress-induced cell death in H9c2 cells where it abrogates Bax-induced release of cytochrome C from the mitochondria in a caspase-independent manner. It is also known to interact with caspases-2 and-8 to inhibit apoptosis [63].

Hsps are stress proteins known to accumulate within cells during stress and mediate cell survival. Hsp70, a chaperone protein, promotes cell survival by physically associating with the lysosomal membrane and resisting chemical and physical

destabilization, thereby inhibiting death-associated permeabilization of lysosomes. Depletion of Hsp70 within cells triggers tumor cell death [109].

cFLIP catalytically inactivates caspases-8/-10 homologues. In the absence of cFLIP, active caspase is released from DISC and mediates apoptosis if downstream signals are set on apoptosis execution. In contrast, if cFLIP is expressed in sufficient concentrations, it will efficiently inactivate procaspase-8 activation to mature enzyme and stay tethered to DISC [114].

Anti-apoptotic protein expression within cells is of great importance because it is the relative balance between the anti- and pro-apoptotic factors that determines whether a cell survives or dies under given conditions. There are certain proteins within cells that can modulate this delicate balance between the pro- and anti-apoptotic factors. NF-κB is a factor that can determine the life-death status of a cell.

II.4. Nuclear factor-kappa B

NF-κB represents a family of ubiquitously expressed [106], redox-sensitive transcription factors [139], conserved from Drosophila to humans. It plays an important role in regulating the transcription of a large number of genes important in the synthesis of antimicrobial peptides, cytokines, chemokines involved in immune response, embryo and cell lineage development, cell apoptosis, cell cycle progression, inflammation, oncogenesis and cell survival [24, 84]. NF-κB family has five major members: RelA

(p65), NF-κB1 (p50/p105), NF-κB2 (p52/p100), c-Rel and RelB. p50 and p52 are first synthesized as large precursors, p105 and p100, which are later processed by proteasomes [84]. The NF-κB family members share a highly conserved Rel homology domain responsible for DNA binding, dimerization, and interaction with IκB, the intracellular inhibitor of NF-κB. In addition, C-terminal regions of p65, RelB and c-Rel contain transactivation domain that is important for NF-κB-mediated gene transactivation [24]. Each member of the NF-κB family, except RelB, can form homodimers as well as heterodimers with one another. NF-κB dimers bind to a cognate 10bp DNA binding site called the κB site and directly regulate gene transcription [83]. NF-κB DNA binding shows great degeneracy, generally the sequence preferred is 5'-GGGRNNYYCC-3' (where R is a purine, Y is a pyrimidine and N indicates any base) [113]. The main activated form of NF-κB is a heterodimer of p65 associated with either a p50 or p52 subunit [83].

II.4.1. Activation of NF-κB

The activity of NF-κB is controlled by the shuttling of active NF-κB dimers from the cytoplasm to the nucleus in response to cell stimulation [84]. A wide range of signals like mitogens, cytokines, toxic metals, intracellular stress, viral or bacterial products, reactive oxygen intermediates, hypoxia, PKC, MAPKs and UV radiation [24, 82, 144] activate NF-κB.

NF-κB activation consists of two phases that occur in different cellular compartments. The **first phase** consists of early cytoplasmic events that lead to rapid translocation of NF-κB to the nucleus [25]. NF-κB proteins are basically sequestered in the cytoplasm by inhibitory proteins known as IκBs. These regulatory proteins are identified by the presence of ankyrin repeats of 33 amino acid motifs that mediate the protein-protein interaction. The degradation of IκB allows active NF-κB to translocate into the nucleus, bind to its cognate DNA binding site and regulate transcription of genes. On activation by a variety of inducers, IκB becomes phosphorylated, ubiquitylated and degraded by proteasomes. Phosphorylation of IκB at specific locations (Ser 32 and 36) is mediated by IKK complex. Phosphorylated IκB is then ubiquitylated at Lys 21 and 22 by β-TRCP, which are targeted for degradation by the 26S proteasome [84]. The most common IκBs include the IκBα, IκBβ and IκBε. IκBα displays nucleo-cytoplasmic-shuttling properties and probably translocates nuclear NF-κB complexes from the nucleus to the cytoplasm, thereby contributing to the termination of NF-κB transcription response [25]. Structural and biochemical studies indicate that there are NLS in an NF-κB dimer that are masked by IκBα. At the same time, the NES located at the amino terminus of the IκBα protein functions to expel the NF-κB-IκBα complex from the nucleus. It has been documented that IκBα regulates transient NF-κB activation and IκBβ maintains persistence of NF-κB activation within the nucleus [84].

Degradation of IkBα and nuclear translocation of NF-κB are not sufficient to promote maximal NF-κB transcription response. NF-κB dimers within the nucleus are further regulated through post-translational modification, particularly by site-specific phosphorylation, acetylation or methylation of NF-κB transcription factor complex or the histones that surround the various NF-κB target genes [25, 84]. This constitutes the **second phase** of post-translational modification, which determines the strength and duration of the NF-κB transcriptional response. Post-translational modification regulates both DNA binding and oligomerization properties of NF-κB. Key phosphorylation members include PKA, TNF-α, GSK3β, AKT/PI3K and NF-κB-activating kinases. Differences in the pattern of phosphorylation and acetylation recruit different transcription cofactors resulting in distinct profile of gene expression. In the absence of these post-translational modifications, NF-κB displays significantly impaired transcriptional activity [25].

II.4.2. Role of NF-κB in cell death

NF-κB plays a prominent role in maintaining the life-death balance within cells. It can be pro- or anti-apoptotic depending on the cell type, extent of NF-κB activation and nature of the apoptotic stimuli. The role of NF-κB in programmed cell death is therefore context-sensitive [24, 53, 78]. However, the mechanisms by which NF-κB induces apoptosis by targeting downstream target genes within cells still forms an important area of research.

Generally, cells defective in NF-κB signaling are found to be sensitive to pro-apoptotic signals compared to normal wild-type cells [150]. It has been noted that transgenic mice embryos incapable of NF-κB activation, due to the lack of RelA subunit, die of massive hepatic apoptosis [9, 78]. Inhibition of NF-κB is reported to trigger apoptotic cell death in B-cells of the immune system and in hepatocyte cell lines, in response to TNF-α stimulation [164]. Apoptosis induced by alpha-virus and kainic acid also requires NF-κB activation [53].

NF-κB is known to transcriptionally regulate about eight pro-apoptotic genes involved in apoptosis, including TNF-α, fas, fasL and c-myc [24, 78]. p53 and cMyc induction are also reported to occur in excitotoxin-induced, NF-κB-mediated, apoptosis in striatal neurons [117]. In addition, nuclear translocation of NF-κB by AMPA receptors leads to transcription of p53, leading to cell death in dopaminergic neurons [36]. It has also been reported that, doxycycline, an anticancer agent, generates superoxides within cells that subsequently stimulate NF-κB-dependent p53 up-regulation, leading to apoptosis [53]. On the other hand, once apoptosis is activated within the cells, NF-κB itself is reported to be a target for executioner caspases [84].

In spite of the well-documented role of NF-κB in cell death, it is better studied as a pro-survival than a pro-apoptotic transcription factor.

II.4.3. Role of NF-κB in cell survival

NF-κB is known to have a major role in cell survival. Recent reports suggest an anti-apoptotic role for NF-κB in different cell types [9, 24, 95a, 106]. The major mechanism by which NF-κB suppresses apoptosis is by the transcriptional regulation of a number of specific anti-apoptotic proteins including cIAP1, cIAP2, xIAP, Bcl-2, cFLIP, A20 zinc finger protein and manganese superoxide dimutase [84]. Among the NF-κB target genes, the IAPs have emerged as a critical cell survival signal, as they can directly bind and inhibit specific caspases [78]. IAPs contain NF-κB binding elements within their promoter region [85, 137]. NF-κB is also required for TNF-α–mediated induction of cIAP2, and over-expression of cIAP2 protein stimulates NF-κB-directed transcription and IκBα degradation, suggesting a positive feed back control on NF-κB via an IκB targeting mechanism [26]. Increased expression of cIAP2 mRNA correlates with survival in mitotically arrested cells [70].

NF-κB has been reported to prevent TNF-α-induced cell death in mouse embryonic fibroblasts and macrophages [9]. In response to TNF-α, hepatocyte cell line response switches from proliferation to apoptosis upon NF-κB inactivation [164]. NF-κB is reported to suppress mitochondrial events, upstream of Smac release [119]. ROS and MAPKs are reported to be the major mediators of NF-κB activation within cells [39, 136]. Cells over-expressing IκB are found to be sensitive to TNF-α-induced apoptosis, suggesting that NF-κB activation suppresses cell death in response to death stimulus

[150]. Also, constitutive expression of NF-κB was reported to confer apoptotic resistance in mature B-cells [6], thymocytes, monocytes, macrophages, neurons and VSMCs [77], Hodgkin's lymphoma cells [5] and in certain tumor cells [67].

The importance of NF-κB has been explored by inhibiting the biological activation of NF-κB. A mutant IκB-sr was constructed that contains a serine to alanine mutation at residues 32 and 36, which inhibits signal-induced phosphorylation and subsequent proteasome-mediated degradation of IκBα, thereby irreversibly sequestering/retaining NF-κB in the cytoplasm [153]. Cells in which NF-κB was bound by this super repressor were more readily susceptible to cell death than cells where NF-κB was functional [6]. It was observed that if NF-κB is inhibited in smooth muscle cells by chemical pyrrolidine dithiocarbamate or by transfecting with a virus that over-expresses IκBα, it dies [49].

II.4.4. NF-κB in the cardiovascular system

NF-κB is activated in the heart in response to various stimuli including ROS, hypoxia and inflammatory cytokines during heart failure [52], myocardial ischemia and reperfusion [80]. It is also reported to play a key role in the pathophysiology of reperfusion injury, ischemia preconditioning [22, 80, 97, 104, 166], atherosclerosis and unstable angina [149].

Within the heart, different cell types respond differently to NF-κB. Cardiomyocytes, VSMCs, and cardiac fibroblasts respond to pro-inflammatory cytokines by NF-κB activation [149]. NF-κB activation is reported to be essential for hypertrophic growth response in primary neonatal rat cardiomyocytes [116]. But in ECs, NF-κB activation causes permeability disturbances and disseminated coagulation leading to apoptosis [95, 149]. In human and rat VSMCs, increased NF-κB expression controls the induction of apoptosis [49]. NF-κB activation is also reported to be essential for Ang II-dependent proliferation and migration of VSMCs [169]. In cardiac fibroblasts isolated from adult male rat hearts, high basal level of NF-κB expression was observed [171] but its involvement in cardiac fibroblast survival remains unclear.

It has been reported that NF-κB-mediated activation of survival proteins like Bcl-2 and IAPs protects adult cardiac myocytes against ischemia-induced apoptosis in murine models of acute myocardial infarction [103]. NF-κB activation up-regulates mitochondrial anti-apoptotic Bcl-2 in cardiomyocytes, by down-regulating IκBα levels, thereby preventing cell death [96]. Moreover, adenoviral-mediated Bcl-2 delivery was found to increase NF-κB activity and prevent TNF-α-mediated apoptosis in ventricular myocytes [37]. Over-expression of Bcl-2 or Bcl-xL is reported to protect ECs from TNF-α–mediated apoptosis [4]. It has also been reported that heme oxygenase-1-derived carbon monoxide requires the activation of NF-κB to protect ECs from TNF-α-mediated

apoptosis [17, 137]. Hsps are reported to modulate DNA-binding activity of NF-κB, thereby reducing inflammation during reperfusion [149].

II.5. Oxygen and the life-death balance: Biological responses to hypoxia

Molecular oxygen is essential for the normal growth and development of most multicellular organisms. Maintenance of oxygen homeostasis is therefore essential for survival. Any decrease in oxygen availability below normal levels has profound physiological consequences [101]. Hypoxia is a state in which diffusive oxygen transport fails to meet the metabolic oxygen demand of the tissue. But mammalian cells have evolved intrinsic mechanisms for the maintenance of oxygen homeostasis at the tissue level, the failure of which can lead to cellular dysfunction and/or irreversible cell damage.

The cells within a tissue are exposed to different concentrations of oxygen depending on the specific localization of the cells and the functional status of the tissue. Atmospheric air contains about 21% oxygen. However, arterial pO_2 is only about 14%. Heart cells receive an oxygen supply of <10% under conditions of systemic normoxia [120]. During mild hypoxia, myocardial pO_2 drops to ~1% to 3% or lower [120].

Hypoxia is encountered in a variety of conditions – both physiological and pathological. The developing fetus may be exposed to hypoxic conditions *in utero* [81,

165]. Further, hypoxia is an extremely common physiological stress, found at high altitudes due to oxygen-thin atmosphere [115, 127]. Hypoxia also manifests under clinical conditions such as wound healing, anemia, myocardial infarction, ischemic heart disease, stroke, retinopathy, chronic obstructive pulmonary disease and cancer [111]. Hypoxic condition within the body activates complex adaptive physiological mechanisms within cells aimed at optimizing oxygen delivery to metabolizing tissues. However, persistence of hypoxia leads to severe pathological consequences both at the cellular and molecular levels [45, 57, 68, 101, 127, 161, 163].

II.5.1. Adaptive response to hypoxia

At the **tissue level**, hypoxia induces activation of oxygen sensors or chemo receptors of the pulmonary vasculature to initiate respiratory changes including increased alveolar ventilation. It also initiates cardiovascular system changes such as pulmonary vasoconstriction, reduced myocardial contractility, decreased maximum oxygen consumption, and switch from aerobic to anaerobic mode of metabolism [115]. Pulmonary vascular smooth muscles of the peripheral coronary and cerebral vessels also constrict/dilate to optimize blood flow to tissues under hypoxia [101]. Increased transport of iron to erythroid tissues, increased heme biosynthesis and erythropoeisis enhance the oxygen-carrying capacity of blood. Hypoxia also enhances angiogenesis, which decreases oxygen diffusion distance, and modulates local blood flow mediated by alterations in vascular tone [163]. Some of these changes may cause right ventricular hypertrophy and pulmonary hypertension that may result in congestive heart failure [115].

At the **cellular level,** hypoxia is known to cause injury and death [43]. Under hypoxia, some cells are irreversibly injured and die whereas others can adapt to the stress and survive. Hypoxia is also reported to modulate the expression of immuno-modulatory factors, cytokines and growth factors, and adhesion molecules, all of which may modify intercellular interactions in disease states by autocrine/paracrine mechanisms [2, 47, 142, 163].

The major metabolic changes associated with hypoxia include the switch from aerobic metabolism (oxidative phosphorylation) to anaerobic metabolism (glycolysis), increase in carbohydrate consumption to compensate for its inefficient utilization under hypoxic conditions, decreased energy usage by shutting down non-essential cell functions, and metabolic depression to a stable hypo-metabolic state consequent upon the coordinated regulation of energy supply and demand processes [68]. Hypoxia is known to reversibly inhibit or delay cell cycle progression within cells that contributes to reduced utilization of available residual energy [16, 45, 54, 59]. Bovine aortic and pulmonary artery ECs [145], mouse embryonic fibroblasts [54, 55, 59, 61] and splenic B-lymphocytes [59] and murine embryo fibroblasts exhibit reduced cell proliferation under hypoxia. However, in certain cell types, hypoxia causes hyperplasia as an adaptive strategy. Hypoxia induces human pulmonary fibroblast and pulmonary smooth muscle cell proliferation [33, 34].

At the **molecular level**, hypoxia is a powerful regulator of several genes modulating cell function. HIFs are known to play a central role in coordinating the cellular response to hypoxia [21, 62, 99, 102, 129, 163]. Apart from HIF proteins, a variety of other transcription factors and signaling molecules are involved in eliciting the hypoxia-induced changes. p53 and NF-κB are among the transcription factors activated by hypoxia [75, 100, 121, 129, 131]. Hypoxia activates NF-κB by tyrosine phosphorylation and by the inactivation and dissociation of IκB [75]. Hypoxic induction of these transcription factors is followed by their translocation to the nucleus where they modulate the expression of a wide array of genes encoding proteins with varied cellular functions [163]. Hypoxic conditions are associated with an increase in intracellular oxidant stress, which is postulated to result from increased ROS production within complex III of mitochondria [64]. Several signaling pathways, including p42/44 MAPK, SAPK or p38 MAPK and PI3K/Akt, mediate the effects of hypoxia through activation/inactivation of hypoxia-sensitive proteins culminating in a functional phenotype that is characteristic of the response to hypoxia [10, 11, 71, 105, 130, 131].

Hypoxia is a well-known cause of cell injury and death. Under hypoxia, cell death pathways are activated to remove irreversibly injured cells. HIF-1α production is observed in most cells, as an adaptive response, during hypoxia; it is reported to mediate hypoxic-cell death via p53 [129]. BNip3 and Noxa, pro-apoptotic Bcl-2 family members, are known to regulate apoptosis in H719 cell lines under the influence of HIF-1α during

hypoxia [72]. Hypoxia induces apoptosis in Jurkat cells via cytochrome C release and caspases-3 activation in the absence of glucose [92]. It is also reported to induce apoptosis caused by DNA cleavage and p53 activation in cultured neonatal rat myocytes [88].

An important response of rat kidney proximal tubule cells to hypoxia is the selective up-regulation of cIAP2 expression that confers resistance to apoptotic cell death. However, neither Bcl-2 nor cIAP1 was significantly induced during hypoxia in these cells [42, 44]. cIAP2 activation was independent of HIF-1α involement [42]. Hypoxic rat kidney proximal tubule cells over-expressing cIAP2 were found to be greatly resistant to staurosporine-induced apoptosis. On the contrary, immunodepletion of cIAP2 from the cytoplasm restored susceptibility of cells to staurosporine-induced apoptosis, showing the importance of IAP in protecting cells from apoptosis during hypoxia [42, 44, 89].

II.5.2. Hypoxia in the heart

The heart is an obligate aerobic organ consuming more oxygen than brain for activity. A constant supply of oxygen is therefore indispensable for cardiac viability and function [58]. However, the heart is exposed to hypoxia under several circumstances including pulmonary diseases, at high altitudes, excessive exercise and during cardiac

arrest. All these factors can lead to myocardial ischemia where hypoxia is a major component.

Significant loss of cardiomyocytes by apoptosis is a prominent and an important pathogenic feature during cardiac ischemia and infarction [160]. Cardiac myocytes are reported to exhibit compromised cell viability even in the presence of hypoxic fibroblast-derived factors [135]. ECs also undergo apoptosis in response to hypoxia [95], through NF-κB-mediated suppression of anti-apoptotic Bcl-2 [95]. In a rat model of chronic myocardial infarction, hypoxia has been shown to promote myocardial angiogenesis via an NF-κB-dependent mechanism, which would be an adaptive mechanism to augment oxygen supply [128].

II.5.3. Cardiac fibroblasts and hypoxia

The effects of hypoxia on cardiac fibroblasts remain largely unclear although these cells are exposed to oxygen deficit in several pathological states of the heart. Hypoxia is reported to enhance collagen type I synthesis but decrease total protein synthesis in cardiac fibroblasts [1]. Hypoxia has also been shown to enhance matrix metalloproteinases-2 synthesis in neonatal rat cardiac fibroblasts and augment the stimulatory effects of ET-1, Ang II and IL-1β on matrix metalloproteinases-2 synthesis [12]. Importantly, however, cardiac fibroblasts are known to be resistant to hypoxia-induced cell death [88, 98] but the underlying mechanisms have not been delineated.

II.6. Cell survival in cardiac fibroblasts

Cardiac fibroblasts have been shown to be resistant to programmed cell death under conditions of stress, unlike the other cell types in the heart. They are reported to be more resistant than fibroblasts of non-cardiac origin (dermal or pulmonary fibroblasts) to mitochondria-dependent cell death [98]. Maintenance of constitutive Bcl-2 expression in cardiac fibroblasts is demonstrated to be responsible for their relative resistance to apoptosis [98]. In contrast to skin and dermal fibroblasts, Bcl-2 is constitutively expressed in cardiac fibroblasts, which blocks mitochondrial cytochrome C release, thereby preventing mitochondria-dependent apoptosis. Even a well-known pro-apoptotic stimulus like staurosporine was not found to activate executioner caspase-3 significantly in cardiac fibroblasts [98]. Screening of the major pro- and anti-apoptotic factors, including Bid to Apaf-1, carried out with heart, lung and skin fibroblasts, showed that Bcl-2 is unique to cardiac fibroblasts. Further, silencing of Bcl-2 in cardiac fibroblasts by siRNA produced a meager 10% increase in cell death, demonstrated by Hoechst 33324 staining [98]. Thus, Bcl-2 was considered responsible for survival in cardiac fibroblasts.

Interestingly, Bcl-2 is reported to be down-regulated in most tissues after birth. In particular, Bcl-2 is reported to be expressed in skin fibroblasts only during their embryonic life and its level represses after birth [112]. In pulmonary fibroblasts, Bcl-2 is lost during lung maturation [19]. The disappearance of Bcl-2 in adult skin and lung fibroblasts may explain their susceptibility to stress. However, its persistence in adult cardiac fibroblasts was not looked into in this study [98]. Thus, there is a need to examine

the Bcl-2 profile in adult cardiac fibroblasts. Moreover, there may be other proteins whose expression is regulated depending on the duration, intensity and type of stress. In summary, the fact that multiple pathways functioning in tandem may enable a cell to survive under conditions of ambient stress prompted the investigations reported in this thesis.

III. MATERIALS AND METHODS

III.1. MATERIALS

III.1.1. Fine chemicals

M199, FBS, BSA, collagenase type I A, trypsin, pancreatin, deoxyribonuclease, HEPES, EDTA, DMSO, glucose, monoclonal anti-vimentin antibody, anti-human von Willebrand antibody, immunostaining kit for desmin, β-actin primary, anti-rabbit and anti-mouse secondary antibodies, TRI-reagent, DEPC, SDS, trisma base, agarose, glycine, sodium acetate, acrylamide, bis-acrylamide, mercaptoethanol, TEMED, APS, and Hoechst 33324 were purchased from Sigma-Aldrich, USA. DakoCytomation LSAB+ systems-HRP kit from Dako, N. America Inc. Fine chemicals for cDNA synthesis including RT buffer, RNase inhibitor, random primers, dNTPs and M-MLV RT, wild type/mutant NF-κB were from Promega Corporation, USA. The Dual Quantitative PCR kit for rat Bcl-2 was purchased from Maxim Biotech, Inc., USA. Annexin-PI apoptosis detection kit, cIAP2 and Bcl-2 primary antibodies were from Santa Cruz Biotechnology, USA. NF-κB subunit antibodies were from Santa Cruz Biotechnology and Cell Signaling Technologies, USA. Cell lysis buffer was obtained from Cell Signaling Technologies, USA. NucBuster nuclear protein extraction kit was from Novagen, USA. BCA protein assay kit and ECL kit were from Pierce, USA, and restriction enzymes from New England Bio Labs, USA. *E.coli* DH5-α, lipofectamine reagent and pre-set 6% non-denaturing gels from Invitrogen, USA. Maxi preps from Qiagen, USA. Non-fat dry milk, LB broth, and LB agar were from Hi Media, Mumbai. Nitrocellulose membrane was from Millipore, USA. Basic nucleofector kit was from Amaxa Biosystems, USA.

III.1.2. Routine chemicals

Calcium chloride, magnesium sulphate, potassium chloride, potassium di-hydrogen phosphate, sodium bicarbonate, sodium chloride, di-sodium hydrogen phosphate, sodium di-hydrogen phosphate, sodium hydroxide, concentrated hydrochloric acid, ethanol, chlorofrom, isopropanol, ether, phonol red and methanol were from Merck, Mumbai.

III.1.3. Cell culture ware

35mm, 100mm cell culture dishes and 15ml centrifuge tubes were purchased from BD Falcon, USA. Cell culture filter and Manifold filter wares from Millipore, USA. GasPak environmental systems and the anaerobic/aerobic envelopes to generate hypoxic/normoxic conditions were from Becton Dickinson, USA. Cell scrapers and 96 well culture plates were from Nunc, USA.

III.1.4. Equipments used

UV-visible spectrophotometer (Shimadzu, Japan); high speed refrigerated centrifuge (Hitachi, Japan); weighing balance (Sartorius, Germany); water bath (LKB, Sweden); ice-flaker (Hoshizaki, Japan); pH meter (Labindia, India); CO_2 incubator (Nuaire, USA); phase-contrast microscope (Nikon, Japan); confocal microscope (Carl Zeiss, Germany); laminar flow hood (CLAS, India); magnetic stirrer (Schott, Germany); EASY pure UV/UF compact reagent grade water system (Barnstead, USA); submerge-gel electrophoresis unit (Bangalore Genei, India); mini-blot electrophoresis unit (Biorad

laboratories, USA); transilluminator (Bangalore Genei, India); programmable thermal cycler (MJ Research Inc., USA); gel documentation unit (Syngene Bio Imaging, Canada); UV transilluminator, dry thermal block, gel dryer (BioRad, USA); kodak film cassette (Kodak, USA); vortexer and orbital shaker (Remi, India); ELISA reader (Bio-Tek Instruments, USA); table-top refrigerated high speed centrifuge (Eppendorf, USA); –80^0C deep freezer (Sanyo, USA); –20^0C deep freezer (Siemens, USA); scintillation counter (Wallac, USA); electroporator (Amaxa Biosystems, USA).

III.2. COMPOSITION OF MEDIA, REAGENTS AND BUFFERS

III.2.1. Acrylamide 30%

29% (w/v) acrylamide and 1% (w/v) N, N'-methylene bisacrylamide in deionized water.

III.2.2. Agarose Gel (1%) for electrophoresis of DNA or RNA samples

For DNA - 200mg agarose in 20ml of 0.5X TBE.

For RNA - 200mg agarose in 20ml of 1X MOPS buffer.

III.2.3. 10% Ammonium persulphate solution

Dissolve 0.2g (w/v) of APS in 2ml of deionized water. Aliquoted and stored at –20^0C.

III.2.4. Blocking solution

5% (w/v) skim milk in TBST containing 0.1% Tween-20.

III.2.5. Bis-Benzimide H 33324 (Hoechst 33324)

Dissolved 10mg Hoechst 33324 powder in 5ml sterile distilled water to get a final concentration of 10mM. A working concentration of 10μM was used for the experiments.

III.2.6. 5% Bovine serum albumin (BSA) solution

Antibodies used for western blotting were diluted in 5% BSA solution (500mg (w/v) BSA dissolved in 10ml TBST).

III.2.7. Bay 11-7085

10mg dissolved in 1ml DMSO to get a stock concentration of 40mM.

III.2.8. Cardiac fibroblast growth medium (pH 7.4)

M199 with Earle's salts containing benzyl penicillin (50U/ml) and gentamycin (0.04mg/ml) was used as growth medium for fibroblasts. 10% or 0.1% FBS was added as required.

III.2.9. 1X Cell Lysis buffer for westerns

20mM Tris-HCl (pH 7.5), 150mM NaCl, 1mM Na_2-EDTA, 1mM EGTA, 1% Triton, 2.5mM sodium pyrophosphate, 1mM β-glycerophosphate, 1mM Na_3VO_4, 1μg/ml leupeptin.

III.2.10. Di-ethyl pyrocarbonate (DEPC) water

1ml of DEPC in one liter of deionized water, stirred overnight at room temperature.

III.2.11. Dissociation medium for fibroblast isolation

The medium consisted of sodium chloride (116.4mM), HEPES (20mM), sodium di-hydrogen phosphate (1.15mM), glucose (5.55mM), potassium chloride (5.37mM), magnesium sulfate (0.81mM) and adjusted to pH 7.4. Deoxyribonuclease (5.5µg/ml), BSA (1mg/ml), $CaCl_2$ (1mM), and antibiotics (50U/ml penicillin and 0.04mg/ml gentamycin) were added to the medium under sterile conditions at the time of isolation. The dissociation medium for the first two digestions had collagenase type I A (1mg/ml) while that for subsequent digestions had trypsin 1:250 (0.75mg/ml) and pancreatin (0.025mg/ml).

III.2.12. DNA/RNA gel loading dye

Bromophenol blue (0.25%), xylene cyanol FF (0.25%), EDTA (1mM) and glycerol (50%) in deionized water.

III.2.13. Electrode buffer (pH 8.3) for SDS–PAGE (Running buffer)

Tris base (25mM), glycine (192mM), SDS (0.1%) in deionized water.

III.2.14. Ethidium bromide

1mg in 1ml deionized water (Stock). 5µl of this stock solution was added to 20ml of 1% agarose gel for DNA/RNA electrophoresis.

III.2.15. Ethylene diamine tetra acetic acid (EDTA) 0.5M (pH 8)

930mg EDTA in 5ml DEPC-treated deionized water.

III.2.16. HEPES buffer

NaCl (137mM), KCl (4.9mM), $MgCl_2$ (1.2mM), NaH_2PO_4 (1.2mM), glucose (15mM), HEPES (20mM), $NaHCO_3$ (5mM), CaCl (2mM). Add Mg^{2+} and Ca^{2+} last to avoid precipitation.

III.2.17. Lysis buffer

0.1M sodium hydroxide containing 0.1% SDS.

III.2.18. LB broth

1g NaCl, 0.5g yeast extract, 1g tryptone in 100ml water. Autoclaved before use.

III.2.19. LB agar

1g NaCl, 0.5g yeast extract, 1g tryptone, 2g bacteriological agar in 100ml water. Autoclaved before use.

III.2.20. MOPS electrophoresis buffer [10X]

MOPS (0.2M, pH 7.0), sodium acetate (3M, pH 5.0), EDTA (0.5M, pH 8.0) in DEPC-treated deionized water. 1X MOPS buffer was prepared from this stock solution by 1:10 dilution.

III.2.21. Phosphate-buffered saline (PBS) (pH 7.4)

Sodium chloride (137mM), potassium chloride (2.7mM), disodium hydrogen phosphate (10.14mM), potassium di-hydrogen phosphate (1.76mM).

III.2.22. Ponceau S stain (10X)

Ponceau S – 2g, trichloroacetic acid – 30g, sulfosalicylic acid – 30g were dissolved and made up to 100ml with water. A working solution was prepared by mixing 1 part of the 10X stock with 9 parts of water.

III.2.23. QIAGEN plasmid isolation kit constituents

a) BufferP1 (Resuspension buffer)

50mM Tris.Cl (pH-8), 10mM EDTA, 100μg/ml RNase A.

b) Buffer P2 (lysis buffer)

200mM NaOH, 1% SDS(w/v).

c) Buffer P3 (neutralization buffer)

3.0M potassium acetate (pH 5.5).

d) Buffer FWB2 (wash buffer)

1M potassium acetate (pH 5).

e) Buffer QBT (equilibration buffer)

750mM NaCl, 50mM MOPS (pH 7), 15% isopropanol (v/v), 0.15% Triton X-100.

f) Buffer QC (wash buffer)

1M NaCl, 50mM MOPS (pH 7), 15% isopropanol (v/v).

g) Buffer QF (elution buffer)

1.25M NaCl, 50mM Tris.Cl (pH 8.5), 15% isopropanol (v/v).

h) Buffer QN (elution buffer)

1.6M NaCl, 50mM MOPS, pH 7, 15% isopropanol (v/v).

III.2.24. a. Resolving Gel for SDS – PAGE (12%)

4ml 30% acrylamide, 2.5ml 1.5M Tris (pH 8.8), 0.1ml 10% SDS, 0.1ml 10% APS and 4µl TEMED were added to 3.3ml of deionized water.

b. Resolving Gel for SDS – PAGE (15%)

5ml 30% acrylamide, 2.5ml 1.5M Tris (pH 8.8), 0.1ml 10% SDS, 0.1ml 10% APS and 4µl TEMED were added to 2.3ml of deionized water.

III.2.25. Resolving gel buffer (pH 8.8)

18.165g Trizma base was dissolved in about 80ml deionized water. pH was adjusted using HCl and was made up to 100ml. Stored at room temperature.

III.2.26. 10% SDS

1g SDS was dissolved in 10ml water. Kept at 37^0C to ensure complete dissolution.

III.2.27. SDS gel-loading buffer [1X]

SDS (2% w/v), bromophenol blue (0.03%), β-mercaptoethanol (0.3%), glycerol (10% v/v) in Tris buffer (0.067M, pH 6.8).

III.2.28. Serum-free medium

M199 containing antibiotics (50U/ml penicillin and 0.04mg/ml gentamycin).

III.2.29. Sodium acetate (3M, pH 5-6)

1.23g sodium acetate in 5ml DEPC-treated deionized water.

III.2.30. Stacking gel for SDS – PAGE (5%)

0.83ml 30% acrylamide, 0.63ml 1M Tris (pH 6.8), 0.05ml 10% SDS, 0.05ml 10% APS and 5µl TEMED were added to 3.4ml of deionized water.

III.2.31. Stacking gel buffer (pH 6.8)

30ml from resolving buffer was measured, adjusted pH to 6.8 using HCl and was made up to 45ml. Stored at room temperature.

III.2.32. Towbin's buffer (Transfer buffer)

3.027g Tris base, 14.4g glycine, 200ml methanol made up to 1L with deionized water.

III.2.33. Tris borate EDTA buffer (TBE) 5X (pH 8.3)

54g Tris base, 27.5g boric acid, 20ml EDTA (0.5M, pH 8.0) made up to 1L with deionized water.

III.2.34. Tris-buffered saline (TBS) 10X (pH 7.6)

24.2g Tris base, 80g sodium chloride in 1L deionized water.

III.2.35. Tris-buffered saline with Tween-20 (TBST) 1X

1X TBS containing 0.1% Tween-20.

III.2.36. Tris EDTA buffer 1X (pH 8)

Tris.Cl 10mM and EDTA 1mM.

III.2.37. Trypsin/EDTA solution

0.25mg/ml trypsin and 0.2mg/ml EDTA in PBS (pH 7.4).

III.2.38. 2xYT medium

16g tryptone, 10g yeast extract and 5g NaCl in 1L water. pH adjusted to 7.0 using NaOH. Autoclaved before use.

III.3. Isolation, culture and characterization of adult rat cardiac fibroblasts

III.3.1. Isolation of cardiac fibroblasts

Cardiac fibroblasts were isolated from young adult male Sprague-Dawley rats (2-3 months, body weight about 200g) following the method of *Kumaran and Shivakumar, 2002* [76], with minor modifications. Following ether-anaesthetization, the heart was excised after thoracic incision under sterile conditions and collected into PBS (*Ref. III.2.21*) containing antibiotics (50U/ml penicillin, 0.04mg/ml gentamycin and 2.5µg/ml amphotericin). The atria were discarded and the ventricular tissue was separated, washed free of blood using PBS (*Ref. III.2.21*), minced into bits of approximately $1mm^3$ size and subjected to a series of 10 digestions in dissociation medium (*Ref. III.2.11*). Digestion was facilitated by gentle shaking of the flask containing the tissue bits on an orbital shaker maintained at 37^0C. Digests from the first two digestions, each of 15 minutes duration with collagenase type I A (1mg/ml), were discarded. The supernatants from subsequent 10-minute digestions in dissociation medium containing trypsin (0.75 mg/ml) and pancreatin (0.025mg/ml) were collected into centrifuge tubes containing M199 with 10% FBS and centrifuged at 1800 rpm for 5 minutes. Cell pellets from the digestions were pooled, re-suspended in M199 containing 10% FBS, seeded into two 35mm cell culture dishes and incubated in a humidified CO_2 incubator at 37^0C in an atmosphere of 95% air and 5% CO_2 for 150 minutes. At the end of this period, the supernatant containing unattached cells and debris was discarded, the dishes with the adherent fibroblasts were rinsed 3-4 times with M199 and supplied fresh M199 with 10% FBS. At

24 hours after isolation, the dishes were washed 3-4 times with growth medium (*Ref. III.2.8*) and incubated in fresh M199 with 10% FBS.

III.3.2. Sub-culture of cardiac fibroblasts

At confluence, the culture supernatant was removed, the cells were washed and trypsinized at 37^0C in trypsin-EDTA solution (*Ref. III.2.37*) for 1-2 minutes. Trypsinization was stopped by addition of M199 containing 10% FBS and the detached cells were pelleted immediately by centrifugation at 1800 rpm for 5 minutes. The cell pellet was suspended in M199 containing 10% FBS and seeded into fresh culture dishes at a split ratio of 1:3.

III.3.3. Characterization of cardiac fibroblasts in culture

Fibroblastic nature of the cells in culture was ascertained by morphology and immunocytochemistry.

III.3.3.1. Morphological analysis

Sub-confluent and confluent cultures were examined under inverted phase contrast microscope for morphological characteristics.

III.3.3.2.Immunocytochemical analysis for vimentin, desmin and vonWillebrand factor

Immunocytochemical staining was done as described by *Eghbali et al (1991)* [48]. Cells from passage 2 or 3 grown to 50-60% confluence were washed thrice with

PBS (*Ref. III.2.21*) and fixed in 70% ice-cold methanol in PBS (*Ref. III.2.21*) for 30 minutes. The fixed cells were washed thrice with PBS (*Ref. III.2.21*), treated with 3% hydrogen peroxide for 5 minutes to quench endogenous peroxidase, incubated for 10 minutes with 2% BSA in PBS (*Ref. III.2.21*). The cells were then treated with primary antibody diluted in PBS (*Ref. III.2.21*) containing 1% BSA for 60 minutes. Cells were washed thrice with PBS (*Ref. III.2.21*) to remove un-bound antibody and incubated for 30 minutes with diluted secondary antibody conjugated with HRP in PBS (*Ref. III.2.21*) containing 1% BSA. Following incubation, cells were washed thrice with PBS (*Ref. III.2.21*) to remove un-bound secondary antibody. The cells were then incubated for up to 10 minutes with HRP-specific substrate reagent containing AEC substrate and observed under a microscope. After colour development, the cells were counterstained with hematoxylin, washed with distilled water, mounted in glycerol and observed under a microscope. All incubations were at room temperature.

Monoclonal anti-vimentin primary antibody was diluted 1:50 in 1% BSA; anti-von Willebrand factor primary antibody was diluted 1:800 in 1% BSA. Dako Cytomation LSAB+ systems-HRP kit was used for processing. Immunostaining for desmin was done using a commercially available kit.

III.4. Isolation, culture and characterization of lung fibroblasts

Lung tissues were excised from young adult male Sprague-Dawley rats (2-3 months) after cervical dislocation. The isolation procedure was essentially the same as that for cardiac fibroblasts, except that 0.1mg/ml pancreatin was used in the digestion medium (*Ref. III.2.11*) as against 0.025mg/ml pancreatin used for cardiac fibroblast isolation. The fibroblastic nature of the isolated cells was ascertained as described for cardiac fibroblasts.

III.5. Isolation of cardiac myocytes

Cardiac myocytes were isolated from young adult rats (3-4 months) by standard enzymatic digestion technique [135]. The cells were maintained in HEPES-buffer (*Ref. III.2.16*) until use.

III.5.1. Preparation of conditioned medium

Confluent cultures of cardiac fibroblasts, made synchronous by serum deprivation for 24 hours, were exposed to hypoxia for 24 hours in serum-free M199 (*Ref. III.2.28*). Supernatants from hypoxic and normoxic cultures were collected under sterile conditions, centrifuged at 10,000rpm for 10 minutes to remove cellular debris and used directly for the experiments without storage.

III.6. Setting up the *in vitro* hypoxia model

III.6.1. In vitro hypoxia system

The GasPak disposable hydrogen + CO_2 generator envelopes containing sodium borohydride and sodium bicarbonate + citric acid tablets and palladium pellets were used to generate hypoxic conditions. Upon addition of deionized water, the sodium borohydride tablet generates hydrogen, which, in presence of palladium catalyst, reduces the chamber oxygen to water, resulting in a chamber pO_2 of about $\leq 0.1\%$, as indicated by anaerobic indicator strips. To generate normoxic conditions, GasPak disposable CO_2 generator envelopes containing sodium bicarbonate + citric acid tablet were used. The sodium bicarbonate + citric acid tablet in both normoxic and hypoxic systems release CO_2 upon addition of deionized water to provide a pCO_2 of about 5%. The desired chamber oxygen and CO_2 levels were achieved within 50 minutes.

III.7. Cell viability

III.7.1. Hoechst 33324 DNA staining

A stock solution of 10mM Hoechst 33324 (*Ref. III.2.5*) was prepared in deionized distilled water and a working concentration of 10μM was used for staining. 70-80% confluent cultures were incubated with the dye for 30 minutes at 37^0C in duplicate and visualized under UV light at ~350nm.

III.7.2. Annexin-PI staining

Cells seeded on sterile cover slips coated with 2% gelatin (~80% confluent) were incubated with Annexin V-FITC conjugate and propidium iodide at 37^0C for 20 min in a humid chamber, as per instructions provided in the kit. Immediately after the incubation, fluorescence was visualized under a fluorescence microscope.

III.8. Electrophoretic Mobility Shift Assay

DNA-binding ability of NF-κB in cardiac fibroblasts was assessed by EMSA.

III.8.1. Preparation of nuclear extract

Nuclear extracts were prepared using NucBuster Protein extraction kit (Novagen) following manufacturer's instructions. Confluent (80-90%) cardiac fibroblast cultures in M199 containing 0.1% FBS were subjected to hypoxic and/or normoxic treatments and were harvested by trypsinization as described earlier, washed in PBS (*Ref. III.2.21*), pelleted, and the standard packed cell volume was measured. The cell pellet was re-suspended in 75–150µl (depending on the pellet size) NucBuster extraction reagent-1 provided with the kit. The mixture was vortexed for 15 sec at high speed, incubated on ice for 5 minutes, vortexed again for 15 sec at high speed and centrifuged at 16,000g for 5 min at 4^0C. The supernatant (the cytoplasmic fraction) was removed and stored at – 80^0C until use. The pellet was re-suspended in 1µl of protease inhibitor cocktail (100X), 1µl of 100mM DTT and 25µl NucBuster reagent-2. The mixture was vortexed for 15 sec

at high speed, incubated on ice for 5 minutes, vortexed again for 15 sec at high speed and centrifuged at 16,000g for 5 minutes at 4^0C. The supernatant (nuclear fraction) was aliquoted and stored at -80^0C until use. Protein concentration of the nuclear extracts was determined by the BCA method.

III.8.2. Protein Quantification

Protein estimation was done using the BCA protein assay kit (Pierce) following the manufacturer's instructions. The protein samples were diluted 100 times for the assay. The water-soluble complex formed as a result of the reaction was quantified spectrophotometrically at 562nm. The kit was sensitive over a broad working range of 20-2,000μg/ml.

III.8.3. Primers

Primers for NF-κB, mutant NF-κB and OCT-1 were procured from Santa Cruz Biotechnologies, USA.

III.8.4. Primer labeling

Reaction mixtures containing NF-κB consensus sequence (A), mutant NF-κB (B) and OCT-1 (C) primers were incubated in separate reaction tubes as follows:

ddH_20	12.0 µl
T4 Kinase buffer	2.0 µl
Oligo (A or B or C)	2.0 µl
T4 kinase	1.0 µl
γ ^{32}P ATP	3.0 µl
	---
	20 µl

Following incubation at room temperature for 90 minutes, the samples were loaded onto separate G-50 columns (that had been washed thrice with TE buffer (*Ref. III.2.36*) and centrifuged at 3000 rpm for 2 minutes. Eluates were then diluted by adding 180µl TE buffer, aliquoted and stored at 4^0C until use. 2µl from each sample was used to assay γ ^{32}P activity by liquid scintillation spectrometry.

III.8.5. DNA binding

All reactions were performed on ice. Normoxic and hypoxic samples were prepared for EMSA in two separate vials as follows:

ddH_20	5.0 µl
5X binding buffer	2.0 µl
Protein	2.0 µl
γ ^{32}P-labeled oligo	1.0 µl
	---
	10 µl

All components except the radiolabelled probe were added into corresponding labeled vials. Constituents were mixed by pipetting up and down. 1µl of radiolabeled oligo was added into each vial and mixed carefully. Vials were then incubated at room temperature for 15 minutes. 2µl loading dye (*Ref. III.2.12*) was added into each vial and mixed gently.

12µl each of the samples was electrophoresed on a 6 % non-denaturing DNA retardation gel at 150V for 50 minutes, in chilled 0.5X TBE (*Ref. III.2.33*), keeping the apparatus on ice. After the run, the gels were processed for autoradiography.

III.9. Competition assay

Nuclear extracts from hypoxic samples were electrophoresed with γ ^{32}P-labeled mutant and wild type NF-κB oligo with an excess of unlabelled oligo, in separate reaction mixtures. Following the run, the gels were dried and prepared for autoradiography.

III.10. Super-Shift Assay

The super-shift assay was performed using antibodies against the five known NF-κB subunits (p50, p52, p65, c-Rel and Rel B) to determine the subunit constitution of active NF-κB in cardiac fibroblasts. The reaction mixture for the super-shift assay consisted of:

ddH_20	4.0 µl
5X binding buffer	2.0 µl
Protein	2.0 µl
Antibody	1.0 µl
γ ^{32}P-labeled oligo	1.0 µl
	------
	10 µl

All components except the antibody and γ ^{32}P-labeled oligo were prepared in a master mix and aliquoted into labeled vials separately for each subunit antibody. 1µl of the corresponding NF-κB subunit antibody was added and the mixture was incubated in ice for 1 hour followed by the addition of 1µl of γ ^{32}P-labeled oligo into each vial. Samples were incubated for 15 minutes at room temperature and resolved on a 6% acrylamide gel as described earlier.

III.11. Construction of IκB-super repressor

pSM001, the IkB-sr plasmid used in this study, was constructed from plasmid pLL143 that carries the IκB-sr gene with the IRES and EGFP (reporter) sequences. A poly-A´tail between the IkB-sr gene and EGFP masked EGFP expression in pLL143, which presented difficulties in screening. Reconstructing the plasmid by deleting the poly-A tail unmasked its otherwise suppressed EGFP expression while retaining its IkB-sr function.

III.11.1. Plasmid isolation

E.coli DH5-α strain carrying pLL143 was maintained as a 8% glycerol stock in LB broth at –80^{0}C. A swab from this stock was inoculated into 250ml of LB broth (*Ref. III.2.18*) with amphicilin and was left overnight in a 37^{0}C incubator shaker. Qiagen's Maxi prep kit was used for plasmid isolation as per manufacturer's instructions. Briefly, cells were harvested, lysed and the lysate was passed through a pre-equilibrated Maxi column. The DNA was eluted with 15ml elution buffer into fresh transparent tubes and precipitated with 10.5ml isopropanol. The pellet was air dried and dissolved in 300µl H_2O. 15µl 4M NaCl and 750µl absolute ethanol were added and the tubes were allowed to stand at room temperature for 30 minutes and centrifuged at 14,000 rpm at 4^{0}C for 10 minutes. The pellet was washed with 70% ethanol, solubilized in distilled water and quantified spectrophotometrically at 260nM. The amount of DNA was calculated using the formula: DNA=(OD at 260 X 50 X100) / 1000.

13.5µl DNA from 100X working stock was mixed with 1.5µl 10X loading dye (*Ref. III.2.12*) and electrophoresed on a 1% agarose gel (*Ref. III.2.2*) stained with ethidium bromide (*Ref. III.2.14*), following standard protocol [93], and the bands were visualized using a UV transilluminator.

III.11.2. Restriction digestion

The poly-A tail of the plasmid was spliced using restriction enzymes, BglII and EcoR1. The restriction digestion reaction mixture comprised:

10X restriction buffer	1.5 µl
1M NaCl	1.5 µl
BglII	1.0 µl
EcoR1	1.0 µl
DNA (pLL143)	1.0 µl
H_2O	9.0 µl
	--------
	15 µl

The tubes were incubated at 37^0C overnight to facilitate restriction.

III.11.3. Klenow fragment synthesis

Restriction digestion generated staggered ends in the plasmid that were blunted to avoid non-specific combinations. The reaction mixture prepared for blunt-end synthesis contained:

10X Klenow buffer	2.5 µl
10mM dNTPs	4.0 µl
Klenow enzyme	1.0 µl
H_2O	2.5 µl

The above mixture was added to the vial containing the restriction digestion mixture, to a total volume of 25µl, and kept at room temperature for 60 minutes. The product was electrophoresed on a 1% low melting agarose gel (*Ref. III.2.2*) for an hour. On visualization using a UV transilluminator, 2 fragments were seen, the larger fragment being the plasmid and the smaller fragment the spliced poly-A tail. The larger fragment was excised from the low melting agarose (*Ref. III.2.2*) into an eppendorf tube and kept at 65^0C for 5 minutes to melt away the gel.

III.11.4. Ligation

To circularize the plasmid, the following reaction mixture containing the linear plasmid was kept overnight in a 16^0C water bath:

10X T4 ligase buffer	5.0 µl
T4 ligase	1.0 µl
Fragment	44.0 µl
	---
	50 µl

III.11.5. Plasmid amplification

Ligation created a functional new plasmid pSM001, which was transfected into competent *E.coli* strain DH5α. 50µl ligation mixture and 150µl competent cells (stored at -80^0C) were mixed and incubated on ice for 20 minutes. The tubes were then subjected to heat shock at 37^0C for 5 minutes and immediately transferred to ice for 2 minutes, which

facilitated the entry of plasmids into the bacterium. The mixture was then transferred to a tube containing 1ml 2xYT medium (*Ref. III.2.38*) and left in a 37^0C shaker incubator for an hour. About 300µl of the above mixture was spread onto a LB agar (*Ref. III.2.19*) plate containing kanamycin for selection. The plate was then left upside down in a 37^0C incubator overnight.

Transfected colonies (seen the next day) were carefully picked and incubated in 250 ml LB broth with kanamycin for amplifying the plasmid, which was later used for isolating pSM001, as described earlier. Plasmid was stored in distilled water or TE (*Ref. III.2.36*) at 4^0C until use.

III.11.6. Mapping and Western blotting

The plasmids were subjected to mapping and western blot analysis.

i) Mapping

Plasmids pLL143 and pSM001 were cleaved with BamH1 to linearize them.

Restriction buffer	1.5 µl
1M NaCl	1.5 µl
Diluted BamH1	1.0 µl
DNA	2.0 µl
H_2O	9.0 µl
	---
	15 µl

The reaction mixture was incubated at 37^0C for 1 hour and analyzed on 1% agarose gel (*Ref. III.2.2*).

In order to confirm the plasmid construction, pSM001 was cut with XhoI and BamH1 that would release an 824 bp product in addition to the liniarized plasmid. The reaction mixture containing was incubated at 37^0C for 1 hour and analyzed on 1% agarose gel (*Ref. III.2.2*).

Restriction buffer	1.5 µl
1M NaCl	1.5 µl
XhoI	0.5 µl
BamH1	0.5 µl
DNA	6.0 µl
H_2O	5.0 µl
	---
	15 µl
	---

ii) Western blot analysis

pSM001 was further analyzed for IkB-sr and EGFP expression by western blotting. CHO cells were transfected with pSM001 (IkB-sr plasmid), EGFP expressing plasmid pJW029 (EGFP control), and pEVRT (vector) (negative control) separately using Lipofectamine reagent. Cell lysates were collected and subjected to western blot analysis for IkB-sr and EGFP protein expression as described earlier.

III.12. Lipofectamine-mediated transfection of cells

For lipofectamine-mediated transfection of cells, the following reagents and protocols were used.

Solution A

Plasmid + 50µl opti MEM

Solution B

Lipo 2000 15µl + 150µl opti MEM

Solutions A and B were mixed and incubated at room temperature for 30 minutes.

70 to 80% confluent cultures of CHO cells were washed with PBS (*Ref. III.2.21*) and, after 30 minutes incubation with the plasmid mixture, the contents were gently added to the corresponding plates and incubated overnight at 37^0C in a CO_2 incubator. Following overnight incubation, green EGFP fluorescence was observed in cells transfected with pSM001 and pJW029 but not in the negative control.

III.13. Transfection of cardiac fibroblasts

Basic Nucleofector kit for primary mammalian fibroblasts (Amaxa Biosystems, USA) was used for the transfection, which allowed non-viral gene transfer directly into the nucleus using the nucleofector solution and the electroporator (Amaxa Biosystems, USA), with the programme recommended by the company.

III.13.1. Harvesting cells for transfection

Cardiac fibroblasts from 2nd passage (near 80% confluence) were trypsinized, pelleted and collected into separately labeled vials. $1x10^6$ cells were taken from each group for the experiment.

III.13.2. Electroporation

Cells from each group were separately re-suspended in 100µl Nucleofector solution provided with the kit. About 5µg of the purified plasmid (1µg/µl) and about 2µg of the EGFP control plasmid were mixed with the nuclefector-cell mixture. The mixture was transferred into sterile cuvettes and exposed briefly to a strong electric field. The samples were removed immediately from the cuvettes, using M199 containing 10 % FBS to dilute the mixture, and transferred to culture plates and incubated at 37^0C in a CO_2 incubator for 12 hours. Transfected cells showed green fluorescence after about 12 hours of transfection.

III.13.3. Hypoxia treatment

After ascertaining EGFP expression (within 12 hours), the cells were washed with M199 containing 10 % FBS to remove dead cells and debris and subjected to hypoxia for 12 hours with appropriate normoxic controls. Viability was analyzed using Hoechst 33324 staining (*Ref. III.7.1*)

III.14. Isolation of total RNA

All glassware used for RNA isolation was DEPC-treated and autoclaved. All reagents were prepared with DEPC-treated RNase-free water (*Ref. III.2.10*).

Total RNA was isolated from 85-90% confluent cultures of cardiac fibroblasts by a single-step method using TRI reagent (4ml/100mm culture dish) to lyse the cells, as per the manufacturer's instructions. Following phase separation with chloroform, RNA was precipitated from the aqueous phase using isopropanol and was dissolved in DEPC-treated water (*Ref. III.2.10*). The intactness of RNA was checked by 1% agarose gel (*Ref. III.2.2*) electrophoresis [93] and the yield was determined spectrophotometrically at A_{260}.

III.15. cDNA synthesis

Complementary DNA was synthesized from total RNA by the following procedure. The cDNA synthesizing mixture consisted of:

5X RT buffer	6.0 µl
dNTPs	2.5 µl
Oligo dT	3.0 µl
RNase inhibitor	0.5 µl
M-MLV RT	2.0 µl
Total RNA	10.0 µl
DEPC treated water	6.0 µl
	---
	30 µl

10µg total RNA, 10µl of DEPC-treated water (*Ref. III.2.10*) and 3.0µl oligo dT primers were initially mixed and heated at 70^0C for 5 min. The heated mixture was then snap-cooled on ice and mixed with the remaining constituents listed above. The reaction mixture was vortexed and incubated at 37^0C for 60 minutes followed by heating for 5 minutes at 90^0C and snap-cooling on ice to inactivate M-MLV RT. The cDNA preparations were stored at -20^0C until use.

III.16. Polymerase Chain Reaction

Dual Quantitative PCR kit for rat Bcl-2, obtained from Maxim Biotech, enabled co-amplification of the target Bcl-2 gene with 18S rRNA in a single reaction tube, according to the manufacturer's instructions. The PCR reaction mix contained 35µl of PCR master mixture *(Bcl-2 and 18S primers in optimized Dual PCR buffer)*, 0.3µl of Taq DNA polymerase and 2-5µl of sample cDNA or positive control made up to 50µl with DNase–free water. The cDNAs of Bcl-2 and 18S rRNA transcripts in the reaction mix were co-amplified over 35 cycles at an annealing temperature of 60^0C, by standard PCR protocol *(Maniatis et al, 1982)* [93]. The PCR-amplified samples were analyzed on 1% agarose gel (*Ref. III.2.2*) stained with ethidium bromide (*Ref. III.2.14*).

III.17. Western blot analysis

Western blot analysis was carried out as described by *Maniatis et al (1982)* [94] with minor modifications. Briefly, cardiac fibroblast cultures exposed to hypoxic/normoxic treatments were lysed in cell lysis buffer from Cell Signaling

Technologies (*Ref. III.2.9*). The lysates were centrifuged at 16,000 rpm for 30 minutes to remove cell debris and the supernatant was aliquoted and stored at -80^0C until use. The protein content of the lysate was determined using the BCA protein assay kit. The lysates were mixed with SDS gel-loading buffer and incubated in a 100^0C thermal block for 10 minutes and cooled on ice. 60µg of protein was electrophoretically fractionated on a 12% SDS-PAGE mini-gel for cIAP2 and 15% SDS-PAGE mini-gel for Bcl-2 and electro blotted onto nitrocellulose membrane. The membrane with the transferred proteins (ascertained by Ponceau S (*Ref. III.2.22*) staining) was blocked for 1 hour with 5% skim milk (*Ref. III.2.4*) and incubated overnight at 4^0C with the primary antibody prepared at a dilution of 1:200 in 5% BSA in TBST (*Ref. III.2.35*). Unbound primary antibody was removed by washing (5x5' times) with TBST (*Ref. III.2.35*) and the membrane was incubated for 1 hour with HRP-conjugated anti-mouse/anti-rabbit secondary antibody diluted 1:1000 in 5% BSA containing TBST (*Ref. III.2.35*). After removal of the unbound secondary antibody by washing the membrane 5x5' times with TBST (*Ref. III.2.35*), the membrane was exposed to ECL for 1 minute and exposed to X-ray film for different durations, ranging from 30 seconds to 30 minutes. The images were captured on the Syngene gel documentation system. The membrane was stripped by washing with TBST (*Ref. III.2.35*) overnight on a rocking platform, re-probed with anti-β-actin primary antibody (1:1000 in 5% BSA containing TBST (*Ref. III.2.35*)) and developed after incubation with HRP-conjugated anti-mouse secondary antibody.

III.18. Statistics

Student's t-test was used to examine differences between experimental groups. Where necessary, overall comparison was made by one-way ANOVA followed by Student's t-test to examine differences between experimental groups. Significance was determined at $p \leq 0.05$.

IV. RESULTS

This study focused on the molecular mechanisms underlying the relative resistance of cardiac fibroblasts to hypoxic injury.

IV.1. Characterization of adult rat cardiac fibroblasts

IV.1.1. Morphological analysis

Cardiac fibroblasts isolated from adult rat ventricular tissue were grown in culture as described under 'Methods'. Pre-plating for 150 minutes post-isolation ensured selective enrichment of fibroblasts, which constituted >99% of the cells in these cultures. Morphological analysis and immunocytochemical staining established the fibroblastic nature of the cells. At 150 minutes after isolation, the cells had a dense nest-like morphology *(Figure 1)* and, by 24 hours, the cells attained spindle-like appearance. At confluence, the cultures exhibited a monolayer pattern and did not exhibit 'cobblestone' or 'hill and valley' morphology, ruling out contamination of the cultures by ECs and VSMCs, respectively *(Figure 2)*. Cells at passages 2 and 3 were used for the experiments.

IV.1.2. Immunocytochemical staining

Cells were tested for immunoreactivity with antibodies against the cytoskeletal proteins, vimentin and desmin, and the perinuclear Factor VIII-associated antigen. The cells were positive for vimentin *(Figure 3)* but negative for Factor VIII-related antigen and desmin (data not shown), confirming their fibroblastic nature and ruling out the presence of ECs and VSMCs in the cultures.

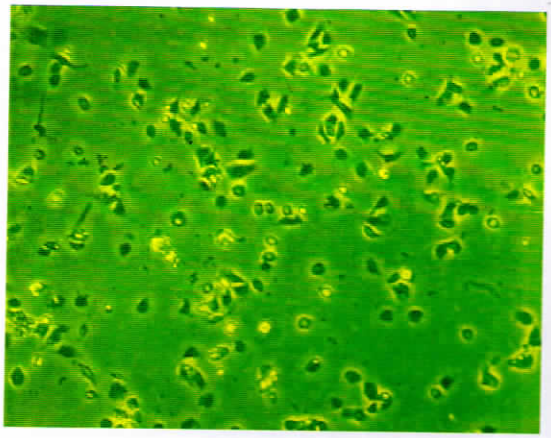

Figure 1: Photomicrograph of adult rat cardiac fibroblasts at 150 minutes after isolation (100X)

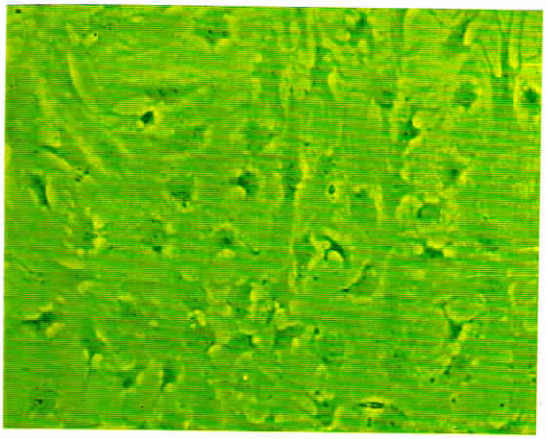

Figure 2: Photomicrograph of adult rat cardiac fibroblasts at confluence (100X)

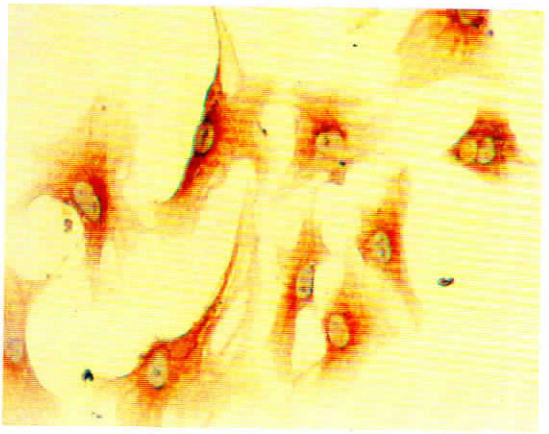

Figure 3: Photomicrograph of vimentin-positive adult rat cardiac fibroblasts (200X)

Sub-confluent cultures were methanol-fixed and incubated with anti-vimentin antibody, AEC-conjugated secondary antibody and AEC-specific chromogen. Nuclei were counter-stained using hematoxylin.

IV.2. The hypoxia model

The *in vitro* hypoxia model was set up using the anaerobic GasPak system from Becton Dickinson, USA *(Figure 4)*.

The system characteristics in terms of the pH and pO_2 of the medium under hypoxic versus normoxic (control) conditions were assessed. The pH of the hypoxic and normoxic media was comparable and was approximately 7.5. pO_2 of the medium under hypoxic culture conditions was ~3%, compared to the normoxic pO_2 of ~15%. pCO_2 in both normoxic and hypoxic systems was ~ 5%.

Figure 4: Anaerobic Gas Pak systems

GasPak anaerobic systems with CO_2 generator or H_2 + CO_2 generator envelope for normoxic or hypoxic conditions, respectively

IV.3. Relative resistance of cardiac fibroblasts

In the initial experiments, the response of cardiac fibroblasts to hypoxia was compared with that of non-cardiac (pulmonary) fibroblasts and cardiac myocytes to ascertain whether these cells are relatively more resistant.

IV.3.1. Hypoxia does not cause loss of viability in cardiac fibroblasts

Flow cytometric analysis of the sub-G_0 population and Syto13-PI staining, carried out earlier in this laboratory, had shown that non-viable cells account for only < 2.5% of the total population of cells after 48 hours of normoxic or hypoxic treatment [124].

In the present study, cardiac fibroblast cultures were exposed to 12, 24, 36 and 48 hours of hypoxia or normoxia and cell survival was monitored at gross morphological level by phase contrast microscopy and by Annexin-PI staining. Cardiac fibroblasts exhibited normal morphology *(Figure 5A)* even after 48 hours of hypoxia treatment. < 2% of the cells were positive for Annexin/PI in both the normoxic and hypoxic groups *(Figure 5B)*. Thus, the data corroborated earlier observations in this laboratory [124] and demonstrated that cardiac fibroblasts are resistant to hypoxia upto at least 48 hours of hypoxic treatment. Cells under hypoxia in presence of 0.1% FBS also gave similar results (data not shown).

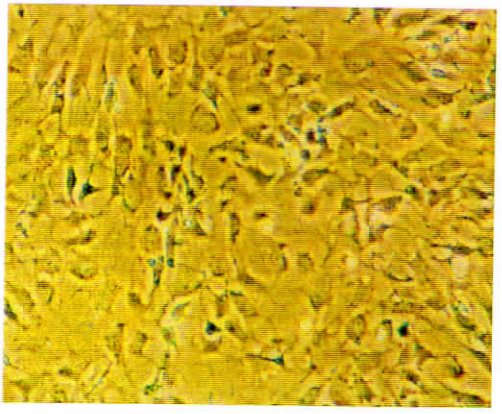

CF-N

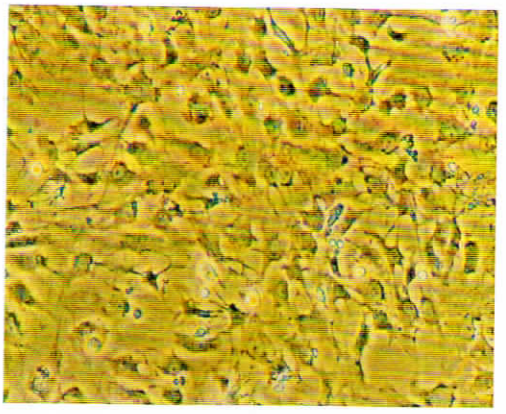

CF-H

Figure 5A: Representative phase contrast micrograph of normoxic (CF-N) and hypoxic (CF-H) cardiac fibroblasts after 48 hours of hypoxia. Cells were observed to have normal morphology even at 48 hours of hypoxia.

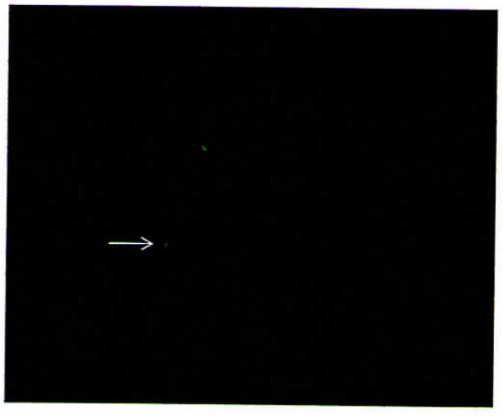

CF-N

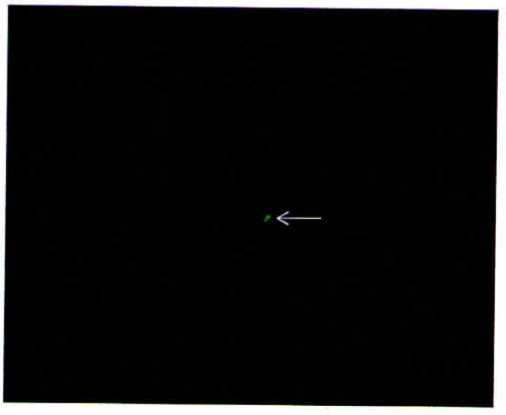

CF-H

Figure 5B: Representative fluorescent micrograph of Annexin-PI stained normoxic (CF-N) and hypoxic (CF-H) cardiac fibroblasts after 48 hours of hypoxia treatment. Cells were washed with PBS and stained with Annexin V–FITC and PI. The arrow shows a non-viable cell that has taken up Annexin and fluoresces green.

IV.3.2. Pulmonary fibroblasts are susceptible to hypoxic injury

Pulmonary fibroblasts were isolated as described under 'Methods' *(Figures 6,7 and 8)* and used as a control cell-type of non-cardiac origin for their response to hypoxia.

Pulmonary fibroblasts cultured in M199 containing 10% FBS were exposed to hypoxia for 12, 24, 36 and 48 hours, with appropriate normoxic controls, and viability changes were monitored. An increase in the number of Annexin-/PI- positive cells was observed after12 hours of hypoxia, compared to normoxic controls *(Figure 9)*. The number increased further by 24 hours of hypoxic treatment. Remarkably, by 36 hours of hypoxic exposure, marked changes in morphology were evident, and the cells were found to peel off *(Figure 10)* by 48 hours of hypoxia. Morphological changes were not observed in the normoxic control groups.

The observations indicated that pulmonary fibroblasts are susceptible to hypoxia-induced cell death, unlike cardiac fibroblasts.

IV.3.3. Conditioned medium from hypoxic cardiac fibroblasts compromises cardiac myocyte viability

Unlike cardiac fibroblasts, cardiac myocytes are reported to be susceptible to cell death under hypoxia [31]. Interestingly, in the present study, it was found that even hypoxic fibroblast-conditioned medium (HFCM), which does not affect the viability of cardiac fibroblasts, was found to compromise cell viability in adult rat cardiomyocytes.

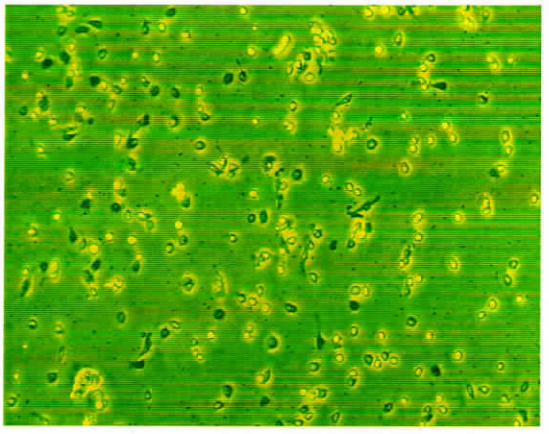

Figure 6: Photomicrograph of adult rat lung fibroblasts at 150 minutes after isolation (100X)

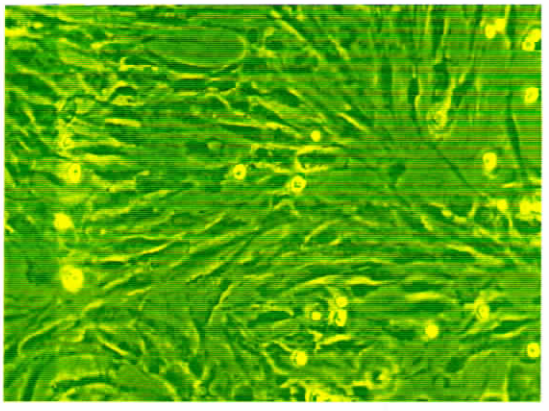

Figure 7: Photomicrograph of adult rat lung fibroblasts at confluence (100X)

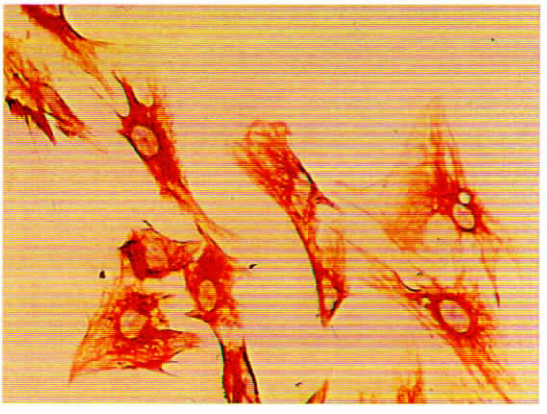

Figure 8: Photomicrograph of vimentin-positive lung fibroblasts (200X)

Sub-confluent cultures were methanol-fixed and incubated with anti-vimentin antibody, AEC-conjugated secondary antibody and AEC-specific chromogen. Nuclei were counter-stained using hematoxylin.

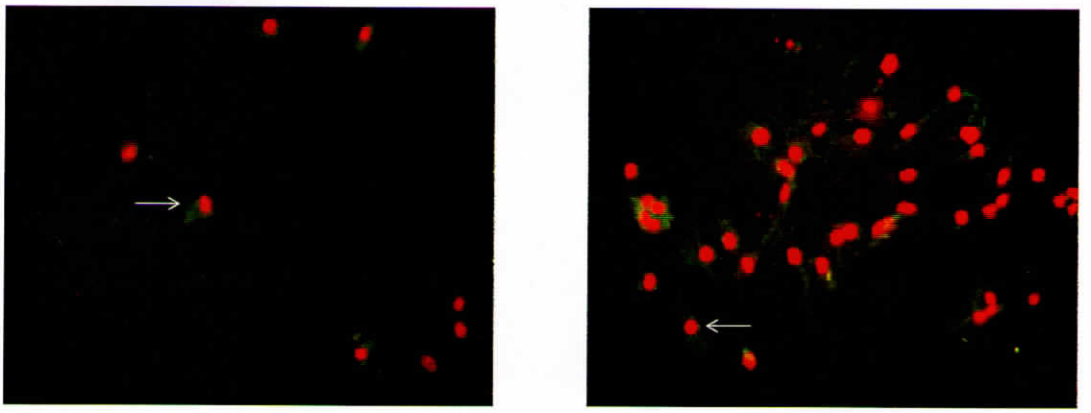

PF-N **PF-H**

Figure 9: Representative fluorescent micrograph of Annexin-PI stained normoxic (PF-N) and hypoxic (PF-H) pulmonary fibroblasts after 12 hours of hypoxia treatment. Cells were washed with PBS and stained with Annexin V–FITC and PI. The arrow shows a non-viable cell that has taken up both Annexin (green) and PI (red).

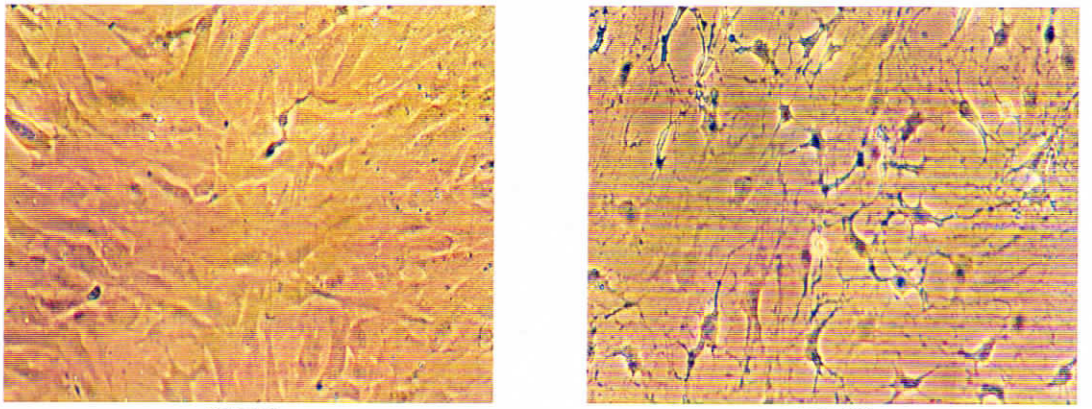

PF-N **PF-H**

Figure 10: Representative phase contrast micrograph of normoxic (PF-N) and hypoxic (PF-H) pulmonary fibroblasts after 48 hours of hypoxia treatment. PF-H were extensively damaged by 48 hours.

Cardiac myocytes isolated from young adult rats *(Figure 11)* were incubated with normoxic fibroblast-conditioned medium (NFCM) *(Figure 12-left)* or HFCM *(Figure 12-right)* for 5 hours. Following wash with HEPES buffer containing 1mM Ca^{2+}, cell viability was analyzed by Annexin-PI staining as described under 'Methods'. Approximately, 500 cells over four fields per dish were counted.

Exposure of myocytes to HFCM for 5 hours resulted in loss of rod-shaped morphology with a significant increase in the number of round myocytes *(Figure 13)*. The treatment also resulted in an upward trend in the number of Annexin-/PI-positive cells *(Figure 14)* compared to cells exposed to NFCM or medium control, suggesting that HFCM may induce apoptotic changes in myocytes. Exposure of myocytes to the conditioned medium for 2 hours was also found to affect cardiomyocyte viability (data not shown) but the effects were more marked at 5 hours of exposure.

HFCM has been reported to have markedly higher levels of TNF-α [135]. Since TNF-α is known to compromise myocyte viability [31], increased levels of TNF-α in HFCM suggested a potential role for the cytokine in the observed loss of myocyte viability upon exposure to HFCM. To examine the possibility, myocytes were exposed to NFCM spiked with TNF-α at 200pg/ml, a concentration comparable to that in HFCM, for 5 hours and cell viability was assayed by morphological analysis and Annexin-PI staining. The treatment also resulted in loss of rod-shaped morphology with a significant

increase in round-shaped *(Figure 13)* and Annexin-/PI-positive cells *(Figure 14)*, compared to the normoxic controls, suggesting loss of viability.

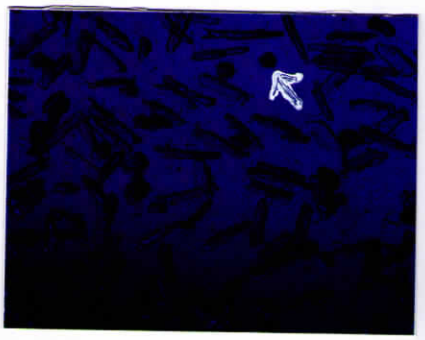

Figure 11: Photomicrograph of isolated adult cardiac myocytes. Healthy cells appeared rod-like and damaged cells had round-shaped morphology (shown by the arrow).

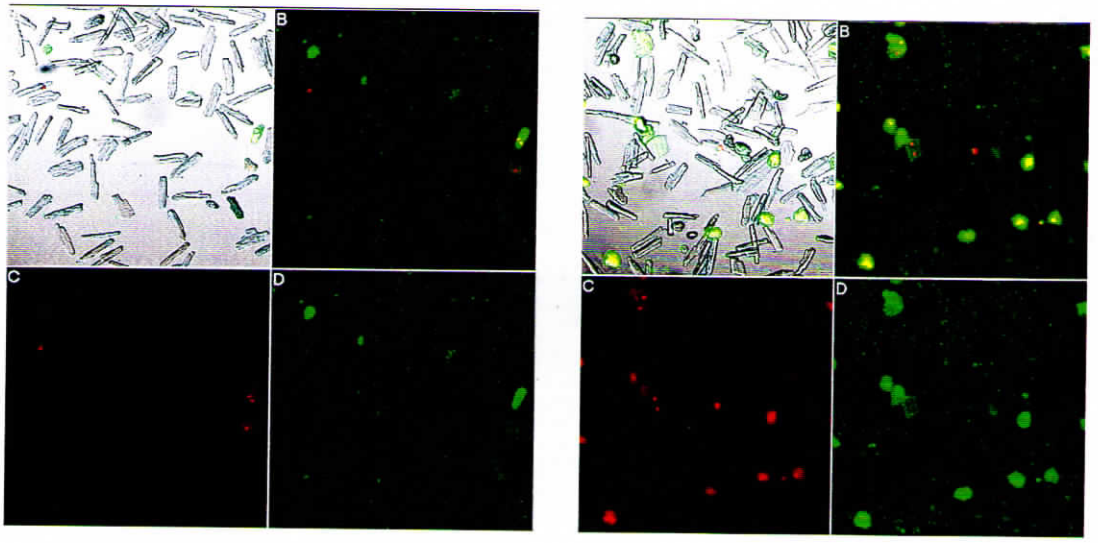

Figure 12: Representative fluorescent micrograph of Annexin-PI stained cardiomyocytes. Cardiomyocytes were exposed to NFCM (left) or HFCM (right) for 5 hours and stained with Annexin-PI as described under 'Methods'. (*A*) Overlay of the bright field and both fluorescence channels (Annexin and PI); rod-shaped and rounded myocytes are seen, (B) Overlay of Annexin-PI fluorescence, (C) PI fluorescence, and (D) Annexin fluorescence. Loss of myocyte viability upon exposure to HFCM is evident.

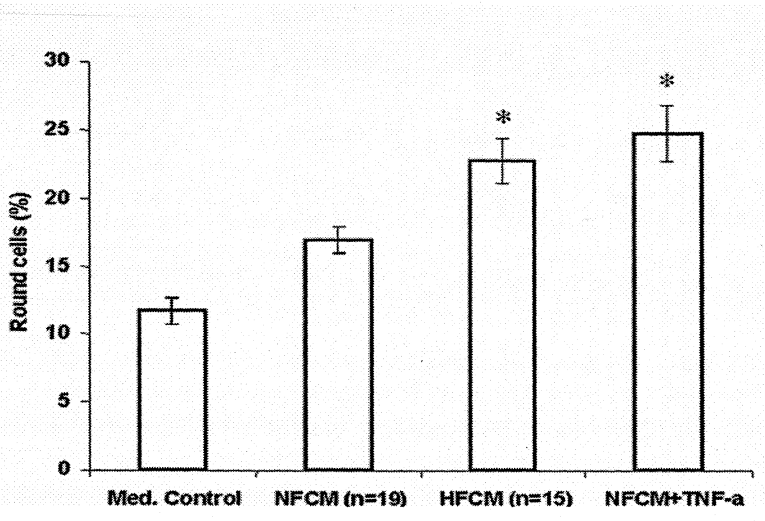

Figure 13: Change in cardiomyocyte morphology (Rod to round) upon exposure to fibroblast-conditioned media. Cardiac myocytes were subjected to the indicated treatments for 5 hours. The percentage of round cells in each group is expressed as Mean ± SEM. "n" denotes the number of dishes per group. * $p < 0.0001$ vs NFCM

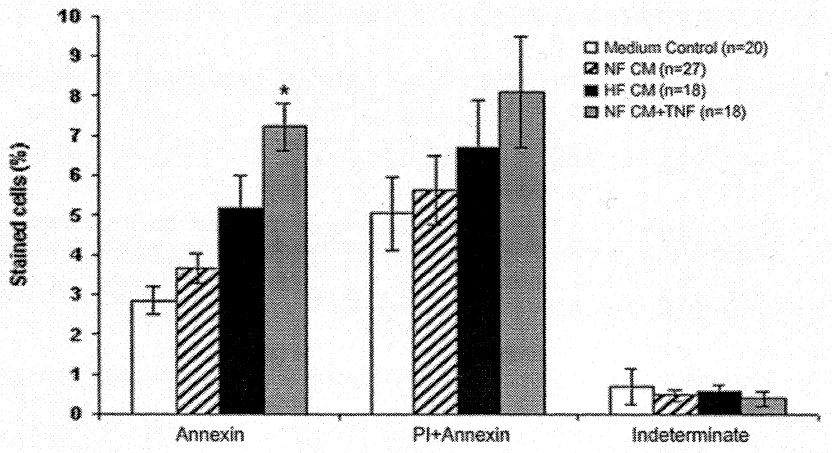

Figure 14: Effects of HFCM and TNF-α on viability of adult rat cardiomyocytes. Cardiac myocytes were subjected to the indicated treatments for 5 hours and viability was assessed by Annexin-PI staining, as described under Methods. Values are expressed as Mean ± SEM. "n" denotes the number of dishes per group. The population marked "indeterminate" was PI positive but Annexin negative. * $p < 0.001$ vs NFCM

IV.4. Mechanisms of resistance of cardiac fibroblasts to hypoxia

The above set of experiments clearly demonstrated the relative resistance of cardiac fibroblasts to hypoxia, compared to pulmonary fibroblasts and cardiac myocytes. Subsequent experiments sought to elucidate the molecular mechanisms responsible for such resistance. The focus was on NF-κB, a major stress-activated transcription factor known for its anti-apoptotic effects in other cell types [9, 24, 106], and cIAP2 and Bcl-2, which are two major anti-apoptotic proteins.

IV.4.1. NF-κB in cardiac fibroblasts

The DNA-binding activity of NF-κB was determined by EMSA, as described under 'Methods'. Nuclear extracts were prepared from cardiac fibroblasts exposed to serum-free conditions for 24 hours followed by normoxic or hypoxic incubation for 6 or 24 hours in M199 containing 0.1% FBS and electrophoresed on a 6% non-denaturing gel. DNA-binding activity of NF-κB under hypoxia is evident in *Figures 15A&15B.* Upon extended exposure of cells to normoxic and hypoxic conditions for 24 hours, DNA-binding activity of NF-κB was observed even in normoxic samples *(Figure 15B)*, which possibly represents pseudo-activation of the transcription factor under prolonged culture conditions. DNA-binding activity of OCT-1 under hypoxia and normoxia served as loading control *(Figures 15C&15D).*

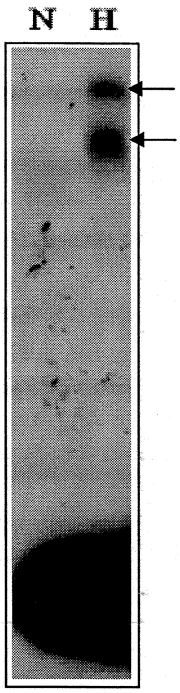

Figure 15A

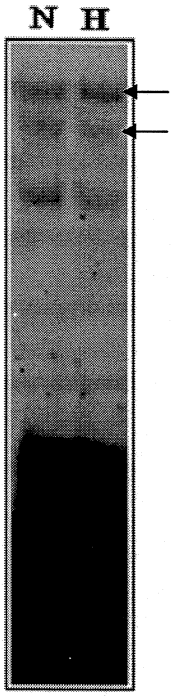

Figure 15B

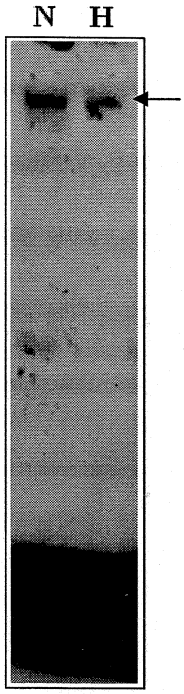

Figure 15C

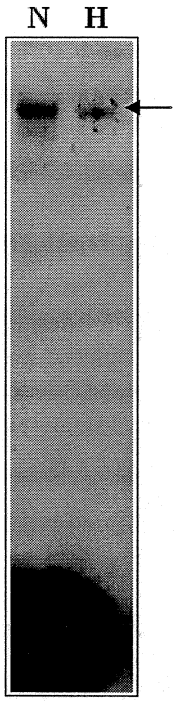

Figure 15D

Figure 15A: Electrophoretic mobility shift assay, performed as described under Methods, showed DNA-binding activity of NF-κB in cardiac fibroblasts exposed to 6 hours of hypoxia.

Figure 15B: Electrophoretic mobility shift assay, performed as described under Methods, showed DNA-binding activity of NF-κB in cardiac fibroblasts exposed to 24 hours of hypoxia.

Figure 15C: Electrophoretic mobility shift assay, showed DNA-binding activity of OCT-1 (loading control) in cardiac fibroblasts exposed to 6 hours of hypoxia.

Figure 15D: Electrophoretic mobility shift assay, showed DNA-binding activity of OCT-1 (loading control) in cardiac fibroblasts exposed to 24 hours of hypoxia.

IV.4.1.1. Competition assay

The specificity of NF-κB for the putative NF-κB binding site was established by the competition assay using oligonucleotides containing binding site for NF-κB. Nuclear extracts with active NF-κB were incubated with γ^{32}P-labeled oligo and an excess of either mutant NF-κB or wild type NF-κB oligo and EMSA was perfomed. As expected, the wild type oligo but not the mutant oligo competitively reduced the binding of NF-κB to the γ^{32}P-labeled oligo (*Figure 16*).

IV.4.1.2. Super-shift assay

Super-shift assay was performed to ascertain the subunit composition of active NF-κB in cardiac fibroblasts. Nuclear extracts with active NF-κB were separately incubated for 1 hour with γ^{32}P-labeled NF-κB consensus sequence and antibodies against the five known NF-κB sub-units (p50, p52, p65, c-Rel (N), and Rel B). The p50 and p65 antibodies, but not the antibodies against the other NF-κB subunits, bound to NF-κB resulting in a ternary complex consisting of NF-κB, the bound antibody and the γ^{32}P-labeled oligo. The electrophoretic mobility of the ternary complex was understandably lower than that of the NF-κB-γ^{32}P-oligo complex without any bound antibody *(Figure 17)*, which showed that active NF-κB in adult rat cardiac fibroblasts is a p65/p50 heterodimer.

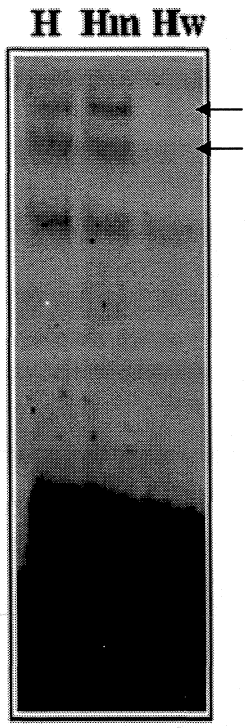

Figure 16

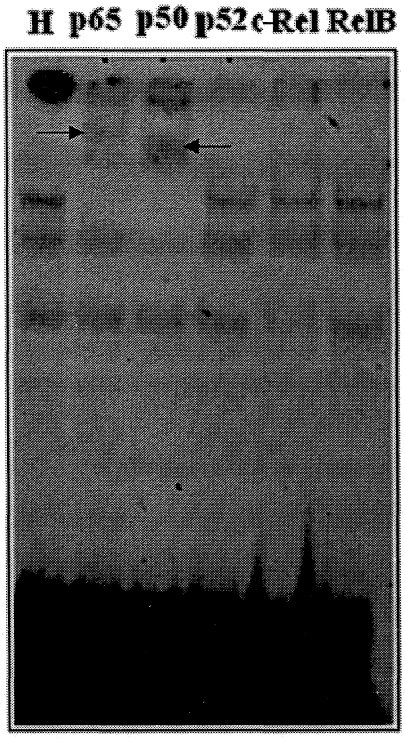

Figure 17

Figure 16: Electrophoretic mobility shift assay profile showing disappearance of NF-κB bands due to competition in presence of excess wild oligo. Nuclear extracts from hypoxic cells were electrophoresed with γ^{32}P-labeled mutant (Hm) and wild type (Hw) NF-κB oligos with an excess of unlabelled oligos, in separate reaction mixtures.

Figure 17: Super-shift assay was performed using antibodies against the five known NF-κB subunits (p50, p52, p65, c-Rel and Rel B) to determine the subunit constitution of active NF-κB in cardiac fibroblasts. Arrows correspond to the shifted p65 and p50 NF-κB bands, demonstrating that NF-κB in cardiac fibroblasts is a p65/p50 heterodimer.

IV.4.2. A role for NF-κB in cardiac fibroblast survival

Having demonstrated the nuclear localization of NF-κB, experiments were designed to determine whether the transcription factor plays any role in the survival of these cells under hypoxic conditions. The strategy consisted in evaluating the effect of inhibiting NF-κB activation on cardiac fibroblast viability under hypoxia.

In subsequent experiments, the nuclear import of NF-κB was abrogated in two different ways: a) gene-based inhibition, and b) pharmacological inhibition.

IV.4.2.1. Gene-based NF-κB inhibition

An IκBα-sr plasmid pSM001 was constructed to abrogate NF-κB activation in cardiac fibroblasts. The IκB-sr plasmid encodes a mutated inhibitor kappa B protein that binds specifically and irreversibly to NF-κB subunits (p65/p50), preventing its nuclear translocation. In the IκB-sr plasmid, amino acids Ser 32 and Ser 36 are replaced by alanine so that these sites cannot be phosphorylated by IKKs, preventing its dissociation from NF-κB.

IV.4.2.1.1. Construction of IκB-super repressor

The IκB-sr plasmid pSM001 was constructed from plasmid pLL143. pLL143 contains IκB-sr gene with the IRES and EGFP sequences. A poly-A tail between the IκB-sr gene and EGFP masked EGFP expression in pLL143, hampering screening. To

circumvent the problem, the plasmid was reconstructed by deleting the poly-A tail to achieve EGFP expression while retaining its IκB-sr capability. *Figure 18* provides a pictorial representation of the procedure.

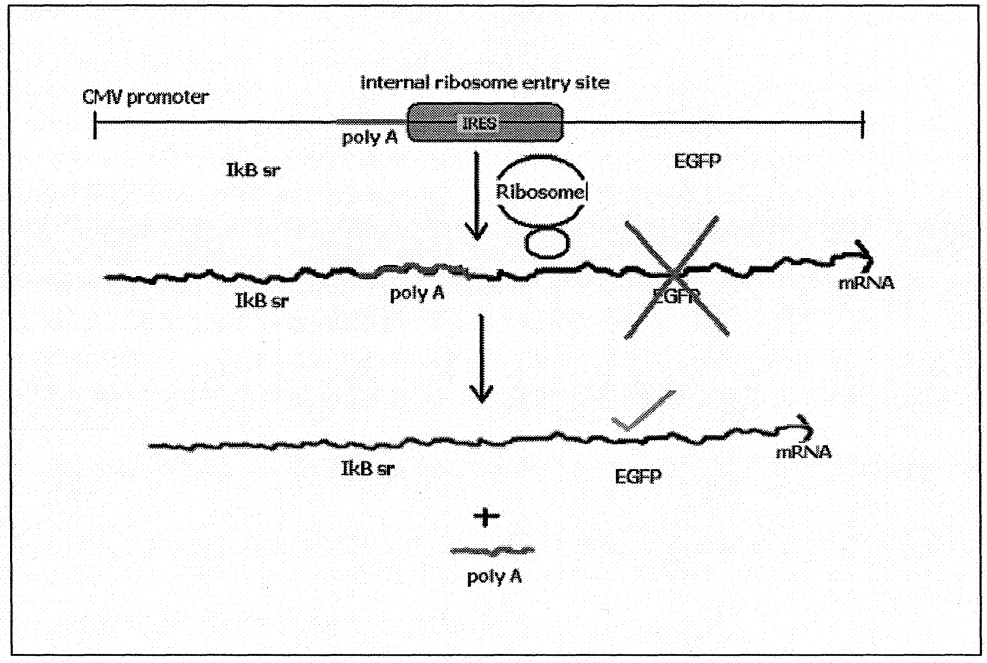

Figure 18: Construction of pSM001. Removal of the poly-A tail, which masked EGFP expression, exposed the EGFP while retaining the super repressor characteristics.

IV.4.2.1.1.A. Plasmid isolation

pLL143 plasmid was isolated as described under 'Methods'. Purity was checked spectrophotometrically and by agarose gel electrophoresis *(Figure 19).* The plasmid was subjected to restriction digestion with specific restriction enzymes.

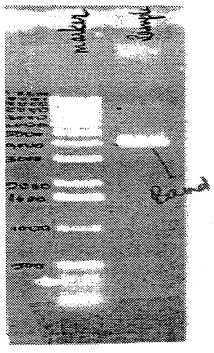

Figure 19: Amplified plasmid pLL143 on 1% agarose gel.

IV.4.2.1.1.B. Restriction digestion

Sequence map analysis of pLL143 revealed single cutting restriction sites BglII and EcoR1 between the IκB-sr gene and the poly-A tail *(Figure 20)*. Splicing the poly-A tail was achieved by restricting the plasmid using BglII and EcoR1 in a restriction mixture cocktail as described under 'Methods'.

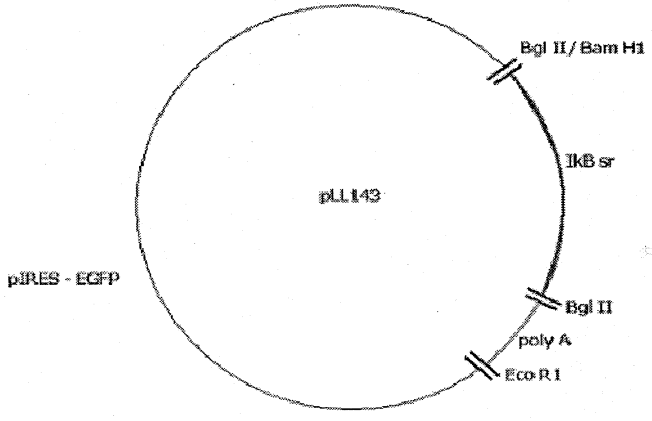

Figure 20: Map of pLL143 showing specific restriction sites.

IV.4.2.1.1.C. Klenow fragment synthesis

Restriction digestion produced a longer fragment (the plasmid) and a shorter fragment (the spliced poly-A tail), both with staggered ends that were blunted as described under 'Methods' *(Figure 21).* The products obtained were subjected to agarose gel electrophoresis (1% low melting agarose), and the larger fragment (the plasmid) was excised for further study.

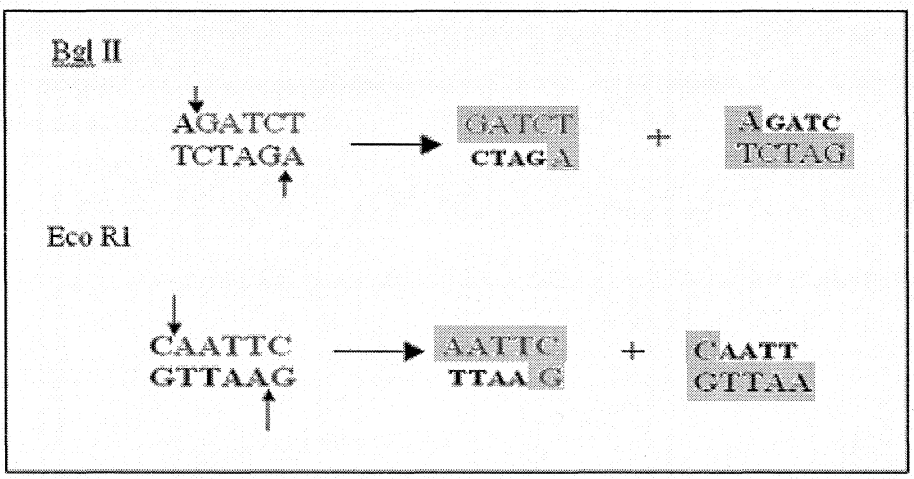

Figure 21: Restriction of pLL143 with enzymes BglII and EcoR1.

IV.4.2.1.1.D. Ligation

Ligation circularized the linear plasmid into a functional plasmid, pSM001 *(Figure 22).* The blunt ends of BglII and EcoR1 were ligated using a ligation mixture as described under 'Methods'. The activity of both the restriction sites (BglII and EcoR1)

was lost in this process. Plasmid pSM001 *(Figure 23)* differs from pLL143 in the expression of EGFP in addition to the IκB-sr gene.

GATCT CTAGA	AATTC TTAAG

OR

AGATC TCTAG	CAATT GTTAA

Figure 22: Ligation circularized the linear plasmid into a functional plasmid, pSM001.

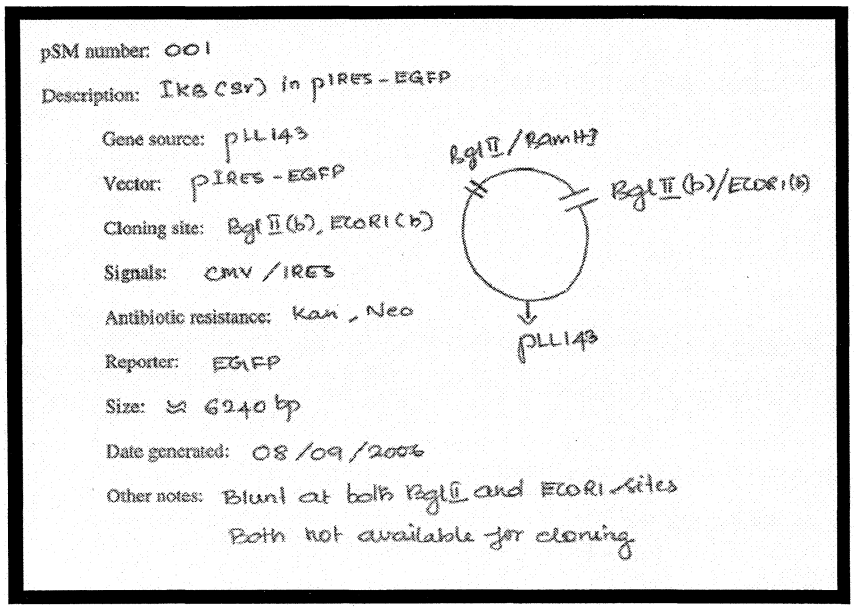

Figure 23: Description of pSM001

IV.4.2.1.1.E. Mapping and western blotting

The plasmid pSM001 was subjected to mapping and western blot analysis. The plasmid was transfected into competent *E.coli* DH5-α strain by a standard procedure as described under 'Methods'. Once amplified, the plasmids were isolated using Qiagen's plasmid isolation kit. After checking plasmid purity, it was stored at 4^0C until use.

(i) Mapping

As a control, plasmids pLL143 and pSM001 were specifically cleaved with BamH1, which linearised the plasmid. In another reaction mixture, pLL143 and pSM001 were cut with XhoI and BamH1. The plasmid construction was validated by restriction with these two enzymes that would specifically release a 824 bp product in addition to the linearized plasmid that is 824 bp less than the control linear plasmid. 1% agarose gel electrophoresis of the mixtures after restriction digestion yielded a profile as shown in *Figure 24.*

(ii) Western blot analysis

Following mapping, pSM001 was subjected to western blot analysis for IκB-sr and EGFP expression. CHO cells were transfected separately with pSM001 (expressing IκB-sr), pJW029 (expressing EGFP), and pEVRT (vector) using Lipo 2000. Western blotting was performed and separate membranes were probed with IκBα and EGFP antibodies and developed using ECL reagent *(Figures 25&26).*

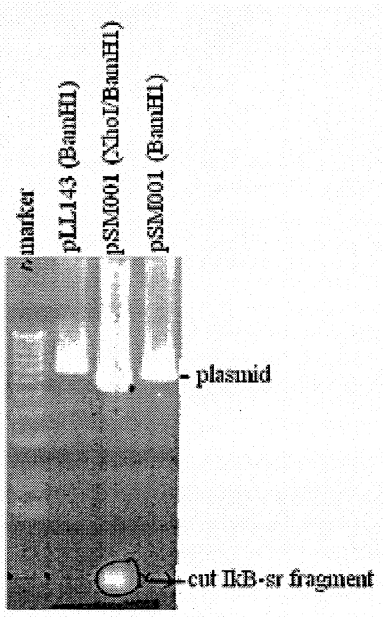

Figure 24: Controlled restriction of pSM001 with specific XhoI and BamH1 generate a 824bp fragment, visualized on 1% agarose gel.

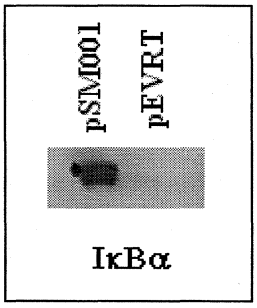

Figure 25: Western blot of pSM001 and pEVRT, probed with IκBα antibody. Band seen only in pSM001.

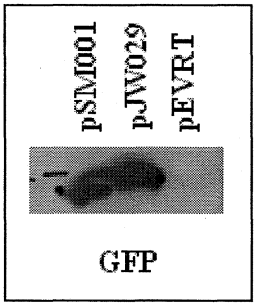

Figure 26: Western blot of pSM001, pJW029 and pEVRT, probed for EGFP expression. Band seen only in plasmid controls and not in vector control.

IV.4.2.1.2. Transfection of cardiac fibroblasts

Initial attempts at transient transfection of adult rat cardiac fibroblasts with pSM001 using the Lipofectamine reagent yielded a low transfection efficiency of 10-20%. However, a markedly higher transfection efficiency of >70% was achieved subsequently using the Basic Nucleofector kit for primary mammalian fibroblasts from Amaxa Biosystems, USA.

Cardiac fibroblasts were trypsinized and transfected with 5μg pSM001 and 1μg EGFP separately. Green fluorescence was detected in both EGFP- and IκB-sr-transfected cells after 12 hours of incubation in M199 containing 10% FBS *(Figure 27)*, indicating successful transfection.

IV.4.2.1.2.1. Response of transfected cardiac fibroblasts to hypoxia

Transfected cardiac fibroblasts were subjected to 12 hours of hypoxia or normoxia and cell viability was analyzed by Hoechst 33324 staining *(Figure 28)*. A significant increase in the percentage of dead cells was evident in IκB-sr-transfected cells subjected to hypoxia, compared to IκB-sr-transfected cells subjected to normoxia. Understandably, marked cell death due to electroporation was noted in normoxic IκB-sr- and EGFP-transfected control groups *(Figure 29)*.

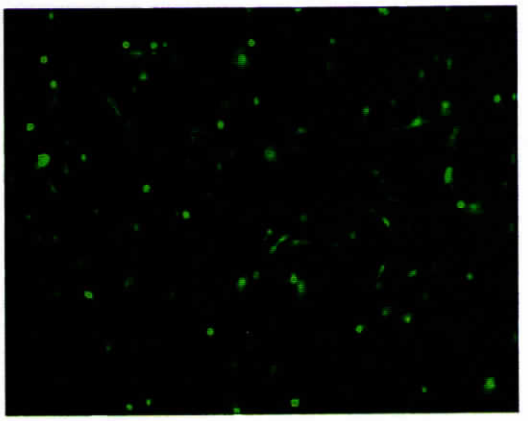

Figure 27: Fluorescence micrograph of cardiac fibroblasts after electroporation. ~ 12 hours after transfection, cells expressed EGFP. Transfection efficiency was >70%.

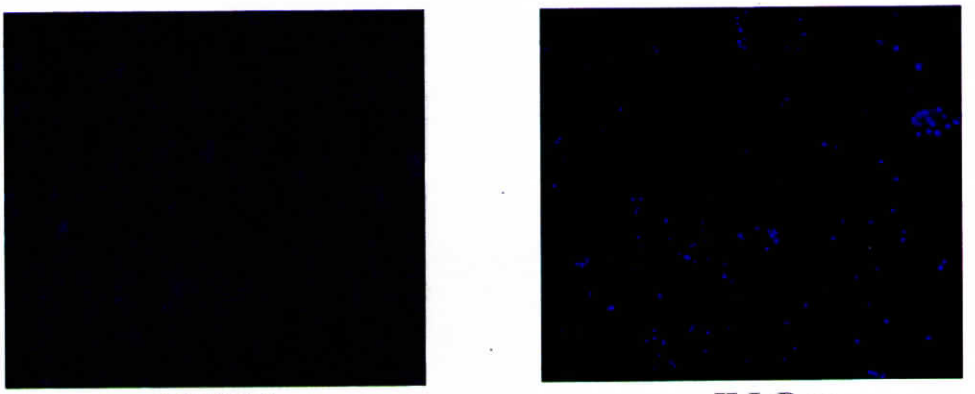

H-EGFP **H-IκB-sr**

Figure 28: Representative fluorescence micrograph of Hoechst 33324-stained cardiac fibroblasts. IκB-sr-transfected fibroblasts, exposed to hypoxia for 12 hours, showed maximum loss of viability, compared to normoxic or hypoxic/normoxic EGFP controls.

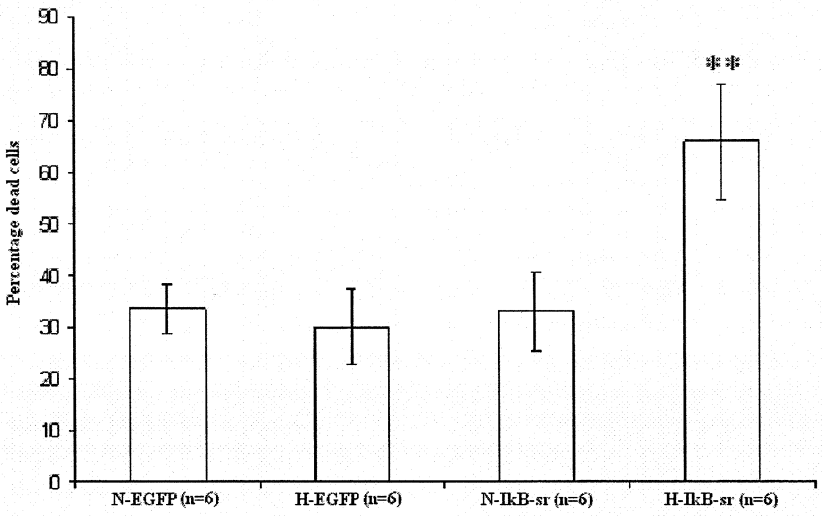

Figure 29: Effect of NF-κB inhibition on cardiac fibroblast viability. Loss of viability, determined by Hoechst 33324-staining, was most marked in NF-κB-inhibited hypoxic cells (H-IκB-sr), compared to normoxic or hypoxic/normoxic EGFP controls. Electroporation *per se* caused considerable loss of viability. The percentage of dead cells in each group is expressed as Mean ± SD. "n" denotes the number of dishes per group. H-IkB-sr vs. N-IkB-sr ** $p < 0.001$

IV.4.2.2. Abrogation of NF-κB activation by pharmacological inhibitors

Bay 11-7085 is reported to effectively inhibit NF-κB activation in different cell types [66, 169]. In the present study, 80-90% confluent cardiac fibroblast cultures were treated with different concentrations of Bay 11-7085 (0.5 to 20μM) for different durations. Cells were then examined by phase contrast microscopy. It was found that exposure of cells to 4μM Bay 11-7085 for 24 hours causes extensive cell damage and cell

loss under hypoxic but not normoxic conditions *(Figure 30),* suggesting that hypoxic cells are more susceptible to these treatment conditions. However, incubation of the cells with 2μM Bay 11-7085 for 24 hours or 4μM Bay 11-7085 for 12 hours did not result in any cell loss under normoxia or hypoxia, facilitating analysis of the cells for Bay 11-7085-induced changes in: a) nuclear import of NF-κB, b) cellular viability, and c) the status of anti-apoptotic proteins.

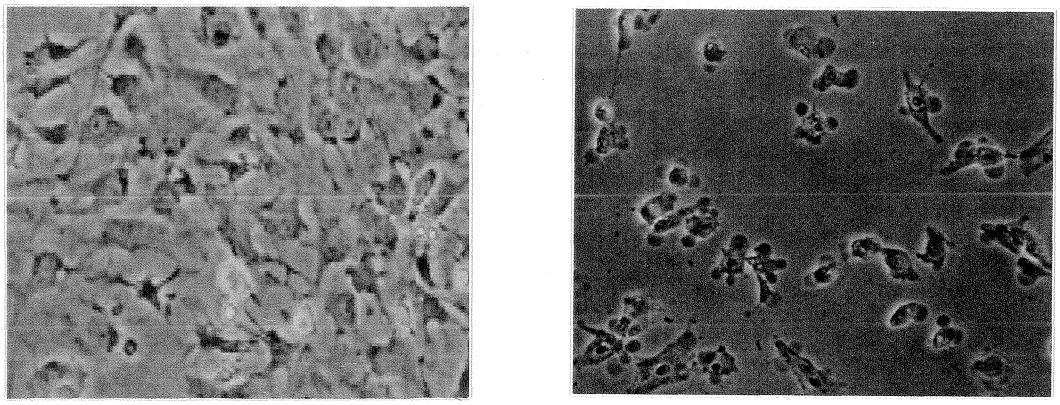

H **H-Bay**

Figure 30: Effect of pharmacological inhibition of NF-κB on cell viability. Extensive loss of viability was observed in cells exposed to hypoxia for 24 hours in presence of 4μM Bay 11-7085.

IV.4.2.2.1. Inhibition of the nuclear translocation of NF-κB by Bay 11-7085

Cells were pre-treated with 4μM Bay 11-7085 for one hour during 12 hours of hypoxic incubation in presence of 4μM Bay 11-7085. Nuclear extracts were then

prepared as described under 'Methods' and EMSA was performed. Treatment of cells with Bay 11-7085 resulted in the total inhibition of the nuclear import of NF-κB in hypoxic cells, as evidenced by the absence of the NF-κB bands in the nuclear extracts from Bay 11-7085-treated cells *(Figure 31)*.

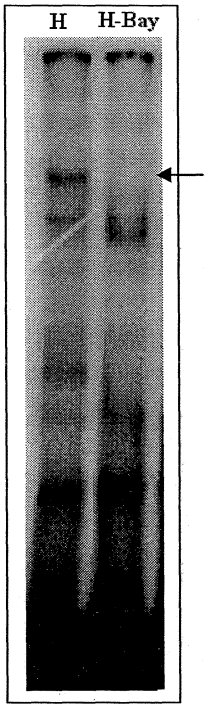

Figure 31: Electrophoretic mobility shift assay showed inhibition of DNA-binding activity of NF-κB in 4μM Bay 11-7085-treated hypoxic cells.

IV.4.2.2.2. Viability of Bay 11-7085-treated cardiac fibroblasts

Cardiac fibroblasts were treated with 4μM Bay 11-7085 for 12 hours under hypoxia and normoxia and cell viability was determined by Hoechst 33324 and Annexin-

PI staining. Bay 11-7085 treatment of cardiac fibroblasts for 12 hours of hypoxia/normoxia resulted in a several-fold increase in cell death, observed as increase in the population of Hoechst 33324- *(Figures 32&33)* and Annexin-PI- *(Figure 34)* stained cells, under hypoxia but not under normoxia.

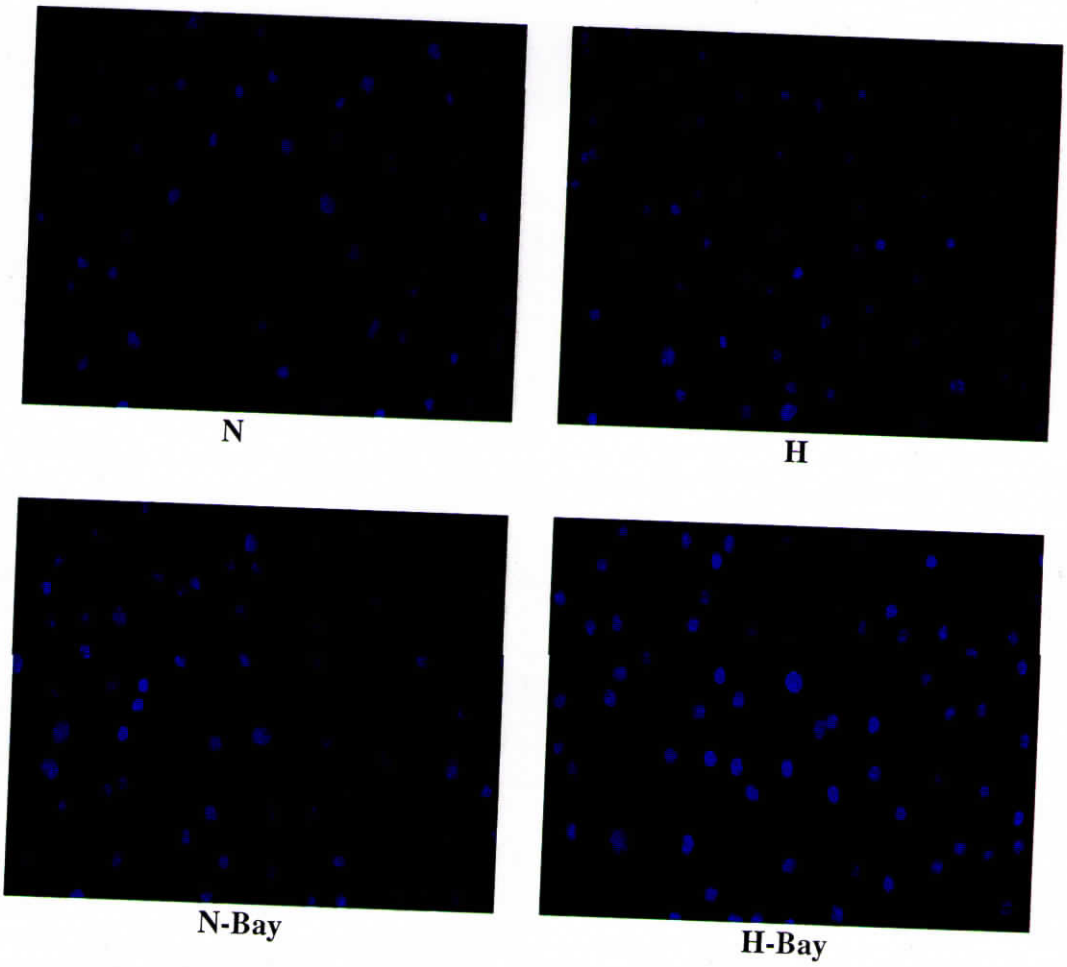

Figure 32: Representative fluorescence micrographs of Hoechst 33324-stained cardiac fibroblasts. Cells exposed to hypoxia for 12 hours in presence of 4μM Bay 11-7085 showed maximum loss of viability.

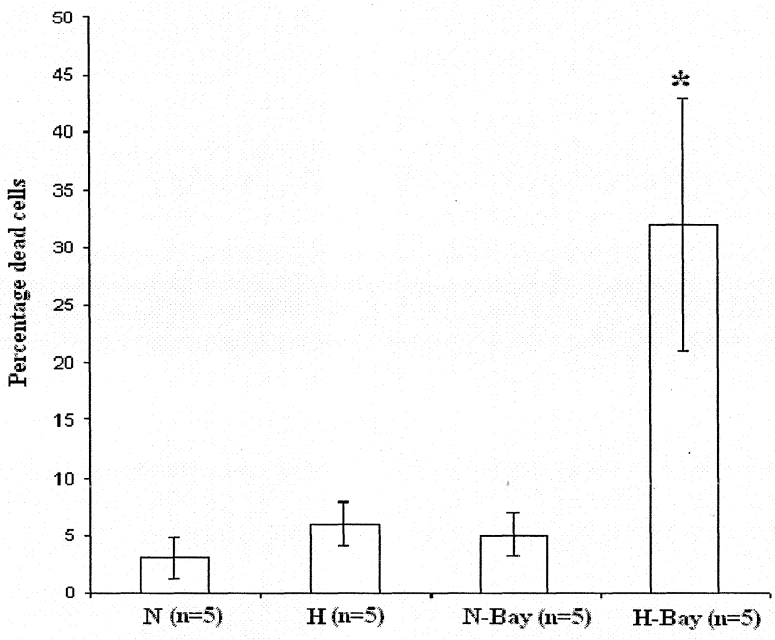

Figure 33: Effect of NF-κB inhibition on cardiac fibroblast viability. Loss of viability, determined by Hoechst 33324-staining, was most marked in NF-κB-inhibited hypoxic cells (H-Bay). The percentage of dead cells in each group is expressed as Mean ± SD. "n" denotes the number of dishes per group. H-Bay vs N-Bay, * $p < 0.0001$.

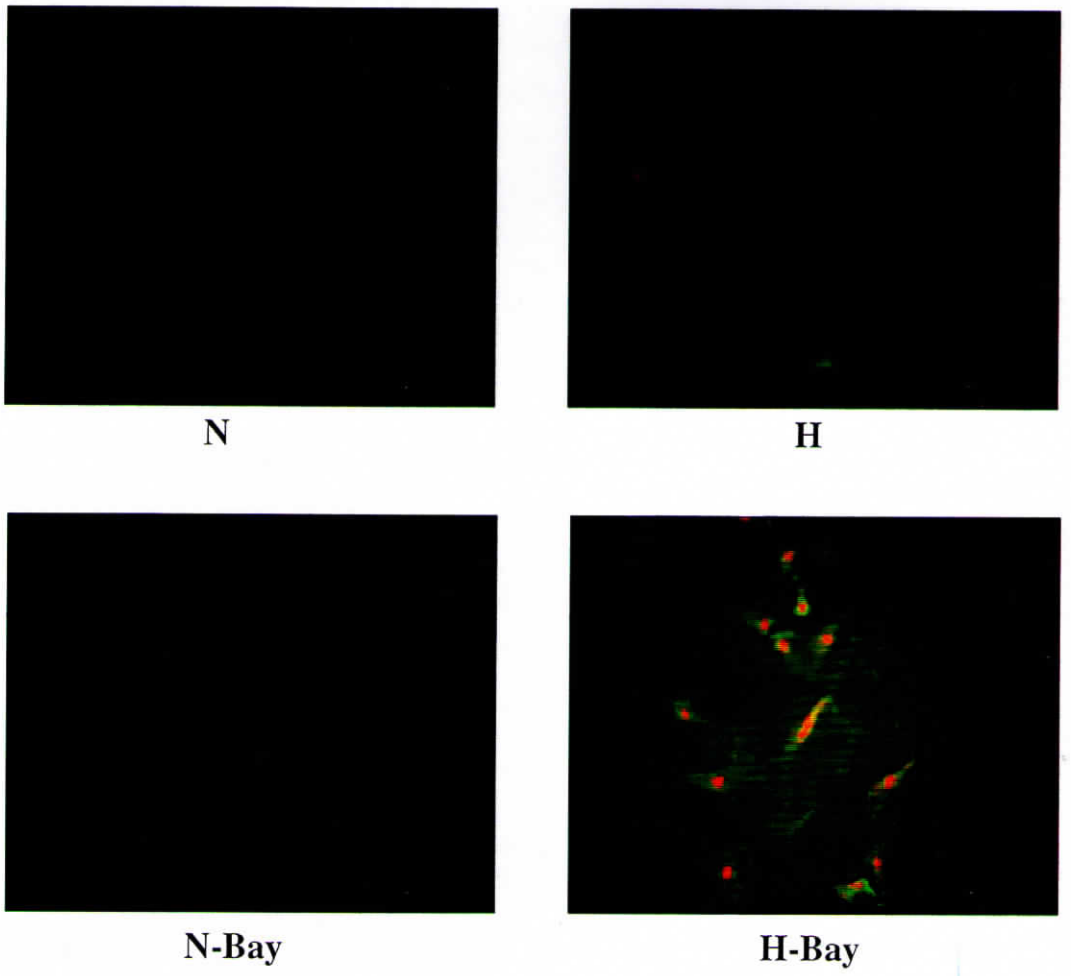

Figure 34: Representative fluorescence micrographs of Annexin-PI-stained cardiac fibroblasts. Cells exposed to hypoxia for 12 hours in presence of 4μM Bay 11-7085 showed maximum loss of viability, as evidenced by increased uptake of Annexin and PI.

Thus, the findings with Bay 11-7085 corroborated those from the gene-based NF-κB inhibition studies. Importantly, in contrast to electroporation, Bay 11-7085 treatment caused meager loss of viability in the control groups and was therefore used in subsequent experiments to inhibit NF-κB activation.

IV.4.3. Expression of pro-survival protein and its regulation by NF-κB

The effect of hypoxia on the expression profile of anti-apoptotic Bcl-2 and cIAP2 was examined in cardiac fibroblasts prior to investigating the possible regulation of these proteins by NF-κB.

IV.4.3.1. Bcl-2 profile in cardiac fibroblasts

To examine the level of Bcl-2 protein in rat cardiac fibroblasts, the cells were subjected to 6,12, 24 and 48 hours of hypoxic treatment, with appropriate normoxic controls. Cell lysates for western blot analysis were prepared and blotting was carried out as explained under 'Methods'.

Bcl-2 was found to be constitutively expressed in hypoxic and normoxic cells at all these time-points *(Figure 35)*.

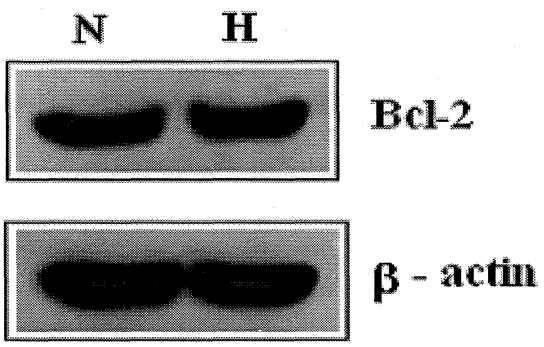

Figure 35: Western blot analysis of Bcl-2 expression in cardiac fibroblasts after 24 hours of treatment. Cells were exposed to normoxic/hypoxic conditions for 24 hours. Western blot analysis was performed as described under 'Methods'. β-actin was used as loading control. A representative profile from one of several experiments showing constitutive expression of Bcl-2.

IV.4.3.1.1. RT-PCR analysis of Bcl-2 mRNA

To examine the level of Bcl-2 mRNA in rat cardiac fibroblasts, cells were exposed to hypoxia and normoxia for 24 hours and semi-quantitative RT-PCR was performed as described under 'Methods'. Briefly, total RNA was isolated, purity was ascertained by 1% agarose gel electrophoresis *(Figure 36)* and cDNA was synthesized from 10μg of RNA by reverse transcription at 37^0C for 60 minutes using random primers. The cDNA was co-amplified over 35 cycles with primers specific for rat Bcl-2 and 18S rRNA (internal control). The PCR products were analyzed by 1% agarose gel electrophoresis followed by densitometric scanning. As is evident from *Figure 37,* no significant differences in Bcl-2 mRNA levels were observed between hypoxic cells and control upon normalization to 18S rRNA.

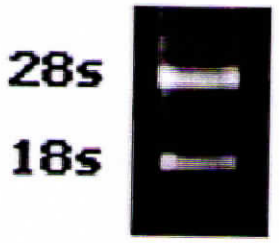

Figure 36: Agarose gel electrophoresis of RNA from cardiac fibroblasts, performed as described under Methods, showing intact 28S and 18S RNA.

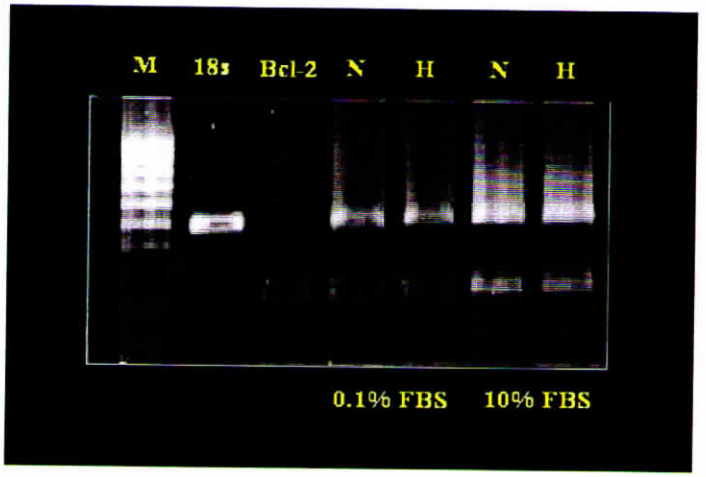

Figure 37: RT-PCR analysis of Bcl-2 transcript levels. Cardiac fibroblasts were subjected to hypoxia for 24 hours and total RNA was isolated as described under 'Methods'. cDNA was synthesized by RT and co-amplified over 35 cycles with primers specific for rat Bcl-2, using 18S rRNA as internal control. The PCR products were analyzed by 1% agarose gel electrophoresis followed by densitometric scanning. Upon normalization to the respective 18S rRNA, no significant differences in Bcl-2 mRNA levels were found between control and hypoxic cells in two separate experiments.

IV.4.3.2. cIAP2 profile in cardiac fibroblasts

Confluent cardiac fibroblast cultures were subjected to 6, 12 and 24 of hypoxia. Western blot analysis showed significant induction of cIAP2 protein under hypoxia but not under normoxia. *Figure 38* shows a representative western blot analysis profile of cIAP2 expression in cardiac fibroblasts at 12 hours of hypoxia treatment.

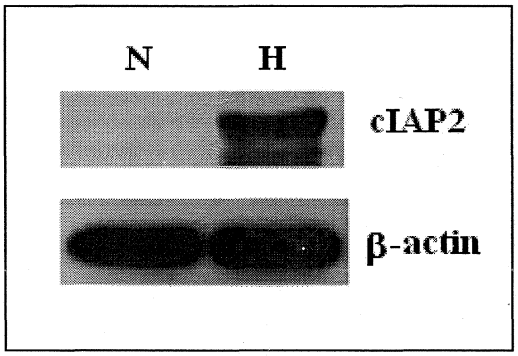

Figure 38: Western blot analysis of cIAP2 expression in cardiac fibroblasts. Cells were exposed to hypoxia for 12 hours and western blot analysis was carried out using anti-cIAP2 antibody, with β-actin as the loading control. Induction of cIAP2 expression was seen in hypoxic but not normoxic samples. A representative profile from one of several experiments showing induction in cIAP2 expression under hypoxia.

IV.4.3.3. Bcl-2 and cIAP2 profile in pulmonary fibroblasts

It was of obvious interest to examine the expression of these proteins in pulmonary cells that were found to be susceptible to hypoxia. Western blot analysis hardly revealed any Bcl-2 and cIAP2 proteins in pulmonary fibroblasts subjected to 6, 12 and 24 hours of normoxia or hypoxia *(Figure 39)*.

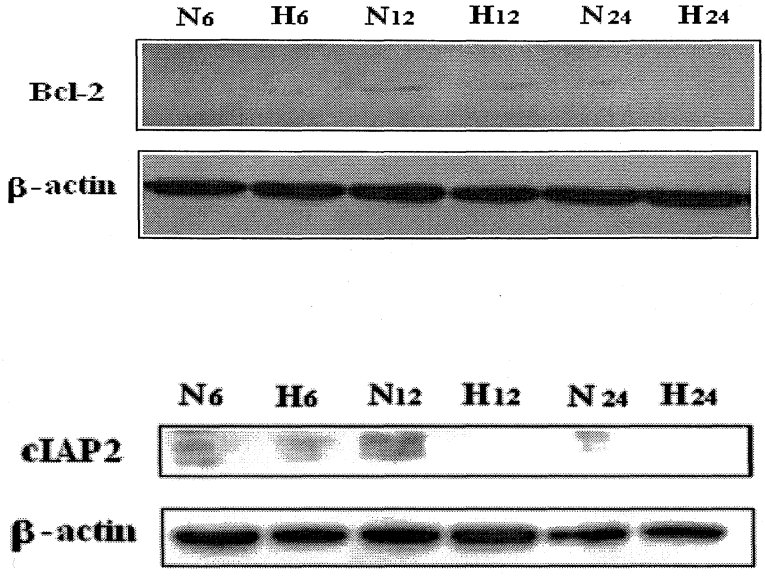

Figure 39: Western blot analysis of Bcl-2 (top) and cIAP2 (bottom) expression in pulmonary fibroblasts. Cells were exposed to hypoxia for 6, 12 and 24 hours and western blot analysis was carried out using anti-Bcl-2 and anti-cIAP2 antibodies, with β-actin as the loading control. A representative profile from one of several experiments revealed hardly any Bcl-2 and cIAP2 protein expression in these cells.

IV.4.3.4. Effect of Bay 11-7085 on the status of anti-apoptotic proteins

The role of NF-κB in the survival of hypoxic cardiac fibroblasts and the hypoxic induction of cIAP2 observed in the present study, along with the reported regulation of Bcl-2 and IAP2 by NF-κB in other cell types [84], prompted investigations into a possible link between the expression of these survival proteins and NF-κB in these cells.

Experiments were performed to ascertain the expression profile of Bcl-2 and cIAP2 in NF-κB-inhibited cardiac fibroblasts.

IV.4.3.4.1. Bcl-2 expression in NF-κB-inhibited cardiac fibroblasts

Western blot analysis of cell lysates from cardiac fibroblasts exposed to 12 hours of hypoxia with 4μM Bay 11-7085 showed comparable levels of Bcl-2 in normoxic, hypoxic and Bay 11-7085-treated cells *(Figure 40)*, suggesting that Bcl-2 expression in cardiac fibroblasts may not be under NF-κB control.

IV.4.3.4.2. cIAP2 expression in NF-κB-inhibited cardiac fibroblasts

In contrast, western blot analysis of cell lysates from cardiac fibroblasts exposed to 12 hours of hypoxia in presence of 4μM Bay 11-7085 showed that hypoxia-induced cIAP2 expression is attenuated by Bay 11-7085 *(Figure 41)*, suggesting the involvement of NF-κB in regulating cIAP2 expression in cardiac fibroblasts under hypoxia.

Together, the data suggest that NF-κB may facilitate cardiac fibroblast survival under hypoxic conditions and that cIAP2 may contribute to the pro-survival role of NF-κB.

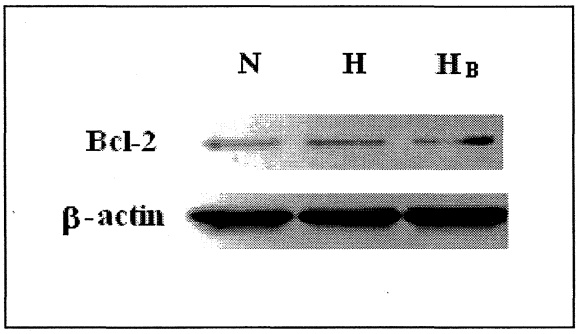

Figure 40: Effect of NF-κB inhibition on Bcl-2 expression in cardiac fibroblasts. Cells were exposed to hypoxia for 12 hours in the presence or absence of 4μM Bay 11-7085. Western blot analysis using anti-Bcl-2 antibody, with β-actin as the loading control, showed no significant change in Bcl-2 levels upon NF-κB inhibition by Bay 11-7085. A representative profile from one of several experiments showing constitutive expression of Bcl-2.

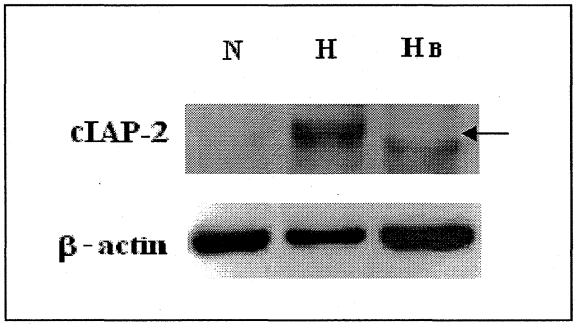

Figure 41: Effect of NF-κB inhibition on cIAP2 expression in cardiac fibroblasts. Cells were exposed to hypoxia for 12 hours in the presence or absence of 4μM Bay 11-7085. Western blot analysis using anti-cIAP2 antibody, with β-actin as the loading control, showed significant attenuation of cIAP2 expression upon NF-κB inhibition by Bay 11-7085. A representative profile showing attenuation in hypoxia-induced cIAP2 expression in NF-κB-inhibited cells.

V. DISCUSSION

V.1. Cardiac fibroblasts in myocardial remodeling

There is increasing appreciation of the role of cardiac fibroblasts in maintaining the structural and functional integrity of the normal and diseased myocardium [18]. Cardiac fibroblasts retain their proliferative potential throughout adult life and are relatively resistant to a variety of factors that are known to damage other cell types, including cardiac myocytes. These two attributes, among others, underlie their ability to influence myocardial remodeling in several pathological states such as myocardial hypertrophy and hypertensive heart disease [18, 110].

Myocardial injury leads to activation of fibroblasts, which involves their phenotypic transformation into myofibroblasts that infiltrate into the site of injury, proliferate and produce matrix components, resulting in scar formation. However, hyper-proliferative response of myofibroblasts also at sites other than the site of injury would result in tissue fibrosis with adverse functional consequences. In fact, it is recognized that fibroblast hyperplasia is always associated with pathological states whereas myocyte hypertrophy can be adaptive or physiological [18].

Normally, wound healing response in tissues of non-cardiac origin is associated with the progression of the granulomatous tissue into a mature scar following myofibroblast apoptosis. However, in the heart, myofibroblasts persist in the mature scar for prolonged periods of time [140], which is consistent with their relative resistance to diverse insults observed in vitro. Failure of the mechanisms of myofibroblast elimination

would contribute to over-expression of the fibro-proliferative response and disturb the quantitative relationship between myocardial parenchyma and stroma, resulting in fibrosis and progressive ventricular dysfunction, eventually leading to heart failure [18, 19a, 115a]. In fact, the term "interstitial heart disease" has been coined to indicate disease states that may predominantly involve the extra cellular space [157, 159].

Of the diverse pathological stimuli prevailing in the injured myocardium, hypoxia is a major factor influencing the extent of cell injury and response. Hypoxia is a potent pro-apoptotic stimulus [31] that is reported to cause cell death in a variety of cells [86, 138, 143] but cardiac fibroblasts are reported to be resistant to hypoxic injury [98]. Apart from a single study that stresses the overriding role of constitutively expressed Bcl-2 in cardiac fibroblast survival under conditions of ambient stress [98], the survival strategies built into these cells remain unclear. Admittedly, diverse mechanisms must be operating in tandem to ensure the survival of these cells under a variety of insults so that they can play a crucial role in tissue response to injury. In this regard, cell survival under conditions of ambient stress can be either by the recruitment of anti-apoptotic defense or by the suppression of pro-apoptotic pathways. The present study aimed at delineating the molecular mechanisms underlying the relative resistance of cardiac fibroblasts to hypoxia, focusing on three well-known anti-apoptotic factors, NF-κB, Bcl-2 and cIAP2.

V.2. An *in vitro* model of hypoxia

Although hypoxia is a powerful regulator of gene expression for multiple regulatory proteins that are involved in processes as distinct, but inter-related, as cell proliferation, cell death and cell survival, the independent effects of hypoxia on cardiac cells have received very little attention. Intrinsic difficulties in evaluating these in the ischemic heart *in vivo* include the existence of a heterogeneous cell population in the heart and the inability to produce a uniform hypoxic insult. It is pertinent to note that stable maintenance of partial blood flow reduction is difficult to achieve in *in vivo* experimental models so that a 1998 National Heart, Lung and Blood Institute Workshop identified the development of *in vitro* models of hypoxia as an area of priority [74, 120]. It is therefore significant that the present study used an *in vitro* cell culture model to evaluate the response of cardiac fibroblasts *per se* to hypoxia in the absence of other confounding influences obtained *in vivo*. The model has generated useful insights into cardiac fibroblast-specific survival strategies recruited in response to hypoxia.

Cardiac fibroblasts isolated from adult rat hearts were characterized and their fibroblastic nature was established in terms of morphology *(Figures 1&2)* and immunocytochemical staining. Confluent cultures did not exhibit 'cobblestone' or 'hill and valley' morphology, ruling out contamination of the cultures by ECs and VSMCs, respectively, as further confirmed by negative immunostaining for factor VIII-related antigen and desmin. The cells stained positive for the cytoskeletal protein, vimentin *(Figure 3),* which is a marker for fibroblasts.

The *in vitro* hypoxia model used in the study provided a hypoxic atmosphere with a pO_2 of <0.1% as against the normoxic pO_2 of ~20%. The pCO_2 in normoxic and hypoxic chambers was ~5%. The medium pO_2 was found to be ~3% in the hypoxic chambers and about 15% in the normoxic chambers [124]. It is important to note that although the atmospheric pO_2 is 20%, the arterial pO_2 is reported to be about 14% and, under conditions of normoxia, cardiac tissue pO_2 is <10% [120]. In the heart, a 30 to 60% decrease in oxygen levels resulting in a pO_2 of ~1 to 3% is considered moderate hypoxia (120). Hence the hypoxic conditions (medium pO_2 ~3%) used in the present study may be considered moderate. Medium pH was comparable in both normoxic and hypoxic chambers and was about 7.5, ruling out a change in pH due to hypoxia.

V.3. Relative resistance of cardiac fibroblasts to hypoxia

Previous studies from this laboratory have conclusively shown that cardiac fibroblast viability is not compromised even after 48 hours of hypoxia [124]. In the present study, cardiac fibroblasts exhibited normal morphology after 48 hours of hypoxia whereas pulmonary fibroblasts were extensively damaged by 48 hours of hypoxia *(Figure 10)*. Further, viability staining (Annexin-PI) of pulmonary fibroblasts showed significant increase in Annexin- and PI-stained cells following 12 hours of hypoxia *(Figure 9)*. These findings clearly demonstrated that cardiac fibroblasts are more robust than fibroblasts of non-cardiac origin.

Further, although cardiac myocytes are reported to be susceptible to hypoxia [31], it was found in this study that even conditioned medium from hypoxic cardiac fibroblasts, which does not affect cardiac fibroblast viability, impairs cardiomyocyte viability, as evidenced by significant increments in the number of round and Annexin-/PI-stained cells *(Figures 12,13&14)*. The results pointed to the presence of factor(s) in HFCM that compromise myocyte viability.

Cytokine profiling of HFCM showed strikingly higher levels of TNF-α, compared to NFCM [135]. In subsequent experiments, when myocytes were exposed for 5 hours to NFCM spiked with 200pg/ml of TNF-α, a significant increase in the number of round cells and Annexin-/PI-stained cells *(Figures 12,13&14)* was observed, indicating that TNF-α may be the factor in HFCM reducing myocyte viability. The observation is consistent with the fact that TNF-α compromises cardiomyocyte viability [151].

Together, the data are consistent with the relative resistance of cardiac fibroblasts vis-à-vis pulmonary fibroblasts and cardiac myocytes.

V.4. Molecular mechanisms underlying relative resistance of cardiac fibroblasts to hypoxia

In looking for mechanisms underlying the resistance of cardiac fibroblasts to hypoxia, this study focused on NF-κB. The choice of NF-κB was dictated by the facts

that, apart from its involvement in immune response, embryo development, apoptosis, cell cycle, inflammation and oncogenesis [24, 84], it is also a well-characterized stress-activated transcription factor known to have a major role in cell survival [9, 49a] and that its involvement in cardiac fibroblast survival under stress has not been established.

V.4.1. Role of NF-κB in cardiac fibroblast survival

V.4.1.1. NF-κB status in cardiac fibroblasts

NF-κB usually exists as homodimers or heterodimes of their five known subunits p65, p50, p52, c-Rel and RelB [84] but the p65/p50 heterodimer is the most widely expressed type of NF-κB in a variety of cell types [83]. Under conditions of stress involving mitogens, cytokines, toxic metals, viral/bacterial products, reactive oxygen intermediates and hypoxia [24, 82, 110a, 144], NF-κB is activated, leading to its rapid translocation to the nucleus [25] where NF-κB dimers bind to cognate DNA binding κB site and directly regulate gene transcription [83]. In this study, NF-κB in cardiac fibroblasts was found to be a p65/p50 heterodimer *(Figure 17)*, and significant DNA-binding activity was observed following exposure to hypoxic conditions for 6 hours *(Figure 15)*. Interestingly, upon extended exposure of cells to culture conditions (24 hours), DNA-binding activity of NF-κB was noted even under normoxic conditions. This may represent "pseudo-activation" which, however, was not probed further.

The first indication of an anti-apoptotic ability of NF-κB came from analysis of Rel $A^{-/-}$ knock out mice, which died at the embryonic stage due to massive apoptosis of hepatocytes in the liver [84]. NF-κB has been reported to prevent TNF-α-induced cell death in mouse embryonic fibroblasts, macrophages [9] and cardiac myocytes [106]. Also, constitutive expression of NF-κB was reported to confer apoptotic resistance in mature B-cells [6], thymocytes, monocytes, macrophages, neurons and VSMCs [77], Hodgkin's lymphoma cells [5] and in certain tumor cells [67]. In light of these observations, the present study examined whether NF-κB may confer death resistance upon these cells under hypoxic conditions.

Generally, involvement of NF-κB in survival is explored by inhibiting its biological activation within cells [153]. A mutant IκB-sr construct containing serine to alanine mutation at residues 32 and 36 is reported to inhibit signal-induced phosphorylation and subsequent proteasomal degradation of IκBα, thereby irreversibly sequestering/retaining NF-κB in the cytoplasm [153]. Cells in which NF-κB was bound to the super repressor were found to be readily susceptible to cell death compared to cells where NF-κB was functional [6]. Based on this principle, the consequence of NF-κB abrogation in cardiac fibroblasts was examined by a gene-based method wherein a super repressor plasmid was constructed that binds and inhibits nuclear translocation of NF-κB.

In the present study, the gene-based inhibition technique was standardized for the first time in adult cardiac fibroblasts. IκB-sr plasmid pSM001 was constructed from pLL143 by deleting an intervening poly-A tail that was masking its EGFP expression while retaining its super repressor capability. The steps involved in cloning included restriction digestion, blunting and re-ligation (explained in detail under 'Methods'). The authenticity of the plasmid was confirmed by western blotting. Subsequently, the electroporation technique was used to transfect the plasmid into cardiac fibroblasts. A striking increase in the number of dead cells was observed by Hoechst 33324 staining in hypoxic IκB-sr-transfected cardiac fibroblasts, in contrast to the control groups *(Figure 32)*. Though the procedure involved in plasmid construction was elaborate, the new plasmid not only finds direct application in NF-κB-mediated survival studies in cardiac fibroblasts but it may also be used as a research tool in inhibiting NF-κB to study its involvement in a number of important processes, including immune response, embryo development, apoptosis, cell cycle, inflammation and oncogenesis [24, 84].

Additionally, Bay 11-7085, which is reported to irreversibly and effectively inhibit NF-κB in many cell types [82, 169], was also used to evaluate the effects of NF-κB inhibition on cell survival. A concentration of 4μM Bay 11-7085 for 24 hours was found to induce gross morphologic changes under hypoxic but not normoxic conditions *(Figure 30),* suggesting that NF-κB inhibition renders cells susceptible to hypoxia. Further, exposure of Bay 11-7085-treated cardiac fibroblasts to 12 hours of hypoxia

produced marked increase in the population of Hoechst 33324- and Annexin-PI-stained cells *(Figures 32,33&34)*. It is important to note that cell death, determined by Hoechst 33324 staining, was around 4-5% in normoxic cultures exposed to Bay 11-7085 as against ~30% in the control groups subjected to electroporation *(Figure 29)*. Thus, in comparison with electroporation, Bay 11-7085-mediated NF-κB inhibition seems more attractive. Moreover, the treatment protocol is less cumbersome compared to the elaborate procedures involved in electroporation.

V.4.2. Mechanisms underlying the pro-survival role of NF-κB in cardiac fibroblasts

NF-κB is widely reported to transcriptionally regulate the expression of a number of specific anti-apoptotic proteins including cIAP1, cIAP2, xIAP, Bcl-2, cFLIP, A20 zinc finger protein, manganese superoxide dimutase within cells [84]. However, in cardiac fibroblasts, very little information is available on the expression of anti-apoptotic proteins or their regulation by NF-κB. Therefore, in addressing cardiac fibroblast resistance to hypoxia, this study focused on the expression profile of pro-survival Bcl-2 and cIAP2 in these cells and the role of NF-κB in regulating their expression under hypoxic conditions.

V.4.2.1. Bcl-2 in cardiac fibroblasts

Constitutive levels of Bcl-2 expression were observed in cardiac fibroblasts subjected to hypoxic and normoxic treatments *(Figures 35&37)*. On the contrary, Bcl-2 was hardly expressed in pulmonary fibroblasts *(Figure 39)*, which were found to be

susceptible to hypoxia-mediated cell death. The data are consistent with the earlier report that constitutive expression of Bcl-2 is responsible for the resistance of neonatal rat cardiac fibroblasts to diverse insults, including hypoxia [98]. It is pertinent to note in this context that Bcl-2 is reported to be down-regulated after birth in most tissues. For example, Bcl-2 is expressed in skin fibroblasts only during embryonic life and its level represses after birth [112]. In pulmonary fibroblasts, Bcl-2 is lost during lung maturation [19]. The disappearance of Bcl-2 protein in adult skin and lung fibroblasts may account for the increased susceptibility of these cells to stress. The persistence of Bcl-2 in adult cardiac fibroblasts, noted in this study, extends the earlier observation on neonatal cells.

Bcl-2 is known to specifically target the mitochondrial route of protection in cells [98]. It is constitutively localized on the mitochondrial outer membrane and inhibits cytochrome C release within cells [31]. Bcl-2 binds to ANT and VDAC on the mitochondrial membranes, inhibiting MPT, Bax activation and apoptosis [133]. Interestingly, it is also known to induce cell cycle delay/arrest [69] by a mechanism involving the cell cycle inhibitor, p27 [98]. Since G_1-S arrest or delay is reported to protect cells from ambient stress [3, 116a], the inhibitory effect of Bcl-2 on the cell cycle may represent yet another mechanism by which it exerts its protective effect on cells. In this context, it is pertinent to point out that recent studies in this laboratory have shown that hypoxia induces G_1-S delay in cardiac fibroblasts, possibly via the induction of p27 [124]. It is tempting to postulate that Bcl-2-mediated delay in cell cycle progression may, at least in part, contribute to the resistance of these cells to hypoxic injury.

V.4.2.2. cIAP2 in cardiac fibroblasts

IAPs promote cell survival mainly by preventing caspase activation [123, 147a]. They directly bind and inhibit upstream caspases like caspases-9 [134] and downstream caspases like caspases-3 and -7 [31, 40, 41]. Release of pro-apoptotic Smac/DIABLO and Omi/Htr2 from the mitochondria opposes the inhibition of caspases by IAPs [46, 141, 152]. These factors bind to IAPs, displacing the caspases, where Omi/HtrA2 act as inhibitors of the 'inhibitor' by cleaving and irreversibly inactivating IAPs through its serine protease activity [167]. In rat kidney proximal tubule cells, hypoxia was reported to selective up-regulate cIAP2 expression, which confers apoptotic resistance in these cells [42, 44]. The study also showed that cIAP2 induction was not a result of secondary effects of hypoxia such as ATP depletion, cellular redox status alteration or respiratory arrest; rather, the key to the induction may be oxygen deficiency *per se* [42, 44]. Also hypoxic expression of cIAP2 was not cell-type specific, as it was detected in 3T3 fibroblasts, primary cultures of HUVEC, human renal carcinoma cells and human kidney proximal tubular epithelial cells [42]. Against these observations, one may postulate that induction of cIAP2 in cardiac fibroblasts *(Figure 38)* may be responsible for their resistance to cell death under conditions of hypoxia. Additionally, as expected, pulmonary fibroblasts hardly showed any cIAP2 induction *(Figure 39)*, consistent with their susceptibility to hypoxia.

The pro-survival role of IAPs is not limited to caspase inhibition. IAPs have been found to promote survival in many cell types by mechanisms independent of caspase

activation [123]. Like Bcl-2, they may regulate the cell cycle under stress and promote cell survival [123]. IAPs are reported to induce cell cycle arrest [79]. It has been reported that cIAP2 expression contributes to G_2/M arrest and promotes survival in He La cells [70]. Clearly, a pro-survival role for cIAP2 and Bcl-2 in cardiac fibroblasts under ambient stress via their cell cycle effects is an important subject for future investigation.

The involvement of NF-κB in the regulation of anti-apoptotic Bcl-2 and cIAP2 has been reported earlier [84] but a link between NF-κB and these survival proteins has not been looked into in relation to cardiac fibroblast survival. In this study, western blot analysis showed comparable levels of Bcl-2 in normoxic and hypoxic cells and in NF-κB-inhibited cells subjected to hypoxia *(Figure 40)*. In contrast, the hypoxia-induced cIAP2 expression was attenuated by Bay 11-7085 treatment *(Figure 41)*. The decrease in cIAP2 but not Bcl-2 levels upon NF-κB inhibition suggests the involvement of NF-κB in the selective regulation of cIAP2 in cardiac fibroblasts under hypoxia.

V.5. Conclusions

The findings suggest that NF-κB plays a pro-survival role in cardiac fibroblasts exposed to hypoxia and that regulation of cIAP2 expression by NF-κB may, at least in part, mediate the pro-survival role of NF-κB during hypoxia. Moreover, constitutive expression of Bcl-2 and hypoxic induction of cIAP2 point to survival strategies in cardiac fibroblasts that are dynamic and involve multiple factors, including (but possibly not

limited to) Bcl-2 and cIAP2. In that sense, the findings significantly enlarge the earlier report that links survival of cardiac fibroblasts under conditions of ambient stress exclusively to basal levels of Bcl-2 [98].

V.6. Limitations of the study

Although the role of NF-κB in cardiac fibroblast survival under hypoxia has been convincingly demonstrated in the present study, evidence of a pro-survival role for cIAP2 as a mediator of the protective effect of NF-κB in hypoxic cardiac fibroblasts hinges on its induction under hypoxia, its well-recognized role as a pro-survival protein and the observed association of compromised viability with reduced cIAP2 levels in NF-κB-inhibited cells. Establishing a direct link between cell survival and cIAP2 by its selective silencing in hypoxic cardiac fibroblasts would considerably enhance the value of the work. The data also do not provide direct evidence of the transcriptional regulation of cIAP2 expression by NF-κB. Further, the findings based on NF-κB inhibition do not rule out a role for other NF-κB-regulated factors, apart from cIAP2, in facilitating cell survival under hypoxia.

VI. SUMMARY

VI.1. Summary

The findings can be summarized as follows:

1. Cardiac fibroblasts, in contrast to cardiac myocytes and fibroblasts of non-cardiac origin (pulmonary), are resistant to hypoxic injury.

2. DNA-binding activity of NF-κB was detected in hypoxic cardiac fibroblasts.

3. NF-κB inhibition by genetic and pharmacological means renders cardiac fibroblasts susceptible to hypoxia, emphasizing the involvement of NF-κB in cardiac fibroblast survival.

4. Cardiac fibroblasts express constitutive levels of Bcl-2 under hypoxic and normoxic conditions.

5. Hypoxia induces cIAP2 in cardiac fibroblasts.

6. Pulmonary fibroblasts do not express cIAP2 and Bcl-2, consistent with their susceptibility to hypoxia.

7. NF-κB inhibition did not affect Bcl-2 expression in hypoxic cardiac fibroblasts.

8. NF-κB inhibition attenuated cIAP2 expression in hypoxic cardiac fibroblasts, suggesting that NF-κB selectively regulates the expression of cIAP2 but not Bcl-2 in hypoxic cardiac fibroblasts.

VI.2. Future directions

- Direct transcriptional regulation of cIAP2 by NF-κB may be examined.

- Selective silencing of cIAP2 by siRNA technology would provide better understanding of its role in cell survival under hypoxia.

- Characterization of downstream events leading to cell death in NF-κB-inhibited cardiac fibroblasts.

VII. REFERENCES

[1] Agocha A, Lee HW, Eghbali-Webb M. Hypoxia regulates basal and induced DNA synthesis and collagen type I production in human cardiac fibroblasts: effects of transforming growth factor-beta1, thyroid hormone, angiotensin II and basic fibroblast growth factor. *J Mol Cell Cardiol* 1997; 29: 2233-44.

[2] Ambalavanan N, Bulger A, Philips IJ. Hypoxia-induced release of peptide growth factors from neonatal porcine pulmonary artery smooth muscle cells. *Biol Neonate* 1999; 76: 311-9.

[3] Amellem O, Stokke T, Sandvik JA, Pettersen EO. The retinoblastoma gene product is reversibly dephosphorylated and bound in the nucleus in S and G2 phases during hypoxic stress. *Exp Cell Res* 1996; 227: 106-15.

[4] Badrichani AZ, Stroka DM, Bilbao G, Curiel DT, Bach FH, Ferran C. Bcl-2 and Bcl-XL serve an anti-inflammatory function in endothelial cells through inhibition of NF-kappaB. *J Clin Invest* 1999; 103: 543-53.

[4a] Banerjee I, Yekkala K, Borg TK, Baudino TA. Dynamic interactions between myocytes, fibroblasts, and extracellular matrix. *Ann N Y Acad Sci* 2006; 1080: 76-84.

[5] Bargou RC, Emmerich F, Krappmann D, Bommert K, Mapara MY, Arnold W, et al. Constitutive nuclear factor-kappaB-RelA activation is required for proliferation and survival of Hodgkin's disease tumor cells. *J Clin Invest* 1997; 100: 2961-9.

[6] Barinaga M. Life-death balance within the cell. *Science* 1996; 274: 724.

[7] Bashey RI, Donnelly M, Insinga F, Jimenez SA. Growth properties and biochemical characterization of collagens synthesized by adult rat heart fibroblasts in culture. *J Mol Cell Cardiol* 1992; 24: 691-700.

[8] Baudino TA, Carver W, Giles W, Borg TK. Cardiac fibroblasts: friend or foe? *Am J Physiol Heart Circ Physiol* 2006; 291: H1015-26.

[9] Beg AA, Baltimore D. An essential role for NF-κB in preventing TNF-α–induced cell death. *Science* 1996; 274: 782-784.

[10] Beitner-Johnson D, Leibold J, Millhorn DE. Hypoxia regulates the cAMP- and Ca2+/calmodulin signaling systems in PC12 cells. *Biochem Biophys Res Commun* 1998; 242: 61-6.

[11] Beitner-Johnson D, Millhorn DE. Hypoxia induces phosphorylation of the cyclic AMP response element-binding protein by a novel signaling mechanism. *J Biol Chem* 1998; 273: 19834-9.

[12] Bergman MR, Cheng S, Honbo N, Piacentini L, Karliner JS, Lovett DH. A functional activating protein 1 (AP-1) site regulates matrix metalloproteinase 2 (MMP-2) transcription by cardiac cells through interactions with JunB-Fra1 and JunB-FosB heterodimers. *Biochem J* 2003; 369: 485-96.

[13] Bialik S, Geenen DL, Sasson IE, Cheng R, Horner JW, Evans SM, et al. Myocyte apoptosis during acute myocardial infarction in the mouse localizes to hypoxic regions but occurs independently of p53. *J Clin Invest* 1997; 100: 1363-72.

[14] Booz GW, Baker KM. Molecular signalling mechanisms controlling growth and function of cardiac fibroblasts. *Cardiovasc Res* 1995; 30: 537-43.

[15] Bosman FT, Stamenkovic I. Functional structure and composition of the extracellular matrix. *J Pathol* 2003; 200: 423-8.

[16] Brischwein K, Engelcke M, Riedinger HJ, Probst H. Role of ribonucleotide reductase and deoxynucleotide pools in the oxygen-dependent control of DNA replication in Ehrlich ascites cells. *Eur J Biochem* 1997; 244: 286-93.

[17] Brouard S, Berberat PO, Tobiasch E, Seldon MP, Bach FH, Soares MP. Heme oxygenase-1-derived carbon monoxide requires the activation of transcription factor NF-kappa B to protect endothelial cells from tumor necrosis factor-alpha-mediated apoptosis. *J Biol Chem* 2002; 277: 17950-61.

[18] Brown RD, Ambler SK, Mitchell MD, Long CS. The cardiac fibroblast: therapeutic target in myocardial remodeling and failure. *Annu Rev Pharmacol Toxicol* 2005; 45: 657-87.

[19] Bruce MC, Honaker CE, Cross RJ. Lung fibroblasts undergo apoptosis following alveolarization. *Am J Respir Cell Mol Biol* 1999; 20: 228-36.

[19a] Bryant JE, Shamhart PE, Luther DJ, Olson ER, Koshy JC, Costic DJ, Mohile MV, Dockry M, Doane KJ, Meszaros JG. Cardiac myofibroblast differentiation is attenuated by alpha(3) integrin blockade: potential role in post-MI remodeling. *J Mol Cell Cardiol* 2009; 46:186-92.

[20] Camelliti P, Borg TK, Kohl P. Structural and functional characterisation of cardiac fibroblasts. *Cardiovasc Res* 2005; 65: 40-51.

[21] Carmeliet P, Dor Y, Herbert JM, Fukumura D, Brusselmans K, Dewerchin M, et al. Role of HIF-1alpha in hypoxia-mediated apoptosis, cell proliferation and tumour angiogenesis. *Nature* 1998; 394: 485-90.

[22] Chandrasekar B, Freeman GL. Induction of nuclear factor kappaB and activation protein 1 in postischemic myocardium. *FEBS Lett* 1997; 401: 30-4.

[23] Chapman D, Weber KT, Eghbali M. Regulation of fibrillar collagen types I and III and basement membrane type IV collagen gene expression in pressure overloaded rat myocardium. *Circ Res* 1990; 67: 787-94.

[24] Chen F, Castranova V, Shi X, Demers LM. New insights into the role of nuclear factor-kappaB, a ubiquitous transcription factor in the initiation of diseases. *Clin Chem* 1999; 45: 7-17.

[25] Chen LF, Greene WC. Shaping the nuclear action of NF-kappaB. *Nat Rev Mol Cell Biol* 2004; 5: 392-401.

[26] Chu ZL, McKinsey TA, Liu L, Gentry JJ, Malim MH, Ballard DW. Suppression of tumor necrosis factor-induced cell death by inhibitor of apoptosis c-IAP2 is under NF-kappaB control. *Proc Natl Acad Sci* U S A 1997; 94: 10057-62.

[26a] Chun-Juan C, Wei Y, Yu-Cai F, Xin W, Ji-Lin L and Wei W. Resveratrol protects cardiomyocytes from hypoxia-induced apoptosis through the SIRT1–FoxO1 pathway. *Biochemical and Biophysical Research Communications* 2009; 378: 389-393.

[27] Claycomb WC. Control of cardiac muscle cell division. *Trends in Cardiovasc Med* 1992; 2: 231-236.

[28] Cleutjens JP, Kandala JC, Guarda E, Guntaka RV, Weber KT. Regulation of collagen degradation in the rat myocardium after infarction. *J Mol Cell Cardiol* 1995; 27: 1281-92.

[29] Cleutjens JP, Verluyten MJ, Smiths JF, Daemen MJ. Collagen remodeling after myocardial infarction in the rat heart. *Am J Pathol* 1995; 147: 325-38.

[30] Colucci WS. Molecular and cellular mechanisms of myocardial failure. *Am J Cardiol* 1997; 80: 15L-25L.

[31] Crow MT, Mani K, Nam YJ, Kitsis RN. The mitochondrial death pathway and cardiac myocyte apoptosis. *Circ Res* 2004; 95: 957-70.

[32] Danial NN, Korsmeyer SJ. Cell death: critical control points. *Cell* 2004; 116: 205-19.

[33] Das M, Bouchey DM, Moore MJ, Hopkins DC, Nemenoff RA, Stenmark KR. Hypoxia-induced proliferative response of vascular adventitial fibroblasts is dependent on G protein-mediated activation of mitogen-activated protein kinases. *J Biol Chem* 2001; 276: 15631-40.

[34] Das M, Dempsey EC, Reeves JT, Stenmark KR. Selective expansion of fibroblast subpopulations from pulmonary artery adventitia in response to hypoxia. *Am J Physiol Lung Cell Mol Physiol* 2002; 282: L976-86.

[35] Datta SR, Brunet A, Greenberg ME. Cellular survival: a play in three Akts. *Genes Dev* 1999; 13: 2905-27.

[36] de Erausquin GA, Hyrc K, Dorsey DA, Mamah D, Dokucu M, Masco DH, et al. Nuclear translocation of nuclear transcription factor-kappa B by alpha-amino-3-hydroxy-5-methyl-4-isoxazolepropionic acid receptors leads to transcription of p53 and cell death in dopaminergic neurons. *Mol Pharmacol* 2003; 63: 784-90.

[37] de Moissac D, Zheng H, Kirshenbaum LA. Linkage of the BH4 domain of Bcl-2 and the nuclear factor kappaB signaling pathway for suppression of apoptosis. *J Biol Chem* 1999; 274: 29505-9.

[38] DeBosch B, Sambandam N, Weinheimer C, Courtois M, Muslin AJ. Akt2 regulates cardiac metabolism and cardiomyocyte survival. *J Biol Chem* 2006; 281(43): 32841-51.

[39] Deshpande SS, Angkeow P, Huang J, Ozaki M, Irani K. Rac1 inhibits TNF-alpha-induced endothelial cell apoptosis: dual regulation by reactive oxygen species. *Faseb J* 2000; 14: 1705-14.

[40] Deveraux QL, Roy N, Stennicke HR, Van Arsdale T, Zhou Q, Srinivasula SM, et al. IAPs block apoptotic events induced by caspase-8 and cytochrome c by direct inhibition of distinct caspases. *Embo J* 1998; 17: 2215-23.

[41] Deveraux QL, Takahashi R, Salvesen GS, Reed JC. X-linked IAP is a direct inhibitor of cell-death proteases. *Nature* 1997; 388: 300-4.

[42] Dong Z, Venkatachalam MA, Wang J, Patel Y, Saikumar P, Semenza GL, et al. Up-regulation of apoptosis inhibitory protein IAP-2 by hypoxia. Hif-1-independent mechanisms. *J Biol Chem* 2001; 276: 18702-9.

[43] Dong Z, Wang J. Hypoxia selection of death-resistant cells. A role for Bcl-X(L). *J Biol Chem* 2004; 279: 9215-21.

[44] Dong Z, Wang JZ, Yu F, Venkatachalam MA. Apoptosis-resistance of hypoxic cells: multiple factors involved and a role for IAP-2. *Am J Pathol* 2003; 163: 663-71.

[45] Douglas RM, Haddad GG. Genetic models in applied physiology: invited review: effect of oxygen deprivation on cell cycle activity: a profile of delay and arrest. *J Appl Physiol* 2003; 94: 2068-83.

[46] Du C, Fang M, Li Y, Li L, Wang X. Smac, a mitochondrial protein that promotes cytochrome c-dependent caspase activation by eliminating IAP inhibition. *Cell* 2000; 102: 33-42.

[47] Durmowicz AG, Stenmark KR. Mechanisms of structural remodeling in chronic pulmonary hypertension. *Neoreviews* 1999; e91-e102.

[48] Eghbali M, Tomek R, Woods C, Bhambi B. Cardiac fibroblasts are predisposed to convert into myocyte phenotype: specific effect of transforming growth factor beta. *Proc Natl Acad Sci U S A* 1991; 88: 795-9.

[49] Erl W, Hansson GK, de Martin R, Draude G, Weber KS, Weber C. Nuclear factor-kappa B regulates induction of apoptosis and inhibitor of apoptosis protein-1 expression in vascular smooth muscle cells. *Circ Res* 1999; 84: 668-77.

[49a] Fan Yeung, Jamie E Hoberg, Catherine S Ramsey, Michael D Keller, David R Jones, Roy A Frye, and Marty W Mayo. Modulation of NF-κB-dependent transcription and cell survival by the SIRT1 deacetylase. *EMBO J* 2004; 23: 2369–80.

[50] Fliss H, Gattinger D. Apoptosis in ischemic and reperfused rat myocardium. *Circ Res* 1996; 79: 949-56.

[51] Foo RS, Mani K, Kitsis RN. Death begets failure in the heart. *J Clin Invest* 2005; 115: 565-71.

[52] Frantz S, Hu K, Bayer B, Gerondakis S, Strotmann J, Adamek A, et al. Absence of NF-kappaB subunit p50 improves heart failure after myocardial infarction. *Faseb J* 2006; 20: 1918-20.

[53] Fujioka S, Schmidt C, Sclabas GM, Li Z, Pelicano H, Peng B, et al. Stabilization of p53 is a novel mechanism for proapoptotic function of NF-kappaB. *J Biol Chem* 2004; 279: 27549-59.

[54] Gardner LB, Li F, Yang X, Dang CV. Anoxic fibroblasts activate a replication checkpoint that is bypassed by E1a. *Mol Cell Biol* 2003; 23: 9032-45.

[55] Gardner LB, Li Q, Park MS, Flanagan WM, Semenza GL, Dang CV. Hypoxia inhibits G1/S transition through regulation of p27 expression. *J Biol Chem* 2001; 276: 7919-26.

[56] Geoffrey M Cooper. The Cell: A Molecular approach (2nd edition). Sinauer Associates Inc; 2000.

[57] Giaccia AJ, Simon MC, Johnson R. The biology of hypoxia: the role of oxygen sensing in development, normal function, and disease. *Genes Dev* 2004; 18: 2183-94.

[58] Giordano FJ. Oxygen, oxidative stress, hypoxia, and heart failure. *J Clin Invest* 2005; 115: 500-8.

[59] Goda N, Ryan HE, Khadivi B, McNulty W, Rickert RC, Johnson RS. Hypoxia-inducible factor 1alpha is essential for cell cycle arrest during hypoxia. *Mol Cell Biol* 2003; 23: 359-69.

[60] Gottlieb RA, Burleson KO, Kloner RA, Babior BM, Engler RL. Reperfusion injury induces apoptosis in rabbit cardiomyocytes. *J Clin Invest* 1994; 94: 1621-8.

[61] Green SL, Freiberg RA, Giaccia AJ. p21(Cip1) and p27(Kip1) regulate cell cycle reentry after hypoxic stress but are not necessary for hypoxia-induced arrest. *Mol Cell Biol* 2001; 21: 1196-206.

[62] Guillemin K, Krasnow MA. The hypoxic response: huffing and HIFing. *Cell* 1997; 89: 9-12.

[62a] Gustafsson AB and Gottlieb RA. Bcl-2 family members and apoptosis, taken to heart. *Am J Physiol Cell Physiol* 2007; 292: C45-C51.

[62b] Gustafsson AB, Gottlieb RA Recycle or die: the role of autophagy in cardioprotection. *J Mol Cell Cardiol* 2008; 44: 654-61.

[62c] Gustafsson AB, Gottlieb RA. Autophagy in ischemic heart disease. *Circ Res* 2009; 104:150-58.

[63] Gustafsson AB, Tsai JG, Logue SE, Crow MT, Gottlieb RA. Apoptosis repressor with caspase recruitment domain protects against cell death by interfering with Bax activation. *J Biol Chem* 2004; 279: 21233-8.

[64] Guzy RD, Mack MM, Schumacker PT. Mitochondrial complex III is required for hypoxia-induced ROS production and gene transcription in yeast. *Antioxid Redox Signal* 2007; 9: 1317-28.

[65] Hacker G. The morphology of apoptosis. *Cell Tissue Res* 2000; 301: 5-17.

[66] Hernandez-Gutierrez S, Garcia-Pelaez I, Zentella-Dehesa A, Ramos-Kuri M, Hernandez-Franco P, Hernandez-Sanchez F, et al. NF-kappaB signaling blockade by Bay 11-7085 during early cardiac morphogenesis induces alterations of the outflow tract in chicken heart. *Apoptosis* 2006; 11: 1101-9.

[67] Hinz M, Krappmann D, Eichten A, Heder A, Scheidereit C, Strauss M. NF-kappaB function in growth control: regulation of cyclin D1 expression and G0/G1-to-S-phase transition. *Mol Cell Biol* 1999; 19: 2690-8.

[68] Hochachka PW, Buck LT, Doll CJ, Land SC. Unifying theory of hypoxia tolerance: molecular/metabolic defense and rescue mechanisms for surviving oxygen lack. *Proc Natl Acad Sci U S A* 1996; 93: 9493-8.

[69] Janumyan YM, Sansam CG, Chattopadhyay A, Cheng N, Soucie EL, Penn LZ, et al. Bcl-xL/Bcl-2 coordinately regulates apoptosis, cell cycle arrest and cell cycle entry. *Embo J* 2003; 22: 5459-70.

[70] Jin HS, Lee TH. Cell cycle-dependent expression of cIAP2 at G2/M phase contributes to survival during mitotic cell cycle arrest. *Biochem J* 2006; 399: 335-42.

[71] Kacimi R, Chentoufi J, Honbo N, Long CS, Karliner JS. Hypoxia differentially regulates stress proteins in cultured cardiomyocytes: role of the p38 stress-activated kinase signaling cascade, and relation to cytoprotection. *Cardiovasc Res* 2000; 46: 139-50.

[72] Kim JY, Ahn HJ, Ryu JH, Suk K, Park JH. BH3-only protein Noxa is a mediator of hypoxic cell death induced by hypoxia-inducible factor 1alpha. *J Exp Med* 2004; 199: 113-24.

[73] Klionsky DJ, Emr SD. Autophagy as a regulated pathway of cellular degradation. *Science* 2000; 290: 1717-21.

[74] Kloner RA, Bolli R, Marban E, Reinlib L, Braunwald E. Medical and cellular implications of stunning, hibernation, and preconditioning: an NHLBI workshop. *Circulation* 1998; 97: 1848-67.

[75] Koong AC, Chen EY, Giaccia AJ. Hypoxia causes the activation of nuclear factor kappa B through the phosphorylation of I kappa B alpha on tyrosine residues. *Cancer Res* 1994; 54: 1425-30.

[76] Kumaran C, Shivakumar K. Calcium- and superoxide anion-mediated mitogenic action of substance P on cardiac fibroblasts. *Am J Physiol Heart Circ Physiol* 2002; 282: H1855-62.

[77] Lawrence R, Chang LJ, Siebenlist U, Bressler P, Sonenshein GE. Vascular smooth muscle cells express a constitutive NF-κB-like activity. *J Biol Chem* 1994; 269: 28913-18.

[78] Lee R, Collins T. Nuclear factor-kappaB and cell survival: IAPs call for support. *Circ Res* 2001; 88: 262-4.

[79] Levkau B, Garton KJ, Ferri N, Kloke K, Nofer JR, Baba HA, et al. xIAP induces cell-cycle arrest and activates nuclear factor-kappaB: new survival pathways disabled by caspase-mediated cleavage during apoptosis of human endothelial cells. *Circ Res* 2001; 88: 282-90.

[80] Li C, Browder W, Kao RL. Early activation of transcription factor NF-kappaB during ischemia in perfused rat heart. *Am J Physiol* 1999; 276: H543-52.

[81] Li G, Bae S, Zhang L. Effect of prenatal hypoxia on heat stress-mediated cardioprotection in adult rat heart. *Am J Physiol Heart Circ Physiol* 2004; 286: H1712-9.

[82] Li N, Karin M. Is NF-kappaB the sensor of oxidative stress? *Faseb J* 1999; 13: 1137-43.

[83] Li Q, Verma IM. NF-kappaB regulation in the immune system. *Nat Rev Immunol* 2002; 2: 725-34.

[84] Lin A, Karin M. NF-kappaB in cancer: a market target. *Semin Cancer Biol* 2003; 13: 107-14.

[85] Liston P, Roy N, Tamai K, Lefebvre C, Baird S, Cherton-Horvat G, et al. Suppression of apoptosis in mammalian cells by NAIP and a related family of IAP genes. *Nature* 1996; 379: 349-53.

[86] Loberg RD, Vesely E, Brosius FC, 3rd. Enhanced glycogen synthase kinase-3beta activity mediates hypoxia-induced apoptosis of vascular smooth muscle cells and is prevented by glucose transport and metabolism. *J Biol Chem* 2002; 277: 41667-73.

[87] Long CS, Brown RD. The cardiac fibroblast, another therapeutic target for mending the broken heart? *J Mol Cell Cardiol* 2002; 34: 1273-8.

[88] Long X, Boluyt MO, Hipolito ML, Lundberg MS, Zheng JS, O'Neill L, Cirielli C, Lakatta EG, Crow MT. p53 and the hypoxia-induced apoptosis of cultured neonatal rat cardiac myocytes. *J Clin Invest* 1997; 99: 2635-43.

[89] Lotocki G, Keane RW. Inhibitors of apoptosis proteins in injury and disease. *IUBMB Life* 2002; 54: 231-40.

[90] MacKenna D, Summerour SR, Villarreal FJ. Role of mechanical factors in modulating cardiac fibroblast function and extracellular matrix synthesis. *Cardiovasc* Res 2000; 46: 257-63.

[91] Maiuri MC, Zalckvar E, Kimchi A, Kroemer G. Self-eating and self-killing: crosstalk between autophagy and apoptosis. *Nat Rev Mol Cell Biol* 2007; 8: 741-52.

[92] Malhotra R, Lin Z, Vincenz C, Brosius FC, 3rd. Hypoxia induces apoptosis via two independent pathways in Jurkat cells: differential regulation by glucose. *Am J Physiol Cell Physiol* 2001; 281: C1596-603.

[93] Mallat Z, Tedgui A, Fontaliran F, Frank R, Durigon M, Fontaine G. Evidence of apoptosis in arrhythmogenic right ventricular dysplasia. *N Engl J Med* 1996; 335: 1190-6.

[94] Maniatis, T, Fritsch EF, Sambrooks J. Molecular cloning: a laboratory manual. New York: Cold Spring Harbor Laboratory, Cold Spring Harbor; 1982.

[95] Matsushita H, Morishita R, Nata T, Aoki M, Nakagami H, Taniyama Y, et al. Hypoxia-induced endothelial apoptosis through nuclear factor-kappaB (NF-kappaB)-mediated bcl-2 suppression: in vivo evidence of the importance of NF-kappaB in endothelial cell regulation. *Circ Res* 2000; 86: 974-81.

[95a] Mattson MP and Meffert MK. Roles for NF-κB in nerve cell survival, plasticity, and disease. *Cell Death and Differentiation* 2006; 13: 852–60.

[96] Maulik N, Goswami S, Galang N, Das DK. Differential regulation of Bcl-2, AP-1 and NF-kappaB on cardiomyocyte apoptosis during myocardial ischemic stress adaptation. *FEBS Lett* 1999; 443: 331-6.

[97] Maulik N, Sato M, Price BD, Das DK. An essential role of NFkappaB in tyrosine kinase signaling of p38 MAP kinase regulation of myocardial adaptation to ischemia. *FEBS Lett* 1998; 429: 365-9.

[98] Mayorga M, Bahi N, Ballester M, Comella JX, Sanchis D. Bcl-2 is a key factor for cardiac fibroblast resistance to programmed cell death. *J Biol Chem* 2004; 279: 34882- 89.

[108] Narula J, Haider N, Virmani R, DiSalvo TG, Kolodgie FD, Hajjar RJ, et al. Apoptosis in myocytes in end-stage heart failure. *N Engl J Med* 1996; 335: 1182-9.

[109] Nylandsted J, Gyrd-Hansen M, Danielewicz A, Fehrenbacher N, Lademann U, Hoyer-Hansen M, et al. Heat shock protein 70 promotes cell survival by inhibiting lysosomal membrane permeabilization. *J Exp Med* 2004; 200: 425-35.

[110] Ohsato K, Shimizu M, Sugihara N, Konishi K, Takeda R. Histopathological factors related to diastolic function in myocardial hypertrophy. *Jpn Circ J* 1992; 56: 325-33.

[110a] Osorio-Fuentealba C, Valdés JA, Riquelme D, Hidalgo J, Hidalgo C, Carrasco MA. Hypoxia stimulates via separate pathways ERK phosphorylation and NF-κB activation in skeletal muscle cells in primary culture. J Appl Physiol 2009; 106: 1301-10.

[111] Ostadal B, Ostadalova I, Dhalla NS. Development of cardiac sensitivity to oxygen deficiency: comparative and ontogenetic aspects. *Physiol Rev* 1999; 79: 635-59.

[112] Pablos JL, Carreira PE, Serrano L, Del Castillo P, Gomez-Reino JJ. Apoptosis and proliferation of fibroblasts during postnatal skin development and scleroderma in the tight-skin mouse. *J Histochem Cytochem* 1997; 45: 711-9.

[112a] Paulina JD, Lieven PB, Matthew GA, Weijia Z, Zhi Z, Jialing L, Brian L and David WA. Bcl-2 changes conformation to inhibit Bax Oligomerization. *The EMBO Journal* 2006; 25: 2287–96.

[113] Perkins ND. Achieving transcriptional specificity with NF-kappa B. *Int J Biochem Cell Biol* 1997; 29: 1433-48.

[114] Peter ME. The flip side of FLIP. *Biochem J* 2004; 382: e1-3.

[99] Michiels C, Minet E, Michel G, Mottet D, Piret JP, Raes M. HIF-1 and AP-1 cooperate to increase gene expression in hypoxia: role of MAP kinases. *IUBMB Life* 2001; 52: 49-53.

[100] Michiels C, Minet E, Mottet D, Raes M. Regulation of gene expression by oxygen: NF-kappaB and HIF-1, two extremes. *Free Radic Biol Med* 2002; 33: 1231-42.

[101] Michiels C. Physiological and pathological responses to hypoxia. *Am J Pathol* 2004; 164: 1875-82.

[102] Minet E, Mottet D, Michel G, Roland I, Raes M, Remacle J, Michiels C. Hypoxia-induced activation of HIF-1: role of HIF-1alpha-Hsp90 interaction. *FEBS Lett* 1999; 460: 251-6.

[103] Misra A, Haudek SB, Knuefermann P, Vallejo JG, Chen ZJ, Michael LH, et al. Nuclear factor-kappaB protects the adult cardiac myocyte against ischemia-induced apoptosis in a murine model of acute myocardial infarction. *Circulation* 2003; 108: 3075-8.

[104] Morgan EN, Boyle EM, Jr., Yun W, Griscavage-Ennis JM, Farr AL, Canty TG, Jr., et al. An essential role for NF-kappaB in the cardioadaptive response to ischemia. *Ann Thorac Surg* 1999; 68: 377-82.

[105] Mottet D, Michel G, Renard P, Ninane N, Raes M, Michiels C. Role of ERK and calcium in the hypoxia-induced activation of HIF-1. *J Cell Physiol* 2003; 194: 30-44.

[106] Mustapha S, Kirshner A, De Moissac D, Kirshenbaum LA. A direct requirement of nuclear factor-kappa B for suppression of apoptosis in ventricular myocytes. *Am J Phsiol Heart Circ Physiol* 2000; 279: H939-945.

[107] Narula J, Acio ER, Narula N, Samuels LE, Fyfe B, Wood D, et al. Annexin-V imaging for noninvasive detection of cardiac allograft rejection. *Nat Med* 2001; 7: 1347-52.

[115] Pierson DJ. Pathophysiology and clinical effects of chronic hypoxia. *Respir Care* 2000; 45: 39-51.

[115a] Porter KE, Turner NA. Cardiac fibroblasts: at the heart of myocardial remodeling. *Pharmacol Ther* 2009; 123: 255-78.

[116] Purcell NH, Tang G, Yu C, Mercurio F, DiDonato JA, Lin A. Activation of NF-kappa B is required for hypertrophic growth of primary rat neonatal ventricular cardiomyocytes. *Proc Natl Acad Sci* U S A 2001; 98: 6668-73.

[116a] Qi Lu, Frances L. Jourd'heuil, David Jourd'heuil. Redox control of G_1/S cell cycle regulators during nitric oxide-mediated cell cycle arrest. *Journal of Cellular Physiology* 2007; 212: 827 – 39.

[117] Qin ZH, Chen RW, Wang Y, Nakai M, Chuang DM, Chase TN. Nuclear factor kappaB nuclear translocation upregulates c-Myc and p53 expression during NMDA receptor-mediated apoptosis in rat striatum. *J Neurosci* 1999; 19: 4023-33.

[118] Reeve JL, Duffy AM, O'Brien T, Samali A. Don't lose heart-therapeutic value of apoptosis prevention in the treatment of cardiovascular disease. *J Cell Mol Med* 2005; 9: 609-22.

[119] Regula KM, Baetz D, Kirshenbaum LA. Nuclear factor-kappaB represses hypoxia-induced mitochondrial defects and cell death of ventricular myocytes. *Circulation* 2004; 110: 3795-802.

[120] Roy S, Khanna S, Bickerstaff AA, Subramanian SV, Atalay M, Bierl M, et al. Oxygen sensing by primary cardiac fibroblasts: a key role of p21(Waf1/Cip1/Sdi1). *Circ Res* 2003; 92: 264-71.

[121] Royds JA, Dower SK, Qwarnstrom EE, Lewis CE. Response of tumour cells to hypoxia: role of p53 and NFκB. *Mol Pathol* 1998; 51: 55-61.

[122] Salvesen GS, Abrams JM. Caspase activation - stepping on the gas or releasing the brakes? Lessons from humans and flies. *Oncogene* 2004; 23: 2774-84.

[123] Salvesen GS, Duckett CS. IAP proteins: blocking the road to death's door. *Nat Rev Mol Cell Biol* 2002; 3: 401-10.

[124] Sapna S. Response of cardiac fibroblasts to hypoxia: a profile of delayed cell cycle progression and augmented production of modulators of inflammation. PhD Thesis-SCTIMST 2007.

[125] Saraste A, Arola A, Vuorinen T, Kyto V, Kallajoki M, Pulkki K, et al. Cardiomyocyte apoptosis in experimental coxsackievirus B3 myocarditis. *Cardiovasc Pathol* 2003; 12: 255-62.

[126] Saraste A, Pulkki K, Kallajoki M, Henriksen K, Parvinen M, Voipio-Pulkki LM. Apoptosis in human acute myocardial infarction. *Circulation* 1997; 95: 320-3.

[127] Sarkar S, Banerjee PK, Selvamurthy W. High altitude hypoxia: an intricate interplay of oxygen responsive macroevents and micromolecules. *Mol Cell Biochem* 2003; 253: 287-305.

[128] Sasaki H, Ray PS, Zhu L, Otani H, Asahara T, Maulik N. Hypoxia/reoxygenation promotes myocardial angiogenesis via an NF kappa B-dependent mechanism in a rat model of chronic myocardial infarction. *J Mol Cell Cardiol* 2001; 33: 283-94.

[129] Schmid T, Zhou J, Brune B. HIF-1 and p53: communication of transcription factors under hypoxia. *J Cell Mol Med* 2004; 8: 423-31.

[130] Seko Y, Tobe K, Ueki K, Kadowaki T, Yazaki Y. Hypoxia and hypoxia/reoxygenation activate Raf-1, mitogen-activated protein kinase kinase, mitogen-activated protein kinases, and S6 kinase in cultured rat cardiac myocytes. *Circ Res* 1996; 78: 82-90.

[131] Seta KA, Millhorn DE. Functional genomics approach to hypoxia signaling. *J Appl Physiol* 2004; 96: 765-73.

[132] Shimizu S, Eguchi Y, Kosaka H, Kamiike W, Matsuda H, Tsujimoto Y. Prevention of hypoxia-induced cell death by Bcl-2 and Bcl-xL. *Nature* 1995; 374:811-3.

[133] Shimizu S, Narita M, Tsujimoto Y. Bcl-2 family proteins regulate the release of apoptogenic cytochrome c by the mitochondrial channel VDAC. *Nature* 1999; 399: 483-7.

[134] Shiozaki EN, Chai J, Rigotti DJ, Riedl SJ, Li P, Srinivasula SM, et al. Mechanism of XIAP-mediated inhibition of caspase-9. *Mol Cell* 2003; 11: 519-27.

[135] Shivakumar K, Sollott SJ, Sangeetha M, Sapna S, Ziman B, Wang S, et al. Paracrine effects of hypoxic fibroblast-derived factors on the MPT-ROS threshold and viability of adult rat cardiac myocytes. *Am J Physiol Heart Circ Physiol* 2008; 294: H2653-8.

[136] Soares MP, Usheva A, Brouard S, Berberat PO, Gunther L, Tobiasch E, et al. Modulation of endothelial cell apoptosis by heme oxygenase-1-derived carbon monoxide. *Antioxid Redox Signal* 2002; 4: 321-9.

[137] Stehlik C, de Martin R, Kumabashiri I, Schmid JA, Binder BR, Lipp J. Nuclear factor (NF)-kappaB-regulated X-chromosome-linked iap gene expression protects endothelial cells from tumor necrosis factor alpha-induced apoptosis. *J Exp Med* 1998; 188: 211-6.

[138] Stempien-Otero A, Karsan A, Cornejo CJ, Xiang H, Eunson T, Morrison RS, et al. Mechanisms of hypoxia-induced endothelial cell death. Role of p53 in apoptosis. *J Biol Chem* 1999; 274: 8039-45.

[139] Sulciner DJ, Irani K, Yu ZX, Ferrans VJ, Goldschmidt-Clermont P, Finkel T. rac1 regulates a cytokine-stimulated, redox-dependent pathway necessary for NF-kappaB activation. *Mol Cell Biol* 1996; 16: 7115-21.

[140] Sun Y, Weber KT. Infarct scar: a dynamic tissue. *Cardiovasc Res* 2000; 46: 250-6.

[141] Suzuki Y, Imai Y, Nakayama H, Takahashi K, Takio K, Takahashi R. A serine protease, HtrA2, is released from the mitochondria and interacts with XIAP, inducing cell death. *Mol Cell* 2001; 8: 613-21.

[142] Tamm M, Bihl M, Eickelberg O, Stulz P, Perruchoud AP, Roth M. Hypoxia-induced interleukin-6 and interleukin-8 production is mediated by platelet-activating factor and platelet-derived growth factor in primary human lung cells. *Am J Respir Cell Mol Biol* 1998; 19: 653-61.

[143] Tanaka M, Ito H, Adachi S, Akimoto H, Nishikawa T, Kasajima T, et al. Hypoxia induces apoptosis with enhanced expression of Fas antigen messenger RNA in cultured neonatal rat cardiomyocytes. *Circ Res* 1994; 75: 426-33.

[144] Thurberg BL, Collins T. The nuclear factor-kappa B/inhibitor of kappa B autoregulatory system and atherosclerosis. *Curr Opin Lipidol* 1998; 9: 387-96.

[145] Tucci M, Hammerman SI, Furfaro S, Saukonnen JJ, Conca TJ, Farber HW. Distinct effect of hypoxia on endothelial cell proliferation and cycling. *Am J Physiol* 1997; 272: C1700-8.

[146] Twomey C, McCarthy JV. Pathways of apoptosis and importance in development. *J Cell Mol Med* 2005; 9: 345-59.

[147] Uchiyama T, Engelman RM, Maulik N, Das DK. Role of Akt signaling in mitochondrial survival pathway triggered by hypoxic preconditioning. *Circulation* 2004; 109: 3042-9.

[147a] Resch U, Winsauer G, Hofer-Warbinek R, Rainer de Martin. X-linked inhibitor of apoptosis protein regulates human interleukin-6 in umbilical vein endothelial cells *via* stimulation of the nuclear factor-*k*B and MAP kinase signaling pathways. *Pharmacological Reports* 2006; 58: 111-17.

[148] Vairo G, Soos TJ, Upton TM, Zalvide J, DeCaprio JA, Ewen ME, et al. Bcl-2 retards cell cycle entry through p27(Kip1), pRB relative p130, and altered E2F regulation. *Mol Cell Biol* 2000; 20: 4745-53.

[149] Valen G, Yan ZQ, Hansson GK. Nuclear factor kappa-B and the heart. *J Am Coll Cardiol* 2001; 38: 307-14.

[150] Van Antwerp DJ, Martin SJ, Kafri T, Green DR, Verma IM. Suppression of TNF-alpha-induced apoptosis by NF-kappaB. *Science* 1996; 274: 787-9.

[151] van Empel VP, Bertrand AT, Hofstra L, Crijns HJ, Doevendans PA, De Windt LJ. Myocyte apoptosis in heart failure. *Cardiovasc Res* 2005; 67: 21-9.

[152] Verhagen AM, Ekert PG, Pakusch M, Silke J, Connolly LM, Reid GE, et al. Identification of DIABLO, a mammalian protein that promotes apoptosis by binding to and antagonizing IAP proteins. *Cell* 2000; 102: 43-53.

[153] Wang CY, Mayo MW, Baldwin AS Jr. TNF- and cancer therapy-induced apoptosis: potentiation by inhibition of NF-kappaB. *Science* 1996; 274: 784-7.

[154] Weber KT, Anversa P, Armstrong PW, Brilla CG, Burnett JC, Jr., Cruickshank JM, et al. Remodeling and reparation of the cardiovascular system. *J Am Coll Cardiol* 1992; 20: 3-16.

[155] Weber KT, Brilla CG. Pathological hypertrophy and cardiac interstitium. Fibrosis and renin-angiotensin-aldosterone system. *Circulation* 1991; 83: 1849-65.

[156] Weber KT, Janicki JS, Shroff SG, Pick R, Chen RM, Bashey RI. Collagen remodeling of the pressure-overloaded, hypertrophied nonhuman primate myocardium. *Circ Res* 1988; 62: 757-65.

[157] Weber KT, Sun Y, Katwa LC, Cleutjens JP, Zhou G. Connective tissue and repair in the heart. Potential regulatory mechanisms. *Ann N Y Acad Sci* 1995; 752: 286-99.

[158] Weber KT, Sun Y, Katwa LC, Cleutjens JP. Connective tissue: a metabolic entity? *J Mol Cell Cardiol* 1995; 27: 107-20.

[159] Weber KT. Cardiac interstitium: Extracellular space of the myocardium. In: Fozzard HA et al. ed. The heart and cardiovascular system. New York: Raven Press; 1992: 1465-80.

[160] Webster KA, Discher DJ, Kaiser S, Hernandez O, Sato B, Bishopric NH. Hypoxia-activated apoptosis of cardiac myocytes requires reoxygenation or a pH shift and is independent of p53. *J Clin Invest* 1999; 104: 239-52.

[161] Webster KA. Evolution of the coordinate regulation of glycolytic enzyme genes by hypoxia. *J Exp Biol* 2003; 206: 2911-22.

[162] Wencker D, Chandra M, Nguyen K, Miao W, Garantziotis S, Factor SM, et al. A mechanistic role for cardiac myocyte apoptosis in heart failure. *J Clin Invest* 2003; 111: 1497-504.

[163] Wenger RH. Cellular adaptation to hypoxia: O_2-sensing protein hydroxylases, hypoxia-inducible transcription factors, and O_2-regulated gene expression. *Faseb J* 2002; 16: 1151-62.

[164] Xu Y, Bialik S, Jones BE, Iimuro Y, Kitsis RN, Srinivasan A, et al. NF-kappaB inactivation converts a hepatocyte cell line TNF-alpha response from proliferation to apoptosis. *Am J Physiol* 1998; 275: C1058-66.

[165] Xu Y, Williams SJ, O'Brien D, Davidge ST. Hypoxia or nutrient restriction during pregnancy in rats leads to progressive cardiac remodeling and impairs postischemic recovery in adult male offspring. *Faseb J* 2006; 20: 1251-3.

[166] Xuan YT, Tang XL, Banerjee S, Takano H, Li RC, Han H, et al. Nuclear factor-kappaB plays an essential role in the late phase of ischemic preconditioning in conscious rabbits. *Circ Res* 1999; 84: 1095-109.

[167] Yang QH, Church-Hajduk R, Ren J, Newton ML, Du C. Omi/HtrA2 catalytic cleavage of inhibitor of apoptosis (IAP) irreversibly inactivates IAPs and facilitates caspase activity in apoptosis. *Genes Dev* 2003; 17: 1487-96.

[168] Yang Y, Fang S, Jensen JP, Weissman AM, Ashwell JD. Ubiquitin protein ligase activity of IAPs and their degradation in proteasomes in response to apoptotic stimuli. *Science* 2000; 288: 874-7.

[169] Zahradka P, Werner JP, Buhay S, Litchie B, Helwer G, Thomas S. NF-kappaB activation is essential for angiotensin II-dependent proliferation and migration of vascular smooth muscle cells. *J Mol Cell Cardiol* 2002; 34: 1609-21.

[170] Zhao L, Eghbali-Webb M. Release of pro- and anti-angiogenic factors by human cardiac fibroblasts: effects on DNA synthesis and protection under hypoxia in human endothelial cells. *Biochim Biophys Acta* 2001; 1538: 273-82.

[171] Zhao X, Eghbali-Webb M. Gender-related differences in basal and hypoxia-induced activation of signal transduction pathways controlling cell cycle progression and apoptosis, in cardiac fibroblasts. *Endocrine* 2002; 18: 137-45.

VIII. LIST OF PUBLICATIONS

Article published:

1) Shivakumar K, Sollott SJ, **Sangeetha M**, Sapna S, Ziman B, Wang S, Lakatta EG. Paracrine effects of hypoxic fibroblast-derived factors on the MPT-ROS threshold and viability of adult rat cardiac myocytes. *Am J Physiol Heart Circ Physiol* 2008; 294: H2653-58.